LONG-TERM IMPACTS OF SUDDEN OAK DEATH AND INTERACTIONS WITH FIRE IN BIG SUR, CA USING COUPLED DYNAMIC SPATIAL TEMPORAL EPIDEMIOLOGICAL MODELING

Chris M. Jones

"A dissertation submitted to the faculty at the University of North Carolina at Chapel Hill in partial fulfillment of the requirements for the degree of Doctor of Philosophy in the Curriculum of Geography."

Chapel Hill
2017

Approved by:

Aaron Moody

Ross K. Meentemeyer

Conghe Song

Diego Riveros-Iregui

Charles Mitchell

ABSTRACT

Chris M. Jones: Long-term Impacts of Sudden Oak Death and Interactions with Fire in Big Sur, CA Using Coupled Dynamic Spatial Temporal Epidemiological Modeling
(Under the direction of Aaron Moody)

Invasive forest pathogens are an increasing risk to forest ecosystems. One such invasive forest pathogen is *Phytophthora ramorum*, a generalist pathogen with asymmetries in host competency and susceptibility. Apparent competition, indirect competition between two or more species mediated by a common enemy (*P. ramorum*), can emerge when asymmetries in host response to a pathogen occur. Additionally, invasive pathogens can interact with natural disturbance regimes to alter forest ecosystems in unexpected ways due to non-linear dynamics. Coupled spatial temporal models provide the ability to examine how disease and interactions with fire alter forest composition over the course of a century. Epidemiological models typically treat forest composition as static and don't account for disease related mortality.

Here, I present the first dynamic spatial epidemiological model that can interact with a FLSM, LANDIS-II, to incorporate changes in forest composition due to disturbance, natural growth, mortality, and regeneration. The model incorporates asymmetries in host susceptibility and competency across species and age classes and changes in inoculum production based on temperature and precipitation. Average odds ratio of the model was 7.9 compared to 7.6 for the current *P. ramorum* spread model. This model was then coupled with a forest composition model and fire behavior model to analyze the effect of disturbance interaction and apparent competition. The model simulated from 1990-2090 using 10-year time steps for the FLSM and a 1-year time step for the disease and fire model in Big Sur, CA using daily projected climate data.

The model was replicated 30 times to account for stochastic variability in climate, disease spread, fire ignition locations, and seedling establishment. Three disturbance scenarios were utilized: fire, disease, and fire and disease. Model results suggest overall disease decreased fire severity, however, when disease related mortality occurred 3 years prior to a fire then fire severity increased. The model results suggest that bay laurel increases relative to other host species due to apparent competition under the disease only scenario. This effect is mitigated in the disease and fire scenario due to individual species response to fire.

To Shannon (my wife and best friend) and Oliver (the greatest little man ever)

ACKNOWLEDGEMENTS

Many individuals contributed to this research. I want to thank my graduate advisor, Aaron Moody, for his years of advice, guidance, mentorship, and flexibility. I also want to thank my graduate committee members - Ross Meentemeyer, Diego Riveros-Iregui, Conghe Song, and Charles Mitchell – for their feedback over the years. I also want to think Megan Creutzburg, Rob Scheller, Melissa Lucash, and Jelena Vukomanovic for their guidance and advice on calibrating and validating LANDIS-II, especially the NECN succession extension. I also wanted to thank the other graduate students and postdocs in the Meentemeyer lab, particularly Devon Gaydos, Whalen Dillon, and Fracesco Tonini. I also wanted to thank all of the graduate students and undergraduates that have collected field data in the Big Sur plot network over the years.

This research was funded in part by the NSF Graduate Research Fellowship, as well as the Microsoft for Research Grant and NVidia GPU Computing Grant. Many of the datasets used in this research were freely provided by the US Forest Service Forest Inventory Analysis, Landscape Ecology, Modeling, Mapping, and Analysis (LEMMA) group for the Northwest Forest Plan Effectiveness Monitoring, Soil Survey Geographic Database, National Atmospheric Deposition Program, LANDFIRE group of the Nature Conservancy, and US Geological Survey GeoData Portal. I also want to think all of the developers who have spent time refining the LANDIS-II core and extensions.

TABLE OF CONTENTS

LIST OF TABLES

LIST OF FIGURES

LIST OF ABBREVIATIONS

ANPP	Above-ground Net Primary Productivity
C/N	Carbon/Nitrogen
CA-BCM 2014	California Basin Characterization Model Downscaled Climate/Hydrology
CAL FIRE	California Department of Forestry and Fire Protection
CBH	Base Height of the Crown
CO_2	Carbon Dioxide
CRM	Component Ratio Method
CVS	Current Vegetation Survey
DBH	Diameter at Breast Height
EDA	Epidemiological Disturbance Agent
FIA	Forest Inventory Analysis
FLSM	Forest Landscape Simulation Model
FMC	Foliar Moisture Content
FWI	Fire Weather Index
GCM	Global Circulation Models
GDD	Growing Degree Days
GNN	Gradient Nearest Neighbor
ISI	Initial Spread Index
LAI	Leaf Area Index
LEMMA	Landscape Ecology, Modeling, Mapping and Analysis
NADP	National Atmospheric Deposition Program
NECN	Net Ecosystem Carbon and Nitrogen
NEE	Net Ecosystem Exchange

NPP	Net Primary Productivity
SHI	Site Host Index
SHIMs	Site Host Index Modifiers
SOD	Sudden Oak Death
SOM	Soil Organic Matter
SSURGO	Soil Survey Geographic Database

CHAPTER 1: INTRODUCTION

Invasive Pest and Pathogen Problem

Invasive forest insects and pathogens are a significant threat to forested ecosystems worldwide (Liebhold et al. 1995; Vitousek et al. 1997; Simberloff 2000; Perles, Callahan, and Marshall 2010; Vitousek et al. 1996). As of 2010, a total of 455 non-native forest pests and 16 pathogens were discovered in the US; these organisms have become an increasingly serious threat to forest productivity and diversity (Aukema et al. 2010; Perles, Callahan, and Marshall 2010). Despite regulatory measures to prevent new introduction, the number of species has continued to increase annually (Aukema et al. 2011). Recently, awareness of both the economic and ecological impacts associated with introduced insects and pathogens has increased (Aukema et al. 2010).

For example, the emerald ash borer (*Agrilus planipennis*), Asian longhorned beetle (*Anoplophora glabripennis*), and sudden oak death (SOD) (*Phytophthora ramorum*) caused damages estimated to be in the billions of dollars due to lost timber resources (GAO 2006). Another study estimated approximately $1.7 billion in local government expenditures and $830 million in lost property value from wood and phloem-boring non-native insects in the United States (Aukema et al. 2011). One study of emerald ash borer estimates that over the course of 10 years the cost to treat and remove infected ash trees would be $10.7 billion (Kovacs et al. 2010). A study of oak wilt (*Ceratocystis fagacearum)* conducted in Anoka County, Minnesota found that the cost of removal of dead trees would range from $18-60 million (Haight et al. 2011). In

the Big Sur region of California, the estimated cost of treatment was $7.5 million and property value loss was $135 million (Kovacs et al. 2011).

In addition to lost property value, these invasive forest pests and pathogens have serious consequences for ecosystem services and stability. These ecosystem effects include both short- and long-term effects. Short-term effects occur on timescales from weeks to years, while, long-term effects are seen over decades or centuries (Lovett et al. 2006). Direct short-term effects of forest and pathogen disturbance are tree defoliation, loss of vigor, or death. Indirect short-term effects of forest pests and pathogens include but are not limited to temporary decrease in primary productivity, increased exchange and leaching of nutrients, increased or decreased decomposition, microclimate changes, and increased light availability (Lovett et al. 2006, 2004; J. C. Jenkins, Aber, and Canham 1999). Long-term effects are primarily driven by a change in tree species competition due to host mortality differentiation, that leads to altered forest structure, primary productivity, nutrient exchange rates, and soil organic matter production and turnover (Lovett et al. 2006). Three main attributes of the pest or pathogen affect the short- and long-term effects to ecosystem functions: mode of attack (how does a pest or pathogen attack the tree?), host specificity (generalist vs. specialist (one host vs. multiple hosts), Virulence (rapid mortality vs. slow mortality and probability of mortality) (Lovett et al. 2006). Additionally, there are important host tree characteristics that also play an important role in ecosystem consequences: dominance (i.e. basal area or leaf area), succession and growth (pure stands vs. mixed, where in the successional process, and regeneration effectiveness), and uniqueness (nitrogen fixation, unusual environmental tolerances, large seed crops) (Lovett et al. 2006; Orwig et al. 2008).

The effects of forest pests and pathogens are typically long lasting due to 2 factors: host selectivity and persistence within the ecosystem (i.e. once established remain a permanent component of the ecosystem). For example, hemlock woolly adelgid has been shown to reduce forest floor moisture, increase rates of nitrogen accumulation, increase nitrate leaching into streams, decrease soil CO_2 efflux, and decrease stream flow in the summer (Den Boer 1968; J. C. Jenkins, Aber, and Canham 1999; Ross et al. 2003; Yorks, Leopold, and Raynal 2003; Cobb, Orwig, and Currie 2006; Orwig et al. 2008). *Cryphonectria parasitica*, the causal agent of chestnut blight, has dramatically altered forest composition in the Eastern US; forests once dominated by American chestnut have become oak/hickory dominant. This is especially true in areas of the Appalachian Mountains where it is estimated that one in four hardwoods was an American chestnut (Jules et al. 2014; Prospero and Cleary 2017). The local dominance, biomass, or functional importance of species killed following infection or infestation determines the magnitude and nature of ecosystem change (Lovett et al. 2006; Ruess et al. 2009). Pathogen impacts range from dramatic stand level population declines to removals of single individuals and can occur over many years (Eviner and Likens 2008).

Modeling Pathogen Effects

Pest and pathogen models – frequently used to predict areas of future infection/infestation – have often ignored the effect of host heterogeneity and asymmetric host susceptibility and competency, except see (Meentemeyer et al. 2011; Fitzpatrick et al. 2012). Landscape epidemiological models frequently treat forest composition and host density as static (Meentemeyer, Haas, and Václavík 2012), meaning that the trees do not age or experience effects of disturbance. This makes it difficult to understand how disease alters species composition at a landscape level (Cobb, Meentemeyer, and Rizzo 2010). Apparent competition

is a form of indirect competition driven by asymmetries in host susceptibility to a pathogen that lead to changes in species composition (Power and Mitchell 2004; Cobb, Meentemeyer, and Rizzo 2010). This lack of realistic changes in host community composition greatly impedes modeling the interactions of other landscape-level disturbances with disease spread (Cobb and Metz 2017). Combining a dynamic epidemiological model with a forest landscape simulation model (FLSM) allows for understanding how disease affects forest community composition and other disturbance dynamics and impacts.

Forest landscape simulation models (FLSMs) have been developed to specifically address management and research questions at landscape scales (>10^5 ha) by projecting forest dynamics over space and time (Mladenoff 2004; Scheller and Mladenoff 2007). These models typically include details such as tree age, species and biomass, and are widely used to analyze the influence of disturbances over time as they affect large-scale forest ecosystem dynamics (Thompson et al. 2016; Scheller and Mladenoff 2004). One of several FLSMs, LANDIS-II stands out as a process-based forest landscape model that can include variable time steps for different ecological processes (e.g. succession, disturbance, seed dispersal, forest management, carbon dynamics) and simulate their interactions as an emergent property of the independently simulated processed (Mladenoff 2005; Scheller and Mladenoff 2007; Mladenoff 2004). LANDIS-II continues to grow its user community and several extensions are available to simulate disturbances like wind, fire, insect spread, or land-use change. To date, the representation of forest pathogen and disease spread in FLSMs including LANDIS-II has been lacking.

Phytophthora Ramorum

Phytophthora ramorum is an oomycete, a fungus like eukaryotic microorganism, which can infect over a hundred plant species (Rizzo, Garbelotto, and Hansen 2005; Davidson, Patterson, and Rizzo 2008). Disease symptoms are expressed in two forms: lethal infections on canker hosts and non-lethal foliar infections. The lethal form of the disease infects stems and branches of several ecologically important tree species, such as, tanoak (*Notholithocarpus densiflorus*), coast live oak (*Quercus agrifolia*), canyon live oak (*Quercus chrysolepsis),* California black oak (*Quercus* kelloggii), and Shreve's oak (*Quercus parvula var. shrevei*). These canker hosts are epidemiological dead ends with the exception of tanoak (Kovacs et al. 2011; Davidson et al. 2005). The foliar hosts can transmit the disease as leaves and twigs of these species produce inoculum. California Bay Laurel produces the most inoculum of all infected species and as such is consider the reservoir host with other hosts considered alternative hosts (Figure 1) (Kelly and Meentemeyer 2002; Meentemeyer, Rank, et al. 2008; Václavík et al. 2010). There are four main factors that make *P. ramorum* a serious threat to many forest ecosystems: the potential for foliar hosts to readily support *P. ramorum* growth, the pathogen's ability to disperse by wind-blown rain (Davidson et al. 2005), the broad range of the host species, and the ability to kill ecologically important species (Garbelotto, Rizzo, and Marais 2002; Rizzo and Garbelotto 2003).

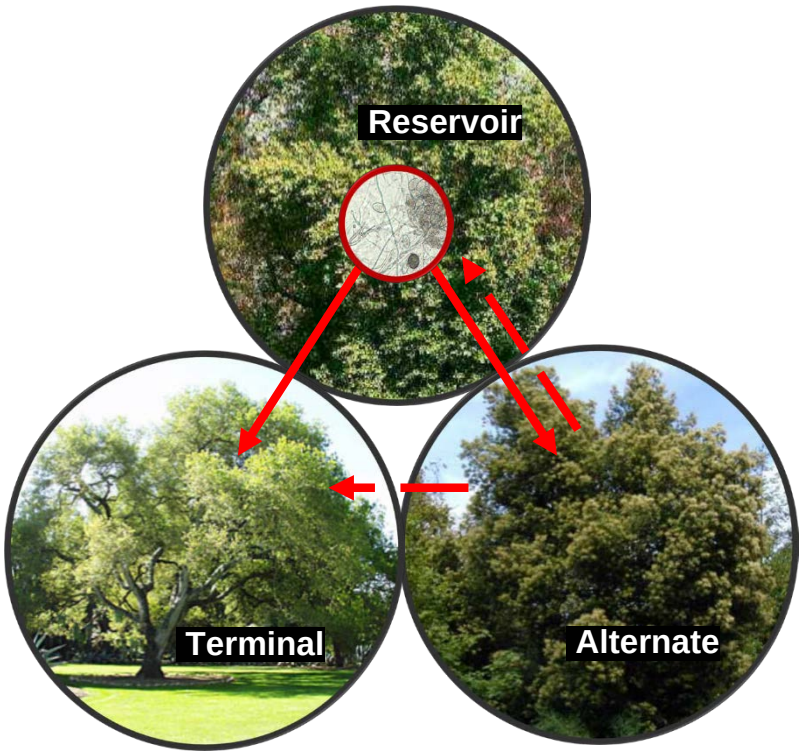

Figure 1: Transmission pathways for the pathogen. Reservoir hosts = primary source of pathogen spread indicated by the solid red lines, alternate hosts = able to spread pathogen but to a lesser extent indicated by the dashed red lines, and terminal hosts = no spread of the pathogen.

The range of sudden oak death is from the Big Sur region (Figure 3) of California to South-western Oregon (Meentemeyer, Rank, et al. 2008; Cobb, Meentemeyer, and Rizzo 2010; Václavík et al. 2010; Cobb, Filipe, et al. 2012) (Figure 2). *P. ramorum* produces two types of spores: chlamydospores (resting spores) and zoospores, which have flagella for swimming. Spores are transmitted via rain-splash and wind driven ran, which can knock spores into watercourse where they can be transmitted great distances. People engaged in outdoor activities can also transmit the disease spores on their equipment, especially in muddy areas (Davidson et

al. 2002). Transmission can be much higher than average during periods of high spring rain fall and much lower during periods of prolonged drought (Cobb and Metz 2017; Haas et al. 2016).

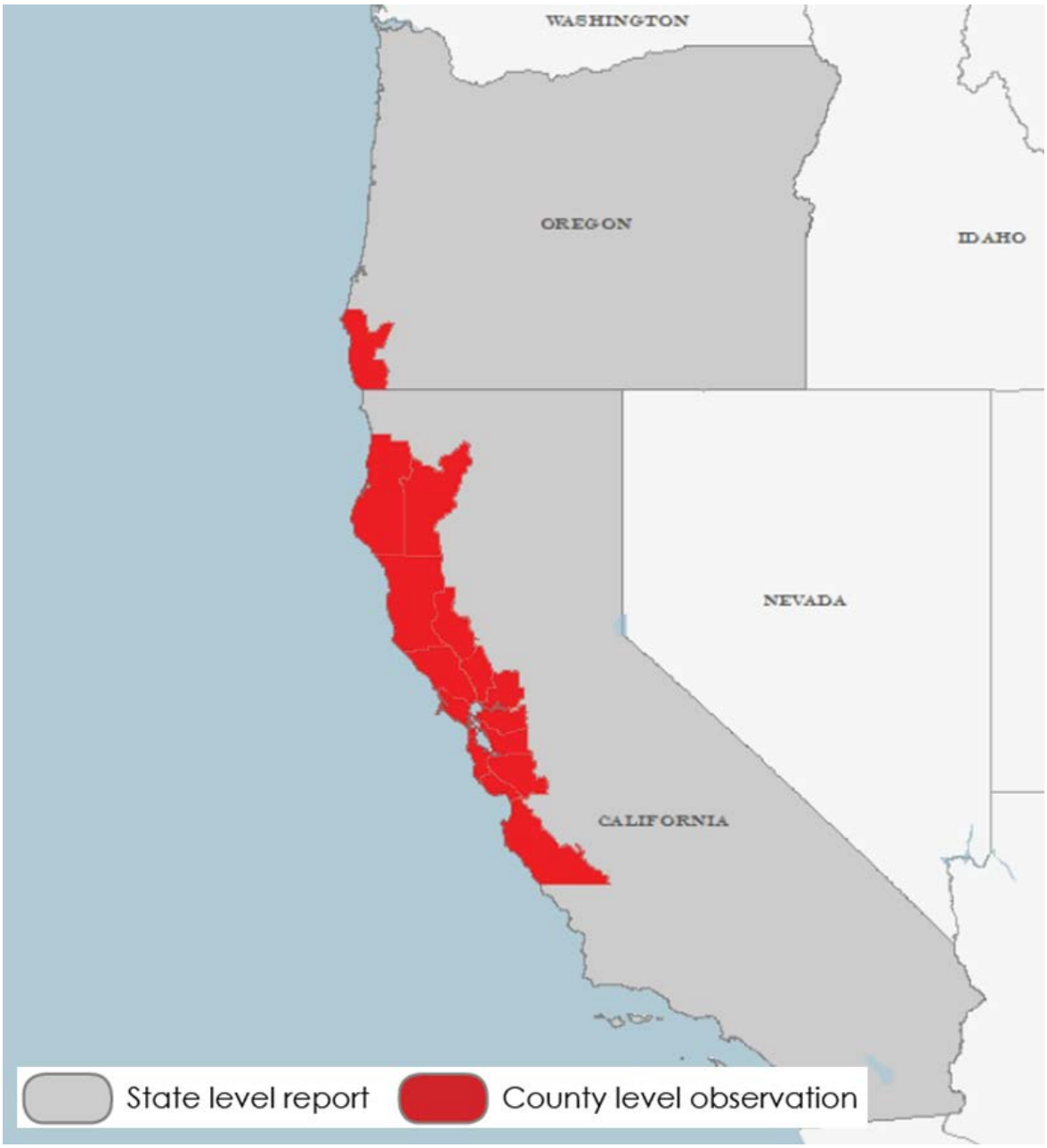

Figure 2: County level infection status of Sudden Oak Death as of 2016 (USDA Forest Service Northern Research Station and Forest Health Protection 2016)

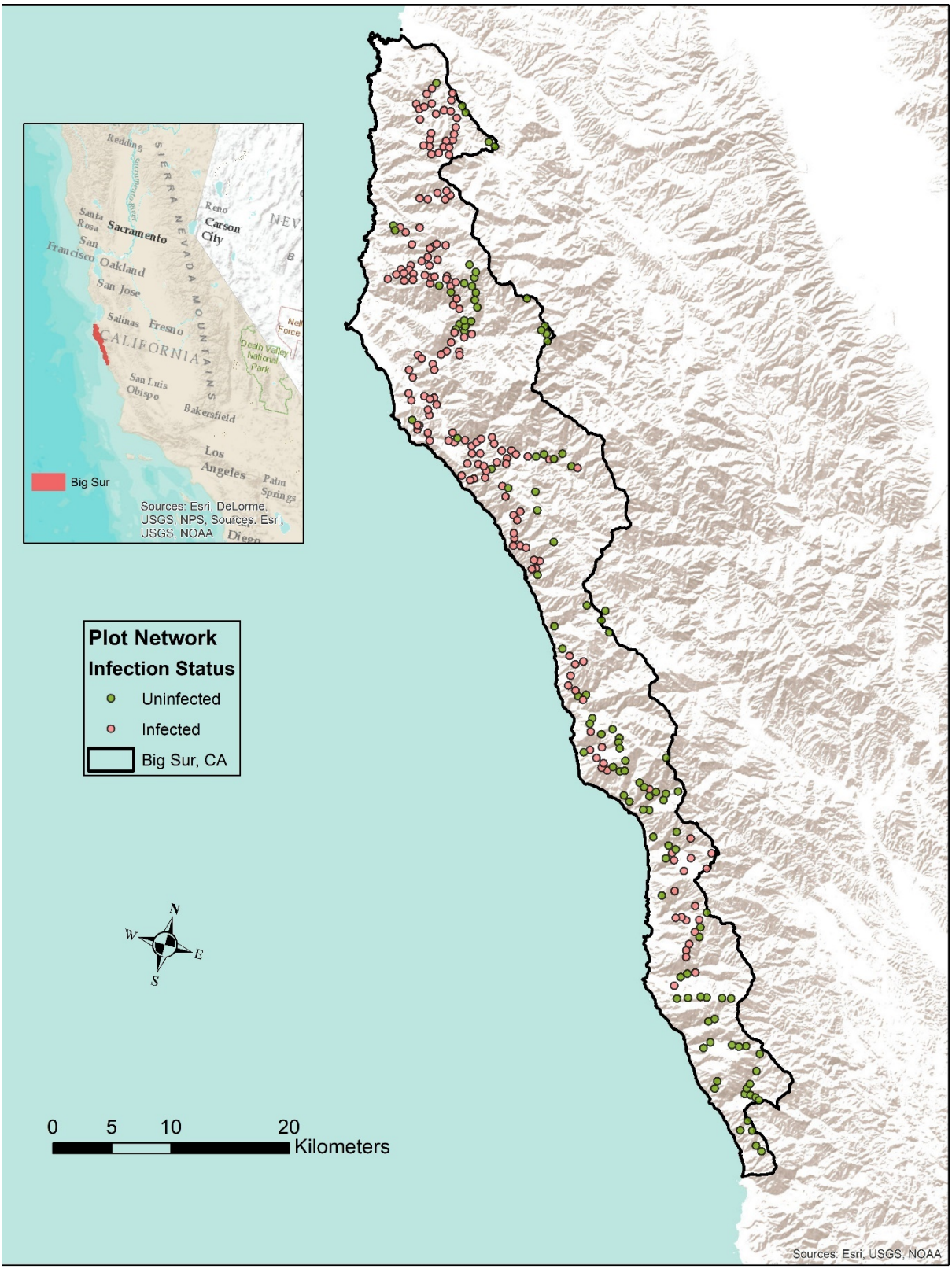

Figure 3: Big Sur study area with most recent plot level infection status shown.

Economic costs of sudden oak death range from removal cost of dead trees, prevention cost, and loss of property value. One study estimated that over a ten year period the cost of treatment, removal, and replacement of 10,000 infected oaks was $7.5 million and that property losses to single family homes were $135 million (Kovacs et al. 2011).

Ecosystem consequences of SOD

P. ramorum is persistent within impacted stands, mortality is constant or increasing over the scale of a decade, and inter-annual climate variability is critical to rates of pathogen spread (Davidson, Patterson, and Rizzo 2008; Cobb, Meentemeyer, and Rizzo 2010; Davis et al. 2010). This dynamic interaction with its environment may prolong mortality and ecosystem effects of *P. ramorum* over a greater time frame compared to other pests or pathogens especially those that spread from discrete contact zones (Hansen and Goheen 2000; Rizzo, Slaughter, and Parmeter 2000; Kauffman and Jules 2006).

In plots affected by SOD, course woody debris accumulation rates increased in both snags and logs compared to uninfected plots (Cobb, Chan, et al. 2012). The number of large live tanoaks decreased dramatically in infected vs. uninfected plots, however, tanoak should be able to persist due to vegetative reproduction (i.e. seedlings or resprouting after fire) (Cobb, Filipe, et al. 2012). Additionally, in redwood-tanoak forests *P. ramorum* infection has led not only to a decline in large tanoak but also redwood while bay laurel became a more dominant part of the forests (Cobb, Meentemeyer, and Rizzo 2010). Thus, incorporating epidemiological processes, particularly factors that determine transmission and host biomass will yield more realistic estimates of carbon accumulation over time and maximum amount of carbon released in infected forests (Cobb, Chan, et al. 2012; Cobb and Metz 2017).

Fire Regime

The frequency of large wildfires in the western USA has increased significantly since the mid-1980s, together with warming temperatures and lengthened fire season (Beh et al. 2012). Wildfire has played a crucial role in shaping the structure and ecological function of coniferous forests throughout the world, including those in the Big Sur area of California (Van Wagtendonk and Cayan 2008; Metz et al. 2010). The relationship between fire and fuels is that recently burned areas limit subsequent fire size by reducing fuel load. Thus, large areas of dense continuous fuels increase the likelihood that fires will become larger and more severe (Valachovic et al. 2011; He and Mladenoff 1999). Large, severe fires can lead to dramatic reductions in mature trees and aboveground and belowground live biomass, leading to cascading ecological effects (Cobb, Meentemeyer, and Rizzo 2016; Sturtevant et al. 2012).

Traditionally forest disturbance events that cause defoliation or damage to a stand are thought to increase fire severity and frequency due to an increase in litter accumulation and increased evapotranspiration due to greater light in the understory (McCullough, Werner, and Neumann 1998; Parker, Clancy, and Mathiasen 2006). However, recent empirical and modelling studies in pine bark beetle disturbance systems have shown that these disturbances are more interactive and may actually cause a decrease in fire severity. This is due to the nonlinear effects of increased dead fuel and thinned canopies (Romme et al. 2006; M. J. Jenkins et al. 2008; Lynch and Moorcroft 2008). The long-term consequences of pathogen disturbance on fire regimes is even more poorly understood due to the need for large temporal data.

Pathogen disturbances influence successional pathways affecting future forest conditions that have subsequent repercussions for future fire and pathogen disturbance (Jasinski and Payette 2005; Kulakowski and Veblen 2007; Bouchard and Pothier 2008). Additionally, wildfire is

frequently considered a major agent of soil and land degradation, some have suggested that it is the single most important agent of geomorphological change (Neary, Ryan, and DeBano 2005). Wildfire and pathogen/pest disturbances are key factors in hydrology of a region given that they have a large influence on evapotranspiration (Neary, Ryan, and DeBano 2005; Shakesby and Doerr 2006; Doerr et al. 2006).

Interacting Disturbances

Disturbances play an important role in maintaining or changing ecosystems. However, many disturbance regimes are being altered by climate change and other anthropogenic factors such as introduced species. Often times interacting disturbances have results that are unexpected based on the individual disturbances but when combined can lead to shifts from one ecosystem state to another (M. G. Turner 2010; Foster et al. 2015). Interactions between fire and disease can modify the other's likelihood, intensity or spatial distribution.

Within the Big Sur study area of California there have been 2 years with large scale wildfires (2008 and 2016) since the establishment of the plot network in 2006. These fires have provided insights into how fire and SOD interact to affect forest composition and services. Forest floor carbon, nitrogen, and phosphorus were significantly greater in plots uninfected by *P. ramorum* compared to those infected within the 2008 Chalk and Basin Complex fire burn area in Big Sur. While no significant difference was found between infected and uninfected plots outside of the burn area indicating that the interaction between fire and SOD have a meaningful impact on post fire forest floor nutrient pools (Cobb and Metz 2017; Cobb, Meentemeyer, and Rizzo 2016).

Host fire tolerance and post fire recovery has feedbacks for disease prevalence, while selective host mortality by *P. ramorum* affects the standing and downed course woody debris which alters the fuel load of the forest thus affecting likelihood and severity of fires (Cobb, Meentemeyer, and Rizzo 2016; Metz et al. 2013, 2010). In some cases, wildfire could directly eliminate the pathogen from burned areas or at a minimum reduce the amount of disease and increase time until reinfection (Beh et al. 2012; Metz et al. 2010, 2013).

Goals

The goal of this dissertation is to use the LANDIS-II FLSM to examine how fire and disease interact and how those interactions affect forest composition. There are two highly important steps to be able to accomplish this goal. First, I needed to create an epidemiological model that could interact with a forest composition model and fire model. Using this model at a 30-m spatial resolution to capture the spatial heterogeneity of the Big Sur was too slow to be used for multiple simulation runs. Thus, I implemented the first parallelization in a FLSM to improve computational time. I have divided the work into three chapters: (1) Parallelization in FLSMs, (2) Dynamic Epidemiological Modelling in FLSMs: A Case Study Using *P. ramorum* in Big Sur, CA, (3) Interacting Disturbances and Their Ecological Impacts: A Case Study Using Fire and *P. ramorum* in Big Sur, CA.

CHAPTER 2: PARALLELIZATION OF FLSMS

Introduction

Forest landscape simulation models (FLSMs) are often used to understand and manage forest dynamics over space and time (Mladenoff 2004; Scheller and Mladenoff 2007). These models typically include details such as tree age, species, biomass and are widely used to analyze the influence of disturbances over time and space on forest ecosystem dynamics (Thompson et al. 2016). Among several types of FLSMs, LANDIS-II stands out as a spatially-explicit forest landscape model that can include variable time steps for different ecological processes (e.g. succession, disturbance, seed dispersal, forest management, carbon dynamics) and simulate their interactions (Mladenoff 2005; Scheller et al. 2007; Mladenoff 2004). LANDIS-II continues to grow its user community and several extensions are made available to simulate disturbances like wind, fire, insect spread, or forest pathogen spread and disease impacts. However, as the model becomes more complex the computational time increases, requiring a tradeoff between spatial extent and spatial resolution (Figure 4).

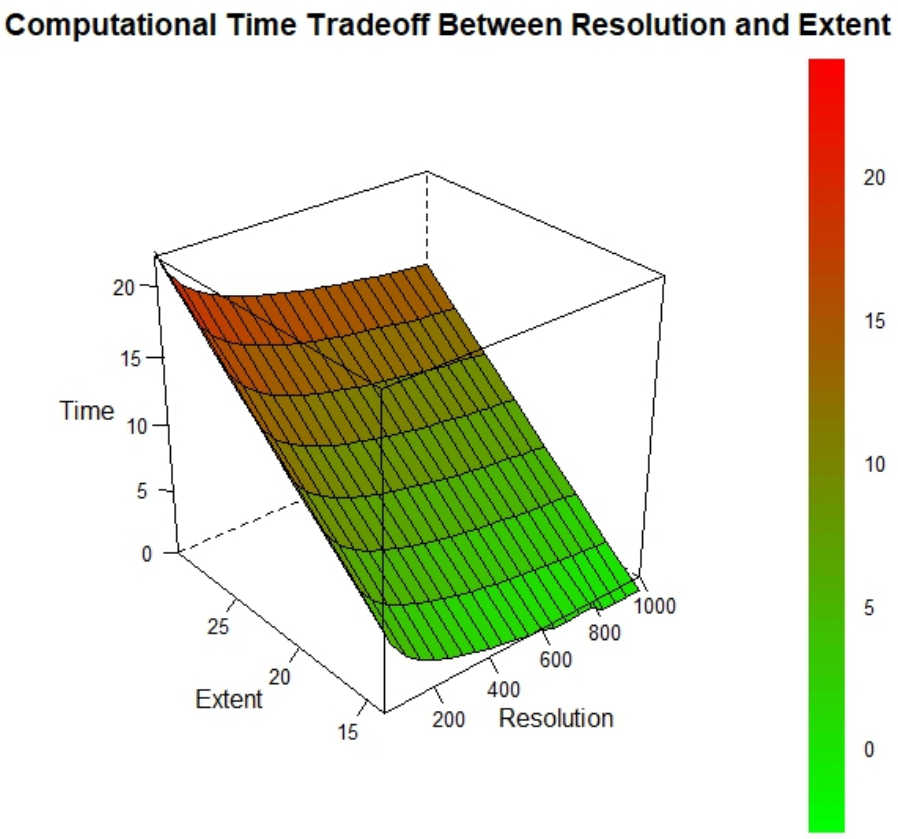

Figure 4: The tradeoff in computational time between resolution and extent. The log of both time and extent are shown here using a single-core model and number of computations for each combination of extent and resolution.

Parallel computing offers a means to reduce computational time by performing many calculations simultaneously. This happens by dividing large calculations into smaller ones and bringing the results back together when all calculations of one type are complete. Care must be taken, however, to ensure that dependent processes still run sequentially. Parallelized FLSMs offer a means to examine processes and capture the effects of highly heterogenous areas on forest processes by allowing higher spatial resolutions within the same size study area. This also dramatically speeds up the calibration and validation process of these models.

In this study, we introduce parallel computing to the LANDIS-II FLSM utilizing the Base Epidemiological Disturbance Agent (EDA) extension for LANDIS-II. Base EDA allows the

linking of forest pathogen spread and tree mortality in forested landscapes. Thus, the feedback between pathogen spread and mortality can be predicted across space and time. The parallelized version of EDA is compatible with all succession extensions and can be used in conjunction with other disturbance extensions (e.g. fire, insect, wind) to simulate their combined effects on forest landscape dynamics. In this paper, we show that a parallel version of the model decreases computational time proportional to the number of cores utilized for the model. This is done using an example application of the EDA extension in Big Sur, California.

Model description

The LANDIS-II modeling framework includes a model core that links, parses, and validates data from multiple extensions and allows the user to select a forest-succession extension and/or any number of disturbance extensions (Scheller et al. 2007). EDA is a disturbance extension compatible with all LANDIS-II forest-succession extensions. It is open source and freely available at the LANDIS-II project website: www.landis-ii.org. The download comes with an installer, user guide and sample data.

To date, no extension or core in LANDIS-II has taken advantage of the benefits of parallel computing. This is partially due to the core utilizing the Microsoft .Net Framework 3.5 instead of 4.0 or higher, which contain built in libraries for implementing parallel algorithms. However, we exported the necessary libraries to a Dynamic-link library that allows us to utilize the parallel functions within the .Net 3.5 framework.

Case study

To demonstrate the effect of parallelization, we ran the model for 20 years in an 8,017 km^2 area of central California at a 30-m resolution (total pixels = 885,588), USA with a 1-year time step. We averaged the time taken for a time step using 1, 2, 4, 6, and 8 cores on the same computer; this is done in order to minimize differences in processor speeds. We then divided the total time for a time-step by the number of pixels in the study area in order to get a per pixel time-step. This allows us to scale up to multiple extents and resolutions as the main formula for computational time is number of pixels multiplied by time per pixel. The decrease in computational time is directly related to the number of cores allocated to the model (1-8 in this case), see Table 1. At some point when much higher cores are used on super computers this relationship will break down and the decrease will no longer be 1:1 based on the amount of the model that is parallel compatible. This extension is 100% parallelizable so Amdahl's law (McCool, Robison, and Reinders 2012) really takes effect at much larger core infrastructure (around 64 cores). Figure 5 shows the difference in computational time at different resolutions for a given extent. This means that the researcher can choose an extent 2 orders of magnitude higher with the same resolution and have a similar computational time when using an 8-core parallel model compared to the single core models that have been used previously.

Cores	Time	Speedup
1	29531	1
2	14621	2
4	7387	4
6	4907	6
8	3676	8

Table 1: Average time for a timestep for a simulation when allotted 1, 2, 4, 6, or 8 cores.

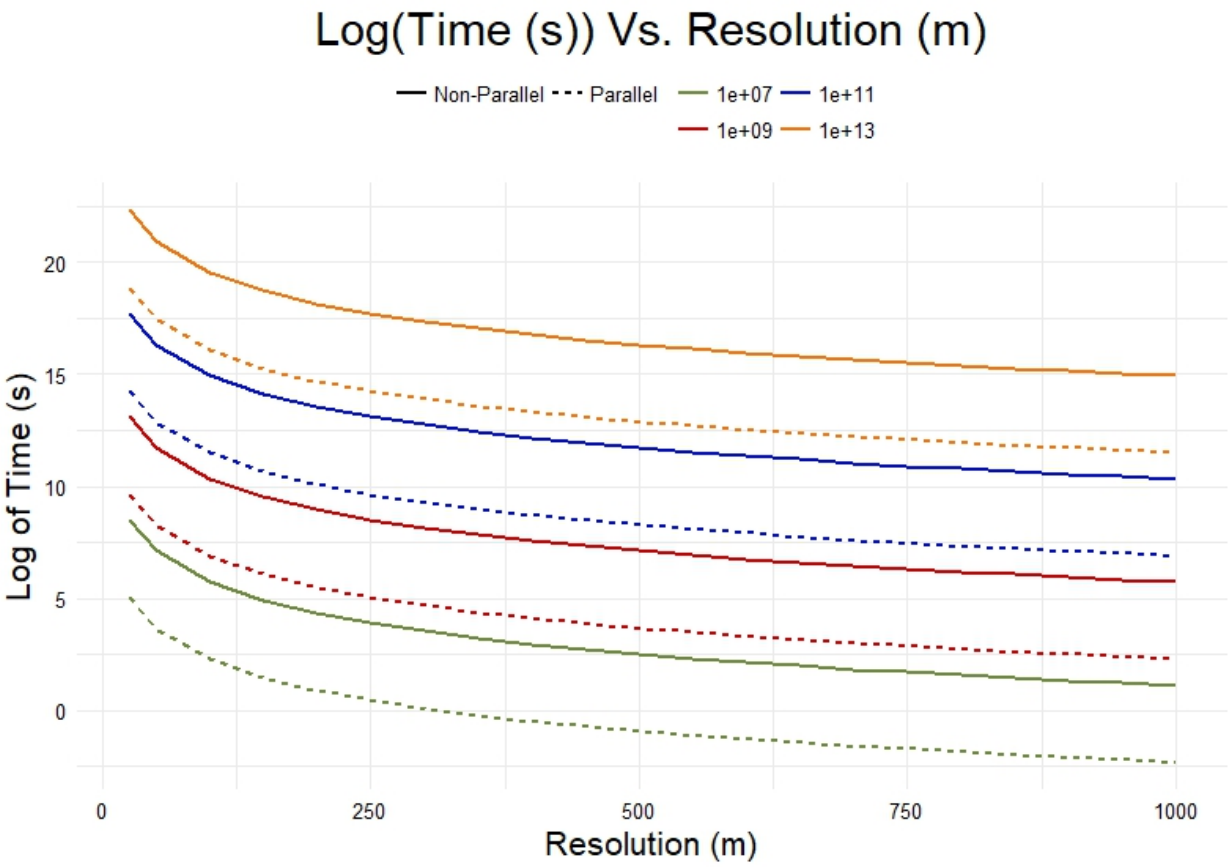

Figure 5: Relationship between the log of time and resolution with extent as factors. The parallel model was ran using 8 cores on the same system as the single core.

Conclusion

We have shown that utilizing the parallel processing can significantly decrease the computational time. This allows the user to choose a spatial extent two orders of magnitude larger or a significantly smaller resolution at the same spatial extent without increasing the computational time. Turner et al (1989) determined that increasing spatial resolution results in the loss of low frequency landcover types (ecoregions) and species especially in areas with low clustering or high heterogeneity. The use of smaller resolutions can greatly increase the understanding gained from processes occurring in highly heterogenous areas. Having shown that parallelization can lead to dramatically lower computational time future work should continue to utilize parallel computing and the opportunities it can provide.

CHAPTER 3: USING COUPLED DYNAMIC SPATIAL TEMPORAL EPIDEMIOLOGICAL MODELS FOR UNDERSTANDING LONG-TERM FOREST COMPOSITION CHANGES WITH ASYMMETRIC DISEASE HOST-COMPETENCY AND SUSCEPTIBILITY.

Introduction

Epidemiological disturbances, such as emerging pathogens and infectious disease outbreaks, are important agents of forest change around the world, causing tree mortality at scales ranging from individual trees of a single species to entire forest patches (Meentemeyer, Rank, et al. 2008; Welsh, Lewis, and Woods 2009). Beyond the complete loss of certain tree species, forest pathogens can significantly alter the functioning of forested ecosystems and the services they provide (Liebhold et al. 1995; Simberloff 2000; Vitousek et al. 1997). For example, pathogens can reduce the capacity of forests to sequester carbon, and can strongly interact with other types of disturbance such as fire, insects, and drought (Anderson et al. 2004; Dale et al. 2009; Elderd et al. 2013; Jactel et al. 2012; Vitousek et al. 1997). Coupled dynamic spatial temporal epidemiological models provide a predictive tool that can inform our understanding of how introduced forest pathogens alter forest ecosystem dynamics, which is crucial for land managers and decision makers (Cobb and Metz 2017; Rizzo, Garbelotto, and Hansen 2005).

One such emerging pathogen is *Phytophthora ramorum*, the causal agent of sudden oak death (SOD), which can infect over a hundred plant species (Rizzo, Garbelotto, and Hansen 2005; Davidson, Patterson, and Rizzo 2008). Disease symptoms are expressed in two forms: lethal infections on canker hosts and non-lethal foliar infections. The lethal form of the disease infects stems and branches of several ecologically important tree species, such as tanoak

(*Notholithocarpus densiflorus*), coast live oak (*Quercus agrifolia*), canyon live oak (*Q. chrysolepis)*, and California black oak (*Q.* kelloggii). These canker hosts are epidemiological dead ends with the exception of tanoak (Kovacs et al. 2011; Davidson et al. 2005). The foliar hosts can transmit the disease as leaves and twigs of these species produce inoculum. California bay laurel (*Umbellularia californica)* produces the most inoculum of all infected species and as such is considered the reservoir host with other foliar hosts considered alternative hosts (Figure 1) (Kelly and Meentemeyer 2002; Meentemeyer, Rank, et al. 2008; Václavík et al. 2010).

One of the key effects that has surfaced at plot level analyses is the effect of apparent competition giving California bay laurel an advantage over tanoak (Cobb, Meentemeyer, and Rizzo 2010). Apparent competition occurs when 2 or more species share a common enemy (*P. ramorum*) that has asymmetric effects on the host species (oaks, tanoak, and bay laurel). In order to capture this effect over time, a ratio of bay laurel to tanoak was created, this ratio should increase if either or both of the following are true: (1) bay laurel increases faster than tanoak and/or (2) tanoak decreases while bay laurel increases or stays the same. Understanding how this emerging infectious disease will change forest composition requires the use of a dynamic epidemiological model linked to a model that simulates forest growth and succession.

Forest landscape simulation models (FLSMs) have been developed to specifically address management and research questions at landscape scales ($>10^5$ ha) by projecting forest dynamics over space and time (Mladenoff 2004; Scheller and Mladenoff 2007). These models typically include details such as tree age, species and biomass, and are widely used to analyze the influence of disturbances over time as they affect large-scale forest ecosystem dynamics (Thompson et al. 2016; Scheller and Mladenoff 2004). One of several FLSMs, LANDIS-II stands out as a process-based forest landscape model that can include variable time steps for

different ecological processes (e.g. succession, disturbance, seed dispersal, forest management, carbon dynamics) and simulate their interactions as an emergent property of the independently simulated processes (Mladenoff 2005; Scheller and Mladenoff 2007; Mladenoff 2004). LANDIS-II continues to grow its user community and several extensions are available to simulate disturbances like wind, fire, insect spread, or land-use change. To date, the representation of forest pathogen and disease spread in FLSMs including LANDIS-II has been lacking.

Landscape epidemiological models frequently treat forest composition and host density as static (Cobb, Filipe, et al. 2012; Meentemeyer et al. 2011), meaning that the trees do not age or experience effects of disturbance. This makes it difficult to understand how disease alters competitive interactions among species, a process known as apparent competition, which can alter species composition at a landscape level (Cobb, Meentemeyer, and Rizzo 2010). Apparent competition can emerge when asymmetries in host susceptibility and tolerances to a pathogen drive changes in species composition (Power and Mitchell 2004; Cobb, Meentemeyer, and Rizzo 2010). Ignoring changes in host community composition limits the realism with which the interactions of other landscape-level disturbances with disease spread can be forecast through modeling (Cobb and Metz 2017).

Here I present the first case study of dynamic epidemiological modeling in a FLSM, utilizing LANDIS-II. The model couples the Net Ecosystem Carbon and Nitrogen (NECN) Succession extension to simulate forest succession and nutrient pools, with the new Epidemiological Disturbance Agent extension (EDA) for LANDIS-II to simulate disease spread. NECN will use a 10-year time-step and EDA will use a 1-year time-step (Figure 6). The model will simulate *P. ramorum* spread and forest succession from 1990 to 2090 in Big Sur, CA using

projected daily climate data. The EDA model accounts for asymmetries in both host susceptibility and competency and couples with the forest succession model to simulate forest composition changes across space and time. Utilizing models coupled in this way allows for examining changes in species composition due to apparent competition.

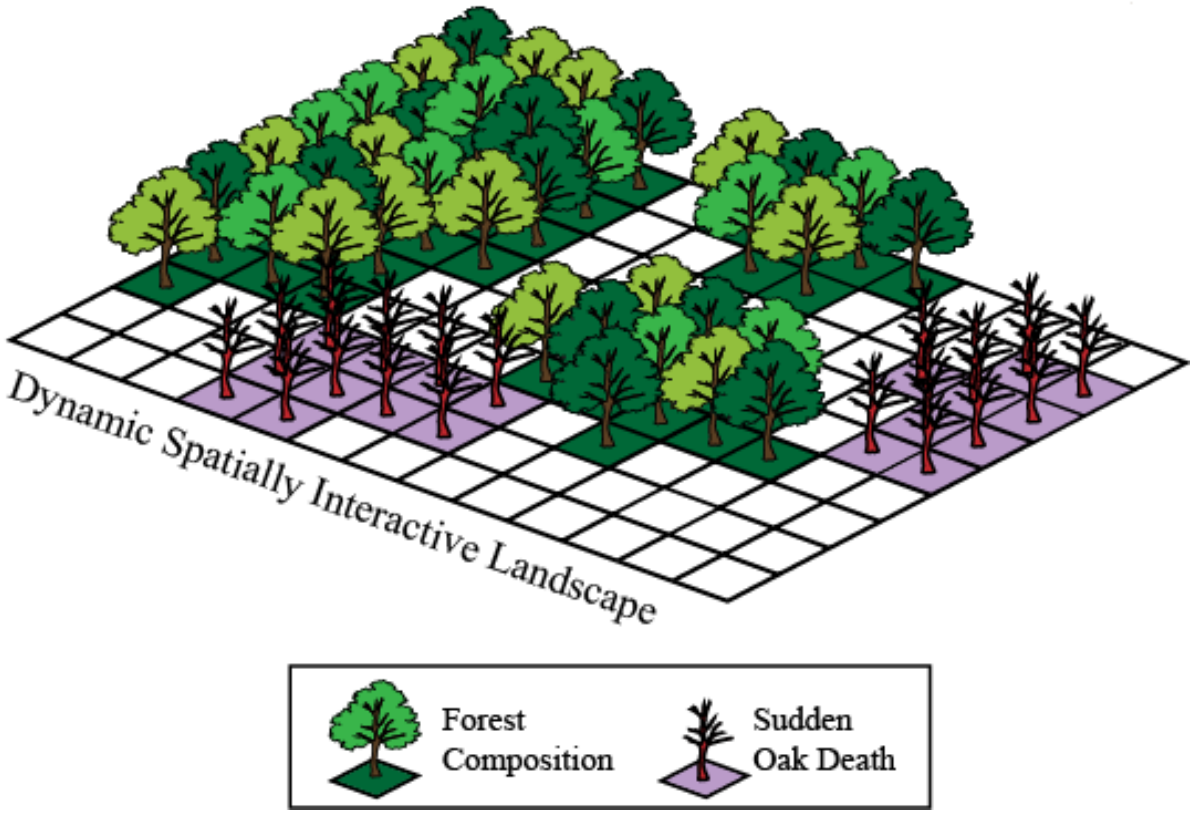

Figure 6: Spatial modeling framework showing disease and forest composition. These two components of the interactive landscape change over time and space and interact with each other within and across time-steps. Sites also interact with each other within a time step (i.e. seeds and inoculum can disperse across the landscape).

Methods

Study Area

This study focuses on the Big Sur region of central coastal California (Figure 7). Forests

in this area are frequently classified into two main categories, redwood and mixed evergreen. There are many other ecosystem types in this study area and species composition varies even within these two broad classes. The topography in the study area is steep with deeply dissected slopes and drainages, elevation ranges from sea level to 1571 m within 5 km of the coast (Henson 1996). In 2006/2007 a long-term monitoring network for *P. ramorum* was established (Metz et al. 2010; Beh et al. 2012). The network consists of 280, 12.5 m radius plots throughout a 79,356 hectares study area within the Big Sur, CA. The plots were randomly located across a range of ecological conditions stratified by elevation, latitude, fire history, and forest community type (mixed evergreen and redwood forests). Plots were also located in areas with and without pathogen presence. All trees ≥1 cm in diameter at breast height (dbh) and shrubs that reached an area ≥ 1 m^2 were measured and species information recorded. *P. Ramorum* symptoms are recorded for hosts that meet these requirements and tissue from symptomatic individuals is brought to the lab for pathogen isolation (Davidson et al. 2005). All plots had plot centers confirmed using survey-grade global positioning system receivers with a horizontal accuracy of 1 m or less after differential correction. A different subset of these plots were resampled in 2008, 2009, 2010, 2011, and 2013. These data will be used to supply LANDIS parameters and for validation.

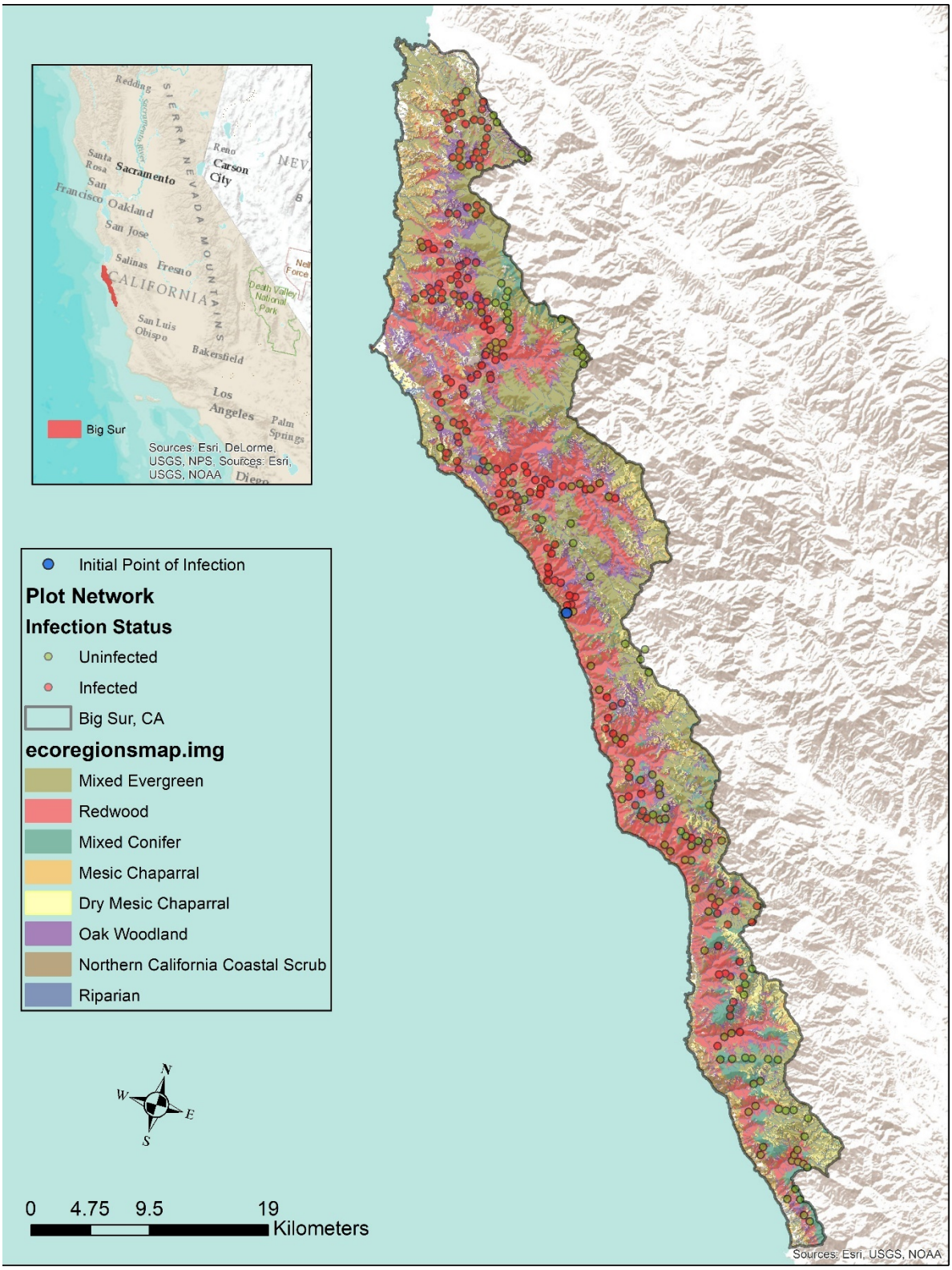

Figure 7: Big Sur Study area with disease status for all 280 plots, point of initial infection, and 8 ecoregions with greater than 1% area.

Modeling Framework

LANDIS-II is a process-based raster modeling framework consisting of a model core that links, parses, and validates data from multiple extensions (modules) and allows the user to "plug in" a forest succession extension and any number of optional disturbance extensions. Forests are represented as tree species-age cohorts (i.e. tanoak 100 for all tanoaks between 91-100 years) within raster cells across the landscape (Scheller et al. 2007). The NECN succession extension (version 4.1) and EDA extension (version 1.1) were utilized for this study.

Succession Extension

The NECN succession extension, originally developed as the Century Succession extension (Scheller et al. 2011), is a combination of the original LANDIS biomass extension and the CENTURY Soil Organic Matter model (Parton et al. 1983). It simulates cohort growth, mortality, and regeneration based on life-history and physiological attributes. Species compete for resources within a grid cell and spatially disperse across cells within the landscape. This allows for species range shifts and the effects of apparent competition due to disease to play out. Additionally, the model estimates above- and below-ground net primary production (NPP), net ecosystem exchange (NEE), multiple pools of live and dead tree biomass (including leaf, wood, fine root, course root, and course woody debris) and active, passive, and slow soil organic matter pools (Parton et al. 1983; Scheller et al. 2011). NECN incorporates a climate library that allows all extensions to utilize the same climate information. The climate data influences soil water content and nitrogen available for tree growth. Growth and competition are simulated based on limitation imposed by temperature, water, nitrogen, leaf area, and light availability instead of operating at a photosynthetic level (Scheller et al. 2011).

Dynamic Epidemiological Extension

Base EDA requires a raster map with location(s) of initial infection. As well as agent-specific parameters such as host transmissivity, host susceptibility, climate tolerances and preferences, mean transmission rate, acquisition rate, maximum dispersal distance, and the appropriate dispersal kernel and exponent (see Sections 2.1-2.3 below). The model can also incorporate parameters defining how other disturbances modify likelihood of infection.

Base EDA is specifically designed to simulate asymmetric weather-driven transmission of pathogen infection within a multi-host landscape. Transmission is modeled as a dynamic process, affecting a meta-population comprised of *N* contiguous subpopulations represented by cells (sites) arranged on a grid. Cells contain forest tree species age cohorts, and (optionally) non-forest vegetation types. Tree mortality simulated by EDA is passed to the succession model that in turn handles vegetation response to that mortality (e.g., changes in light, water, and/or nutrients, depending on the succession extension used). Epidemiological disturbances within the EDA are probabilistic at the site level, where each site is assigned a probability of being in one of the following states: Susceptible (S), Infected (infectious non-symptomatic) (I), Diseased (infectious and symptomatic) (D) (Figure 8).

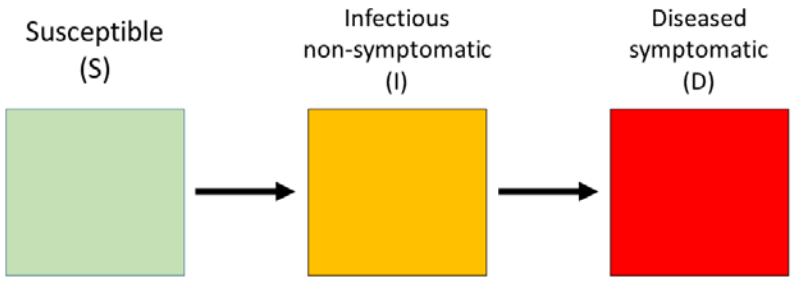

Figure 8: Compartmental structure of the epidemiological model used by the LANDIS-II Base Epidemiological Disturbance Agent (EDA) extension.

Probabilities are compared with a uniform random number to determine whether the site becomes infected or, if already infected, to become diseased. Disease causes species- and cohort-specific mortality in the cell. The epidemiological model is similar to that in Meentemeyer et al. (2011) with adjustments made to fit the LANDIS-II framework and account for mortality. Additionally, the model can handle more than one EDA agent (pathogen), especially those with aerial dispersal.

Site Host Index

Site host index (SHI) was adapted from the "site resource dominance" concept in the LANDIS-II Biological Disturbance Agent Extension (Sturtevant et al. 2004). SHI accounts for the spatial distribution of known hosts of the EDA agent and is a combined function of tree-species composition and the age cohorts present on that site. This approach allows the quantification of susceptibility for each non-infected cell to become infected, and the suitability of each infected cell to produce infectious spores. The relative host index value of a given species cohort is defined by its host competency class, where low, medium, and high competency classes are user-defined values ranging between 1 and 10, with non-hosts having a value of 0. The EDA extension compares a look-up table with the species cohort list at each cell generated by LANDIS-II to calculate SHI at time *t* using one of two methods: 1) the host value from the maximum host competency class present, or 2) an average host value of all tree species present, where the host value of each species is represented by the one assigned to the oldest cohort. Species identified as "ignored" do not contribute to the calculation of average resource value, while non-host species that are not ignored contribute a value of 0. Non-sporulating hosts

(i.e. hosts that do not contribute to pathogen or disease transmission) are not included in the host index calculation.

Site host index modifiers

Site host index modifiers (SHIMs) are optional parameters used to adjust SHI to reflect variation introduced by both site environment (i.e., landtype (ecoregion)) and recent disturbances (Sturtevant et al. 2004). Land type modifiers (LTMs) and disturbance modifiers (DMs) can range between -1 and +1, and are added to the SHI value of all affected sites where host species are present (SHI > 0). LTMs are assumed to be constant for the entire simulation, while DMs have a defined duration and decline linearly with the time since last disturbance (t_{DST}) as follows:

$$DM_{DST}(t) = DM_{max,DST} * \frac{DM_{duration,DST} - t_{DST}}{DM_{duration,DST}} \quad \text{(Equation 1)}$$

Disturbances that may affect a given EDA agent include fire, wind, other EDA agents and insects, as well as timber harvest. SHI is then modified by LTM and the sum of all DMs:

$$SHIM(t) = SHI(t) + LTM + (DM_{wind}(t) + DM_{fire}(t) + \cdots) \quad \text{(Equation 2)}$$

The user should calibrate the two modifiers to reflect the relative influence of species composition/age structure, the abiotic environment, and recent disturbance on SHI. SHIM is normalized by its mean over the entire study area, $SHIM(t) = \frac{SHIM(t)}{SHIM_{mean}}$, and modifies the disease transmission rate, β (see Section 2.2). Normalization of SHI allows comparison of β to homogeneous landscape conditions (where SHIM = 1) and to interpret β as the rate of secondary infection of cells by a single infected neighboring cell in an otherwise uninfected landscape.

Weather

An *annual weather index*, $w(t)$, is used to account for the effect of weather conditions on the probability of uninfected hosts becoming infected, and infected hosts sporulating and spreading an individual EDA agent. Weather predictors (or transformations thereof) should be selected based on their relevance to the chosen EDA agent. The weather index is multiplied by a baseline transmission rate, β_0, to produce a time-dependent transmission rate, $\beta(t) = w(t)\beta_0$, where β_0 is defined by the user. The basic weather index for year *t*, $W(t)$, comprises the cumulative effects of *N* weather predictors (e.g. rainfall alone, or rainfall and temperature) over a range of months, specified by the user (e.g. April to June), and is calculated as follows:

$$W(t) = \sum_{d \in [month_A(t),\ldots,month_B(t)]} X_1 * X_2 * \ldots * X_N \quad \text{(Equation 3)}$$

where $X_1 * X_2 * \ldots * X_N$ represent the weather predictors and the cumulative-sum runs over days *d* included between two user-defined months ($month_A$ and $month_B$) for the current year *t*. If necessary, weather predictors in (1) can be replaced by derived (e.g., aggregated, or transformed) versions. As an example, a predictor can be aggregated (summed or averaged) over *N* consecutive days of a week or month (e.g., cumulative precipitation). Transformed predictors are expressed by a function, (X). In the current version of the extension (v1.0), only a polynomial transformation is available, defined as:

$$f(X) = A + B + exp(C * \left[\ln\left(\frac{X}{D}\right)/E\right]^F) \quad \text{(Equation 4)}$$

where A, B, C, D, E, F are constants specified by the user to adjust the shape of the polynomial (e.g., improving polynomial fit to empirical data on response of EDA agent to changes in temperature). As an example, such a transformation can reflect changes in rate of pathogen sporulation at increasing temperature values. The actual weather index, $w(t)$, is normalized by the mean W_{mean} over the available time series of historical weather predictors: $w(t) =$

$W(t)/W_{mean}$. Normalization means that β_0 can be interpreted as the annual transmission rate under average (or under constant) weather conditions. The weather index built this way varies annually, but is spatially uniform within each ecoregion.

Epidemiological Processes

The epidemiological model shares features with spatially-structured metapopulation models and relies on a few important assumptions: First, only the presence/absence of infection in each cell is accounted for. This simplification ignores a transient effect (occurrence, spread and intensification) within the same cell, assuming that an effective level of inoculum is reached rapidly (but still below the maximum sporulating capacity of the cell). Improving this approximation would require a much larger computational effort in the parameter estimation procedure described in Filipe et al. (2012). Second, infected cells immediately become infectious, which is particularly true for an EDA with a small latent period across its host range. Third, infected sites remain infectious for an undetermined (i.e., long) period; hence no species can recover from infection throughout the simulation. However, if a cohort is killed by fire and resprouts, it is no longer infected.

At every time step *t*, a susceptible cell (site) *i* can become *cryptically infected* subject to a force of infection $\Lambda_i(t)$ and, once infected, it can become diseased at rate r_D. Despite potentially containing dead hosts, *symptomatically infected* (diseased) cells have the same transmission rate, i.e., are as infectious as cryptically infected cells. The probabilities that cell *i* is in each of the possible states (Susceptible, Infected, Diseased), $P_{i,S}$, $P_{i,I}$, and $P_{i,D}$, respectively, are governed by a system of differential equations:

$$\frac{\Delta P_{i,S}}{\Delta t} = -\Lambda_i(t)P_{i,S} \quad \text{(Equation 5)}$$

$$\frac{\Delta P_{i,I}}{\Delta t} = \Lambda_i(t)P_{i,S} - r_D P_{i,I} \quad \text{(Equation 6)}$$

$$\frac{\Delta P_{i,D}}{\Delta t} = r_D P_{i,I} \quad \text{(Equation 7)}$$

The initial conditions for each cell, at the estimated time of onset of the outbreak, are $P_{i,S} = 1$, $P_{i,I} = 0$, $P_{i,D} = 0$, except at the cell estimated to be the location of the first infection, where $P_{i,S} = 0$, $P_{i,I} = 1$, $P_{i,D} = 0$. The force of infection, $\Lambda_i(t)$, is given by:

$$\Lambda_i(t) = \beta(t) \sum_{j \neq i} SHIM_j(t) * SHIM_i(t) * P_{j,I+D|i,S} * K(d_{ij}) \quad \text{(Equation 8)}$$

where $\beta(t) = w(t)\beta_0$ is the transmission rate, with $w(t)$ the annual index of weather fluctuation about a *N*-year average (see Section 2.2) and β_0 the baseline rate; $K(d_{ij})$ is a dispersal kernel (see Section 2.3.1) for a given distance *d* between target and source cells; $P_{j,I+D|i,S}$ is the conditional probability that source cell *j* is infectious (either cryptic or symptomatic infection) given that target cell *i* is susceptible. To achieve a first order of approximation, we assume that $P_{j,I+D|i,S} \approx P_{j,I} + P_{j,D}$ which we expect to be a reasonable approximation to the infection pattern, especially when dispersal is not too localized (e.g. within short distance from source of infection).

Dispersal kernel

The dispersal kernel used in Base EDA is derived from, and shares code with, the seed dispersal kernel developed by Lichti and colleagues (N. Lichti, Purdue University, unpublished manuscript). This dispersal function and associated distributions are especially suitable for aerially dispersed EDA agents including a range of fungi, bacteria, and mistletoes. The probability that the agent disperses a distance *d* from the source was expressed by two main functional forms, often used in the literature: a power-law and a negative exponential. Their generic form can be defined as follows:

$$K_{PowerLaw}(d) = d^{-\alpha} \quad \text{(Equation 9)}$$

$$K_{NegExp}(d) = e^{-d/\alpha} \quad \text{(Equation 10)}$$

An EDA agent produced in a source cell can only be deposited in a cell different from the source, i.e., transmission in force of infection (Λ, see Section 2.3 above) is conditional on the agent being dispersed outside the source cell. The rationale for this choice is that infection processes within a cell are not tracked (no transient effect). In addition, the kernel must integrate to 1 within a chosen 2D spatial neighborhood window (excluding the source cell). The 2D window accounts for all possible pathways through which the target cell can become infected by a given source cell. A user-defined maximum radial distance is used to limit EDA agent dispersal within a chosen neighborhood size. For cases where only local, short-distance dispersal events are considered, this parameter becomes essential to reduce computational burden. Only isotropic dispersal (no wind-assisted directional spread) was considered for version 1.0 of the Base EDA extension.

Tree species cohort mortality

Within each diseased cell, the mortality of individual tree species age cohorts is a probabilistic function of the mortality probability of the cohort's vulnerability class. The user defines which species and ages fall into each vulnerability class (low-high), and the probability of cohort mortality for each class. Probabilities are compared with a uniform random number to determine whether an entire age-cohort dies (i.e. is removed) or not, where tree species cohort mortality is then passed to the succession extension which handles the removal of the cohort(s) and updates the cohort list. We acknowledge that complete cohort removal rather than a partial one may be a simplistic assumption in the current version of the model, but for many landscape-

level processes or dynamics it should not cause significant changes in outcome. The Base EDA time step concludes updating the time since last disturbance, outputting maps of cell states (1 = Susceptible, 2 = Infected, 3 = Diseased) and cohort mortality, and by updating the Base EDA log file (Figure 9).

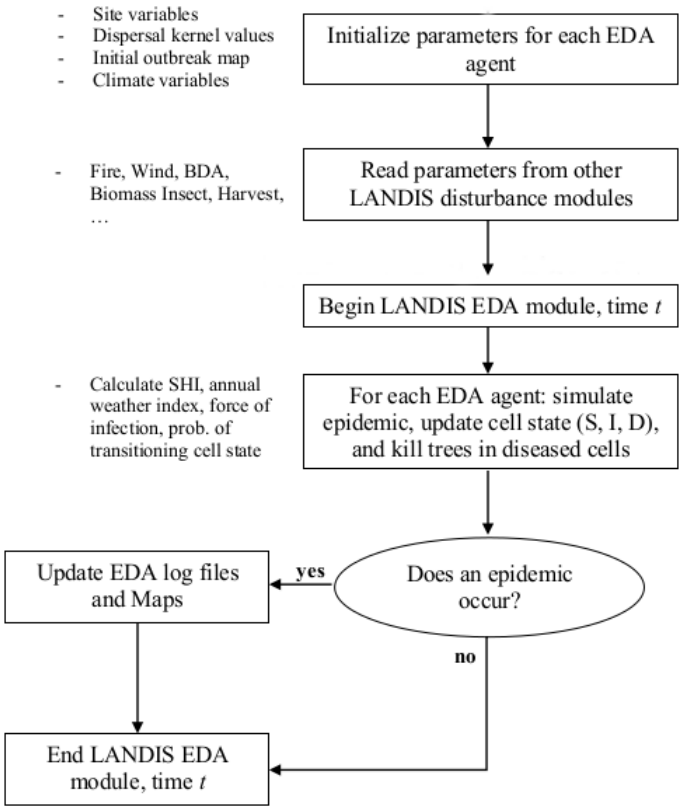

Figure 9: Flow diagram illustrating the main logical structure of the LANDIS-II Base Epidemiological Disturbance Agent (EDA) extension.

Model Inputs

LANDIS-II model inputs include initial vegetation data, ecoregion data, species and functional group trait data, epidemiological data, and climate data (Table 2). See Appendix 1 for all tables with NECN and EDA extension parameters.

Table 2: Data and Sources.

Parameter Groups	Source	Data
Species Specific	Silvics Manual, Literature, LEMMA GNN	Seed dispersal; fire regeneration; resprout probability; resprout age limits; shade, fire, and drought tolerance; sexual maturity; longevity; min temp; GDD min and max; leaf, wood, and root lignin and C/N ratios.
Functional Groups	Silvics Manual and previous Century models	Mortality shape curves; max LAI; growth parameters; leaf drop month; and fraction of carbon in fine and course roots.
Ecoregion Types	LandFire Biophysical Regions	Groups regions with similar climate, topography, and soil
Ecoregion Parameters	SSURGO, NADP	Soil depth; percent clay; percent sand; field capacity; wilting point; drainage; nitrogen
Climate (Daily)	CA-BCM 2014	Precipitation, TMIN, TMAX, Wind

Acronyms: LEMMA = Landscape Ecology, Modeling, Mapping & Analysis, GNN = Gradient Nearest Neighbor, GDD = growing degree days, C/N = Carbon/Nitrogen, LAI = Leaf Area Index, SSURGO = Soil Survey Geographic Database, NADP = National Atmospheric Deposition Program, CA-BCM 2014 = California Basin Characterization Model Downscaled Climate and Hydrology.

Vegetation Data

Initialization of the current vegetation on the simulated landscape, used the gradient nearest neighbor (GNN) map for the California Southern Coastal Range (map region 233) produced by the Landscape Ecology, Modeling, Mapping and Analysis (LEMMA) group for the Northwest Forest Plan Effectiveness Monitoring (Ohmann et al. 2011; Ohmann and Gregory 2002). The GNN method imputes forest inventory plot data to every pixel in the map, characterizing tree species composition, age structure, biomass, and other variables. The inventory plots come from various sources, with the predominant ones being the US Forest Service Forest Inventory and Analysis (FIA) and Current Vegetation Survey (CVS) programs

(Ohmann et al. 2011). Age information for each individual tree within the imputed forest inventory plots was obtained from the supplemental TREE_LIVE database provided by the LEMMA group. These data were used to classify species-age cohorts at 10-year intervals for each plot. Age cohorts range from 10 to the maximum age of the species.

Ecoregions

LANDIS-II uses ecoregions to divide the study area into regions that have homogeneous soils and climate. I use LANDFIRE Biophysical Settings for the California Southern Coastal Range (map region 4) to define the ecoregions. LANDFIRE Biophysical Settings are classified based on topography, soil, and climate data and were developed by the LANDFIRE group of the Nature Conservancy to describe vegetation states prior to Euro-American settlement (names represent this purpose) (Rollins 2009). There are 17 ecoregions in the study area (Table 3). Ecoregion parameters include soil properties such as percent clay and sand, SOC decomposition rates, drainage class, and pools of nitrogen and carbon. SSURGO National Soil Survey for Monterey County, California ("Web Soil Survey" 2014) data was spatially averaged to a depth of 1 m across the ecoregions to obtain the necessary data at the ecoregion level. Percent clay and sand, field capacity, and drainage class were calculated directly from the SSURGO data, while wilting point was calculated as field capacity minus available water content. Soil organic carbon and nitrogen pools were calculated using browns-transect data collected across the 280 plots in the Big Sur plot network (Cobb and Metz 2017; Cobb, Chan, et al. 2012). Nitrogen inputs were assumed to come from wet and dry deposition, biological fixation, soil, and decaying logs (Zhang et al. 2012; Fenn et al. 2003). Wet and dry deposition were calculated from National Atmospheric Deposition Program (NADP) data across the study system (NADP Program Office 2017).

Table 3: Ecoregions with percentage of total study area.

Ecoregion	**Area (%)**
Water	0.1%
Barren	0.2%
Mixed Evergreen Woodland	31.7%
Coastal Redwood Forest	26.7%
Mixed Conifer Forest	5.0%
Black Oak Conifer Forest	0.1%
Southern California Coastal Scrub	0.7%
California Maritime Chaparral	0.7%
California Mesic Chaparral	4.3%
Woodland Savanna	0.9%
Dry Mesic Chaparral	5.0%
Coastal Live Oak Woodland	11.5%
Northern California Coastal Scrub	4.6%
Southern Coastal Grassland	1.1%
Northern Coastal Grassland	0.8%
Riparian	6.3%
Closed Cone Conifer Forest	0.2%

Species and Functional Group Parameters

I simulated 27 tree species based on the data from LEMMA GNN: bristlecone fir, grand fir, bigleaf maple, California buckeye, white alder, red alder, pacific madrone, tanoak, knobcone

pine, Coulter pine, sugar pine, singleleaf pinyon, ponderosa pine, Monterey pine, gray pine, California sycamore, balsam poplar, big-cone Douglas fir, Douglas fir, California live oak, canyon live oak, blue oak, Oregon white oak, California white oak, interior live oak, redwood, and California bay laurel. These 27 species were grouped into 5 functional groups: Redwood, Evergreen-Conifer, Deciduous Conifer, Evergreen Broadleaf, and Deciduous Broadleaf. See Appendix 1 for data tables containing species and functional group parameters.

Epidemiological Data

The model was initialized at the estimated true location of initial infection based on knowledge of invasion history in central coastal California (Rizzo, Garbelotto, and Hansen 2005; Mascheretti et al. 2008; Meentemeyer et al. 2011). Data on host species vulnerability were based on species mortality within both the Big Sur plot network as well as Sonoma County plot data. Host Index is the measure of the host ability to produce inoculum and to become infected (Davidson et al. 2005; Davidson, Patterson, and Rizzo 2008) and is derived from information from the plot network (Meentemeyer et al. 2011). The dispersal kernel utilizes the power law distribution in order to account for long-distance dispersal events such as accidental human assisted dispersal. The effect of precipitation is simulated by summing the previous 5 days and temperature effects are simulated using a polynomial transformation of daily temperature using parameters in Table 4.

Table 4: Shape parameters for fitting temperature effects on *P. ramorum* inoculum production using equation 4. These parameters are derived using methods in Meentemeyer et. al. (2011).

Variable	Temp
a	108.6
b	904.8
c	-0.5
d	15.87
e	0.2422
f	2

Climate Data

The NECN Succession extension requires monthly temperature and precipitation data for model spin-up and future projections. The EDA extension, however, requires daily data. We modified the climate library to take daily data and apply the proper temporal scaling for each extension and are able to supply daily data to the model while still having the ability to provide monthly data to the NECN succession extension. Climate data was obtained from the US Geological Survey GeoData Portal (https://cide.usgs.gov/gdp/) as an area weighted average for each ecoregion. Climate data is from the Western US Hydroclimate Scenarios Project Observations and Statistically Downscaled Data at 1/16th degree resolution (Hamlet, Salathé, and Carrasco 2010). This method uses the Modified Delta approach (Littell et al. 2011), based on 10 models from Phase 3 of the Coupled Model Intercomparison Project to create daily temperature and precipitation values for historical and future climate (1950-2099) (Figures 10-12). The model only uses the 10 best performing GCMs for a given area in this case the California Basin.

Data from 1950 to 1990 was used for model spin-up, while 1990 to 2090 data was used for model projections. Simulating from 1990 to 2090 was necessary to be able to recreate the disease dynamics during the early stage of infection.

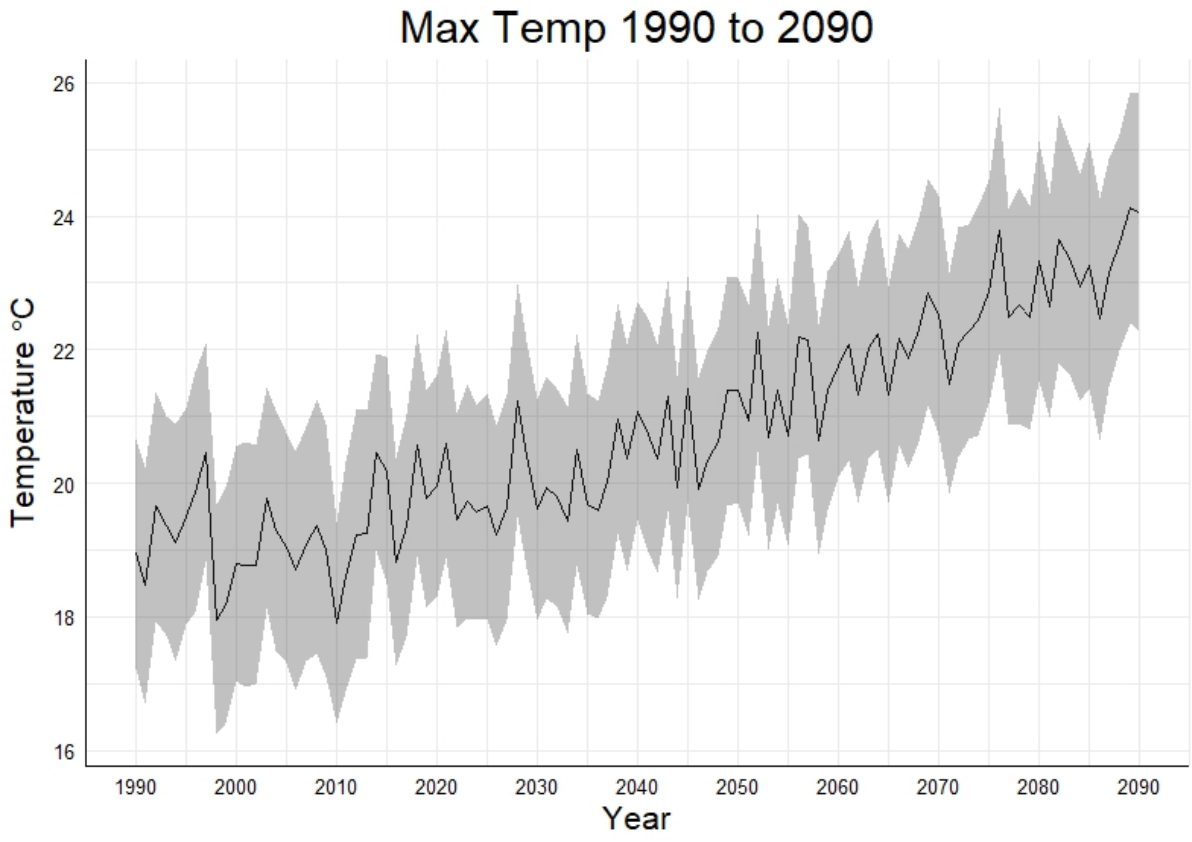

Figure 10: Average maximum temperature of the 10 GCMs from 1990 to 2090 with shaded grey region representing one standard deviation.

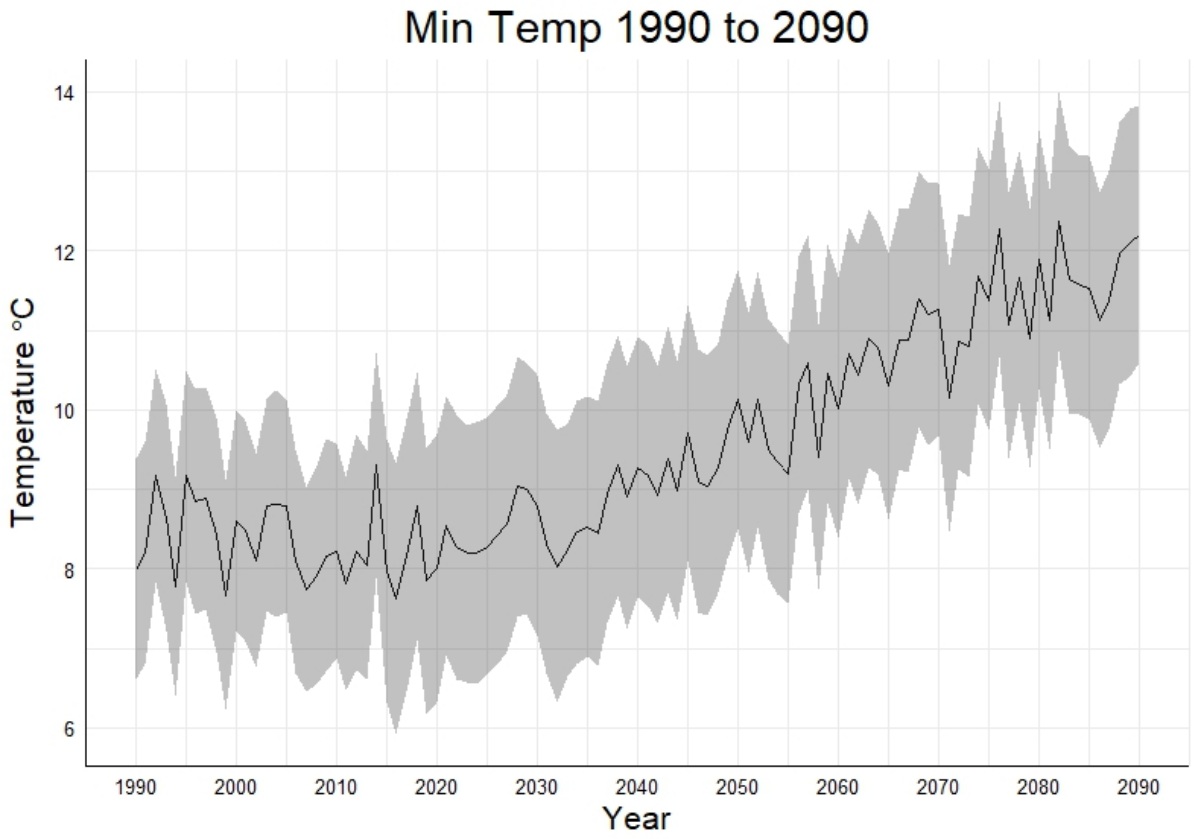

Figure 11: Average minimum temperature from the 10 GCMs from 1990 to 2090 in °C with shaded grey region representing one standard deviation.

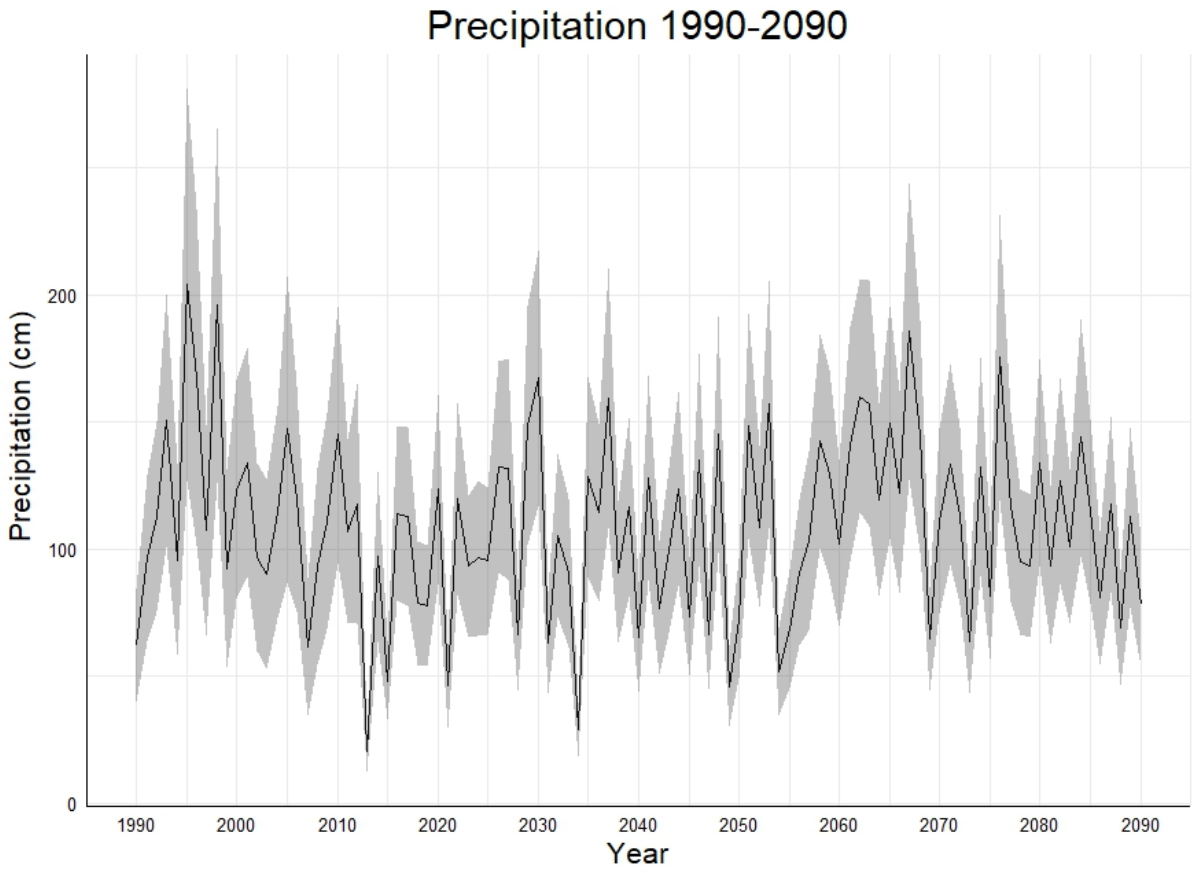

Figure 12: Average annual precipitation from the 10 GCMs from 1990 to 2090 with shaded grey region representing one standard deviation.

Model Calibration

The NECN succession was calibrated using literature review and data for central coastal California. Expected patterns of growth, NEE, carbon accumulation, and stand age were determined from literature review (Henson 1996; D. P. Turner et al. 1995; Vogt 1991; Waring 1983; Noss 1999; Johnson, Shifley, and Rogers 2009; Callaway and D'Antonio 1991; Battles et al. 2008; Pelt and Franklin 2000; Smith, Rizzo, and North 2005; Waring and Running 2010). Calibration of the NECN Succession extension begins with single-cell simulations, adjusting parameters (e.g. temperature response and moisture sensitivity shape parameters) to match patterns of growth and NEE in literature (Ewing et al. 2009; G. Turner 2008; D. P. Turner et al.

1995; Waring and Running 2010). The other parameters (e.g. soil organic carbon decay rates and shade tolerance) were calibrated across the entire Big Sir to ensure that starting conditions matched input data and landscape-scale processes were simulated correctly. Biomass estimates from the LEMMA GNN maps were created using the component ratio method (CRM) (Heath et al. 2009). The CRM computes aboveground biomass as the sum of three components: bole of the tree, stump of the tree, and the top of the tree. The biomass of the tree bole is calculated using regional volume equations, while the biomass of additional tree components is calculated using a series of ratios established by Jenkins et. al. (2003). The GNN biomass estimates were used to calibrate the initial aboveground biomass estimates of model spin-up (Figure 13). Final calibration was based on: (1) initial aboveground carbon was within 10% of GNN estimates across all ecoregions (Figure 13), (2) projected aboveground NPP and carbon matched trends in literature based on stand age, and (3) soil organic carbon accumulated 5-20% in all pools over the 100-year simulation.

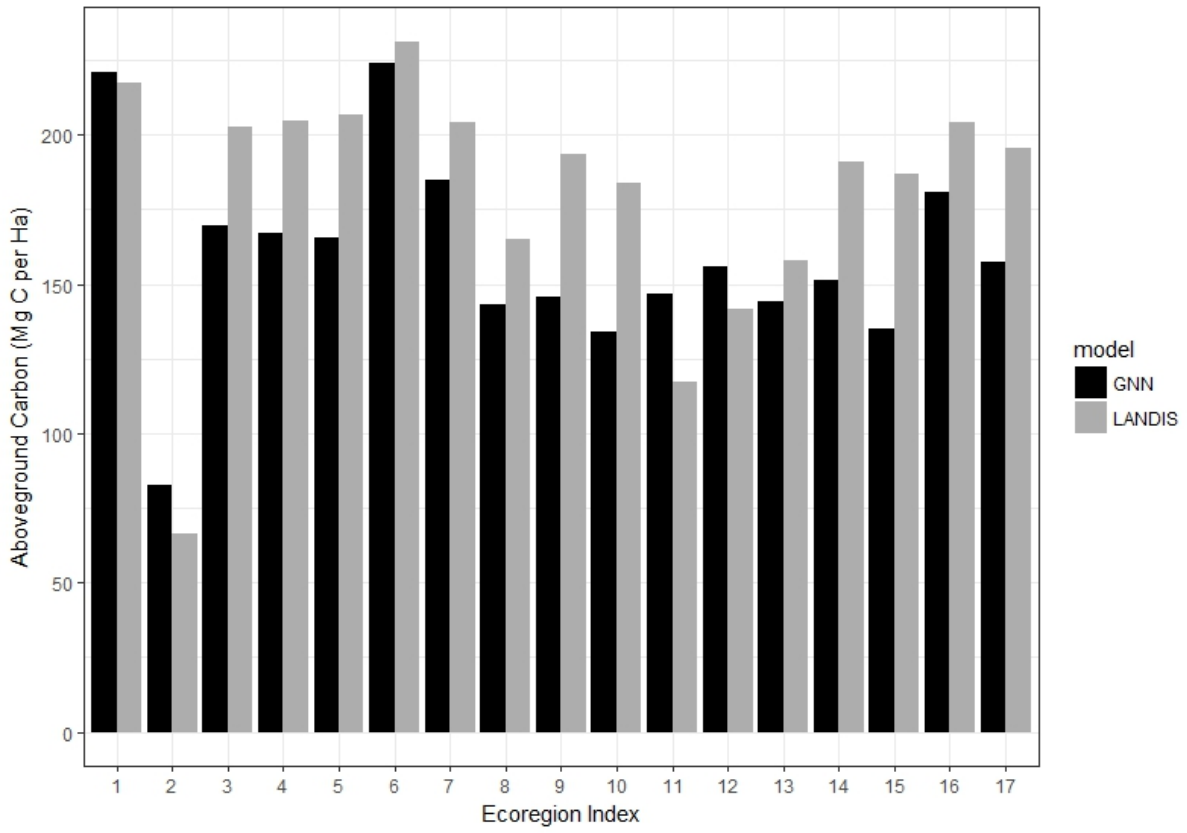

Figure 13: Aboveground carbon estimates for ecoregions in the Big Sur, CA from GNN imputation and LANDIS-II at the beginning of the simulation (year 1990).

Simulation Model Runs

The model simulated from 1990-2090 using 10-year time steps for NECN and a 1-year time step for EDA. The model was replicated 30 times using different random seeds for each simulation in order to account for stochastic variability in climate, disease spread, and seedling establishment. Model results were aggregated to the entire study region to look at the effect of disease across the entire landscape (i.e. large-scale impacts). Results were also aggregated to the ecoregion level to determine if the results at the landscape level are universal across the study system or vary based on biophysical attributes.

Results

EDA Model Accuracy

We compared the disease spread results from the model to plot-level data using two methods: (1) aggregating all plot-level data to 2013 using the disease status of the most recent sampling year (i.e. if plot was last sampled in 2009 that information was used for that plot) (full method) and (2) comparing individual plot sampling results with the model results for that sample year (yearly method) (plots were sampled in 2006, 2007, 2008, 2009, 2010, 2011, and 2013). The first method had 280 plots sampled while the second method ended up with 428 total comparisons (only a portion of the plots were sampled during a sample year and some plots are sampled during more than one year). Method 1 had a lower overall accuracy, higher average true positive rate, and a much lower average true negative rate. Method 2 clearly performed better which was to be expected as it compares the results during the year sampled to model results during the same year. The aggregate method had higher average positive results due to many false negatives associated with the fact that if the plot was last sampled in 2009 then showing results for 2013 may not be indicative of actual disease status in the plot. Total model accuracy using the yearly method was 73.02 (Figure 14). The average odds ratio for the 30 simulations was 7.90 ± 3.21 using the yearly method.

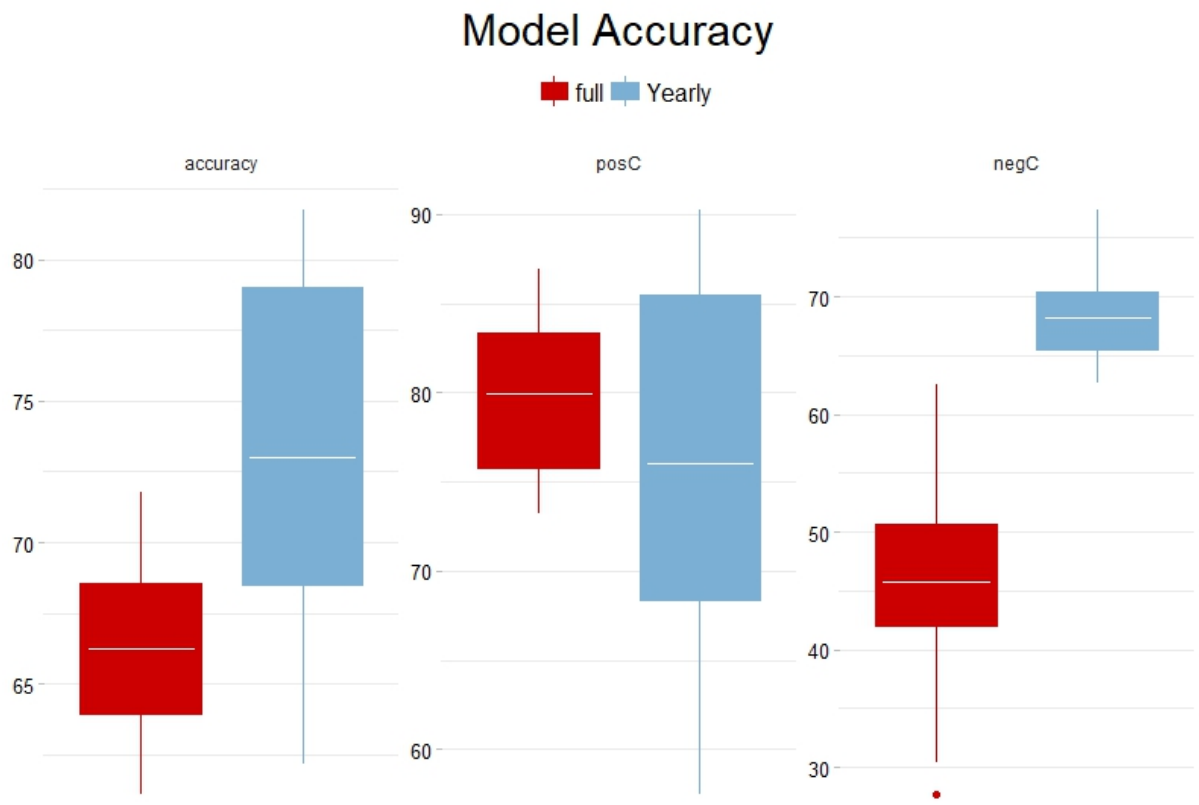

Figure 14: Boxplots of model accuracy comparison using the 2 methods full (all comparisons at year 2013) and Yearly (model results compared to plot data for every sampling year). Accuracy = total model accuracy for both positive and negative disease status, posC = True positive identification (i.e. both plot and model results showed disease present), and negC = True negative identification (i.e. both plot and model results showed no disease)

Impacts of Disease on Forest Composition

When aggregated to the landscape level (entire study area) the impact of disease on the forest composition, as measured using the bay/tanoak ratio, stayed roughly constant from 1990 (0.680) to 2000 (0.684) (Figure 15). From 2000 to 2020 the bay/tanoak ratio more than doubled (0.684 to 1.319) and continues to increase at a more modest rate through 2090 (1.835). This effect of disease on bay/tanoak ratio exhibited notable differences between ecoregions (Figure 16). The higher the relative abundance of bay laurel compared to tanoak initially, the greater and more rapid the increase in the bay/tanoak ratio over time (Figure 16).

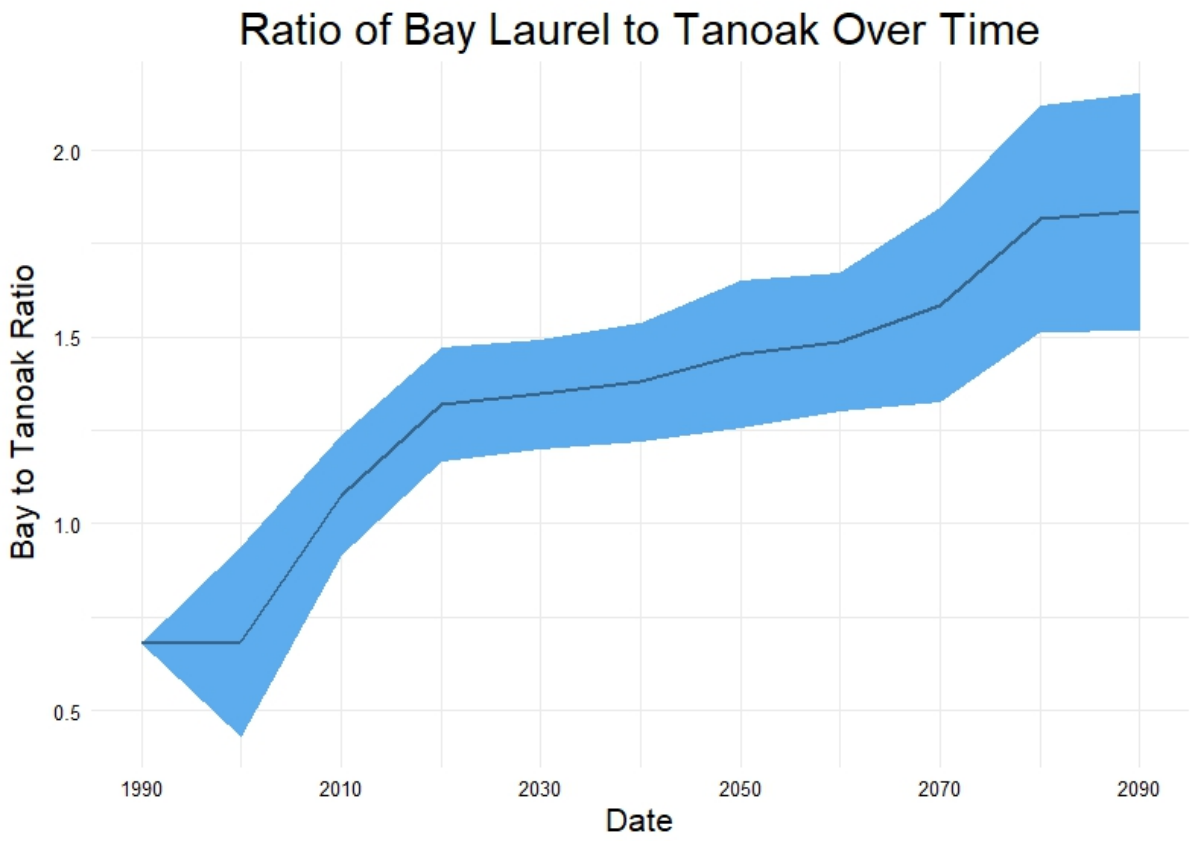

Figure 15: Ratio of Bay Laurel to Tanoak over time with shaded region representing one standard deviation and the dark blue line representing the average from the 30 simulations

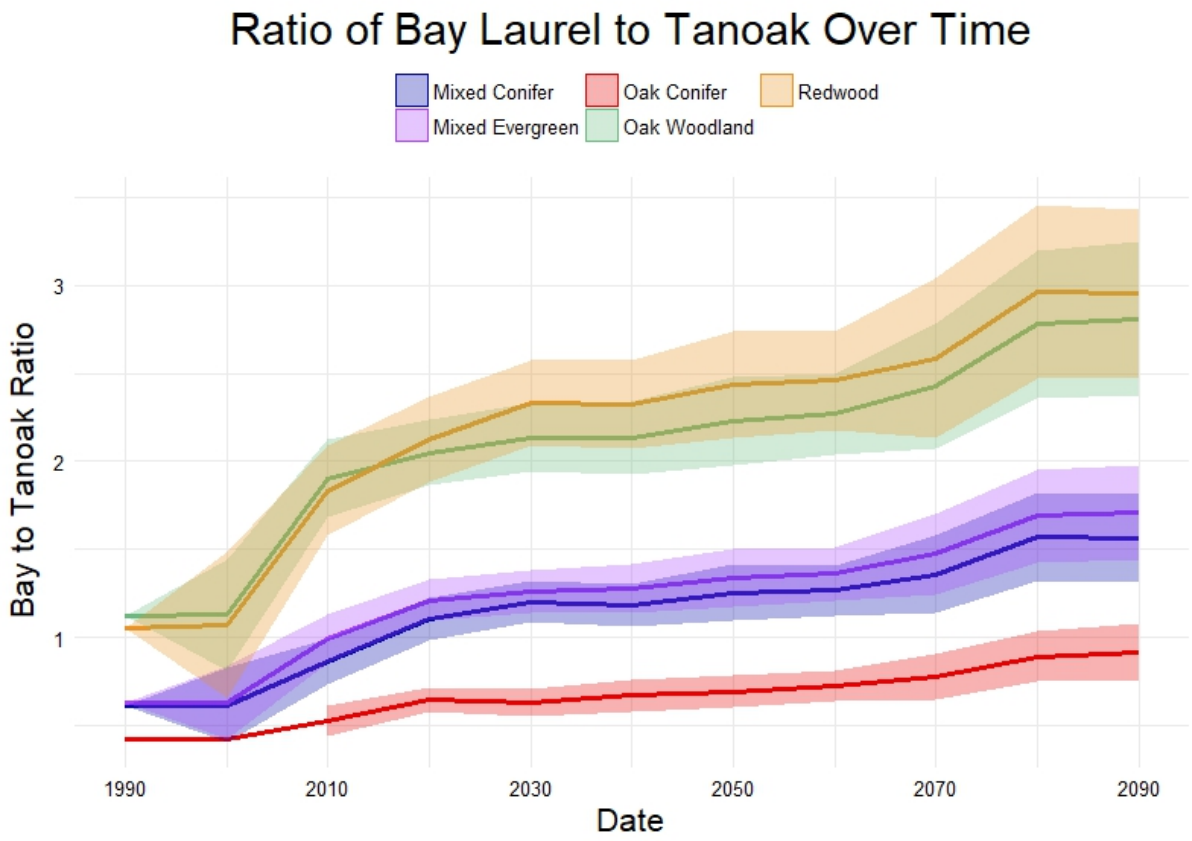

Figure 16: Average ratio of bay laurel to tanoak over time by ecoregion. Solid line indicates the average and the shaded region represents the standard deviation.

Discussion and Conclusions

The dynamic epidemiological model developed to work with LANDIS-II and calibrated for *P. ramorum* spread had an overall accuracy of 73% and odds ratio of 7.90 ± 3.21. These results are especially promising given the patchy nature of disease and the highly heterogeneous terrain and forest composition in the Big Sur. Also, the results are comparable to accuracy results (odds ratio = 7.6) from Meentemeyer et al (2011) in the central western ecoregion, the region in their study where the Big Sur is located. The model presented here achieves several advances compared to other forest epidemiological models: (1) separates host competency from host

susceptibility, (2) includes disease related mortality, (3) includes link to model of species composition due to forest growth, succession, and regeneration, (4) includes asymmetries in host competency and susceptibility by species and age classes. Separating host competency from host susceptibility allow us to more accurately capture disease dynamics. For instance, oaks play no role in the spread of *P. ramorum* (no competency) but experience disease related decline and mortality (medium susceptibility). Tanoak produces moderate levels of inoculum (medium competency) and experiences disease related decline and mortality (high susceptibility). Bay laurel produces the most inoculum (high competency) but experiences no disease related decline (no susceptibility). Previous models (Meentemeyer et al. 2011) have included asymmetries in host competency by species but not by age class. This distinction allows for increased inoculum production as trees age, grow, and have more leaf area for spore production. Despite these advances the model could be improved by: (1) allowing disease build up in a site over time, (2) include an option for anisotropic (wind or topography driven) spread (3) include an option for inoculum production based on leaf biomass within a site rather than by age class. Future work will seek to incorporate these and other improvements into EDA to more accurately capture disease dynamics. By incorporating this dynamic epidemiological model into a forest landscape simulation, we are able to not only track disease spread but also disease effects on forest composition.

Generalist pathogens often have asymmetries in host susceptibility and/or competency that can lead to changes in species composition. This asymmetric impact on host species by a generalist pathogen is known as apparent competition. Apparent competition has been shown in experimentally controlled field studies using barley yellow dwarf virus where the presence of *Avena fatua*, a highly susceptible reservoir species, decreased the abundance of two other host

species (Power and Mitchell 2004). Empirical observational data has suggested apparent competition in *P. ramorum* infected redwood forests (Cobb, Meentemeyer, and Rizzo 2010; Cobb, Filipe, et al. 2012). The model suggests an increase in bay laurel relative to tanoak across the entire study area. This is true across all ecoregions but the rate and magnitude of change varies greatly between ecoregions. The ecoregions with the greatest increase in the ratio of bay laurel to tanoak are the ones with the greatest initial ratio of bay laurel to tanoak (i.e. redwood). In redwood systems in the Big Sur the three-primary species are bay laurel, tanoak, and redwood. The model results suggest that apparent competition mediated through asymmetric host susceptibility and competency lead to changes in species composition within the landscape, with bay laurel becoming more important (increasing from 10% to 13% for the entire study area) and tanoak becoming less important (decreasing from 14.7% to 7.1% across all ecoregions). The increase in bay laurel in the study area suggests that the disease will not only be maintained in the system but increase due to bay laurel producing the most inoculum of all hosts.

It is important to note that our model tracks species biomass not individual trees and our calculations are not based on the number of individuals of a species but rather species biomass. By having calculations by biomass rather than number of individual trees makes species like redwood with larger than average biomass per tree relatively more important than they would be in an analysis based on number of stems, however, changes in species biomass relative to each other should still show similar trends to an analysis of individual trees. Model results support empirical data from other studies on SOD impact on forest composition and add support for the theory that tanoak will persist despite SOD impacts due to reproductive ability (Cobb, Filipe, et al. 2012; Cobb, Meentemeyer, and Rizzo 2010).

CHAPTER 4: UNTANGLING THE INTERACTING EFFECTS OF DUEL DISTURBANCES: SUDDEN OAK DEATH AND FIRE

Introduction

Forest pests and pathogens can have large scale impacts on forest composition and can interact with natural disturbance regimes to dramatically change forest composition (Aukema et al. 2010; B. Buma and Wessman 2011; M. G. Turner 2010; Cobb and Metz 2017). But the long-term impacts of and interactions with natural disturbance regimes for newly introduced pests and pathogens are not well understood. Therefore, we are combining a dynamic epidemiological model, a fire-behavior model, and a forest landscape simulation model (FLSM) (Figure 17) to understand how these disturbances interact and change forest composition over the course of a century using *Phytophthora ramorum* as our case study invasive pathogen. Three disturbance scenarios (fire, disease, and fire and disease) will be used in order to understand the interacting effects of fire and disease on forest composition.

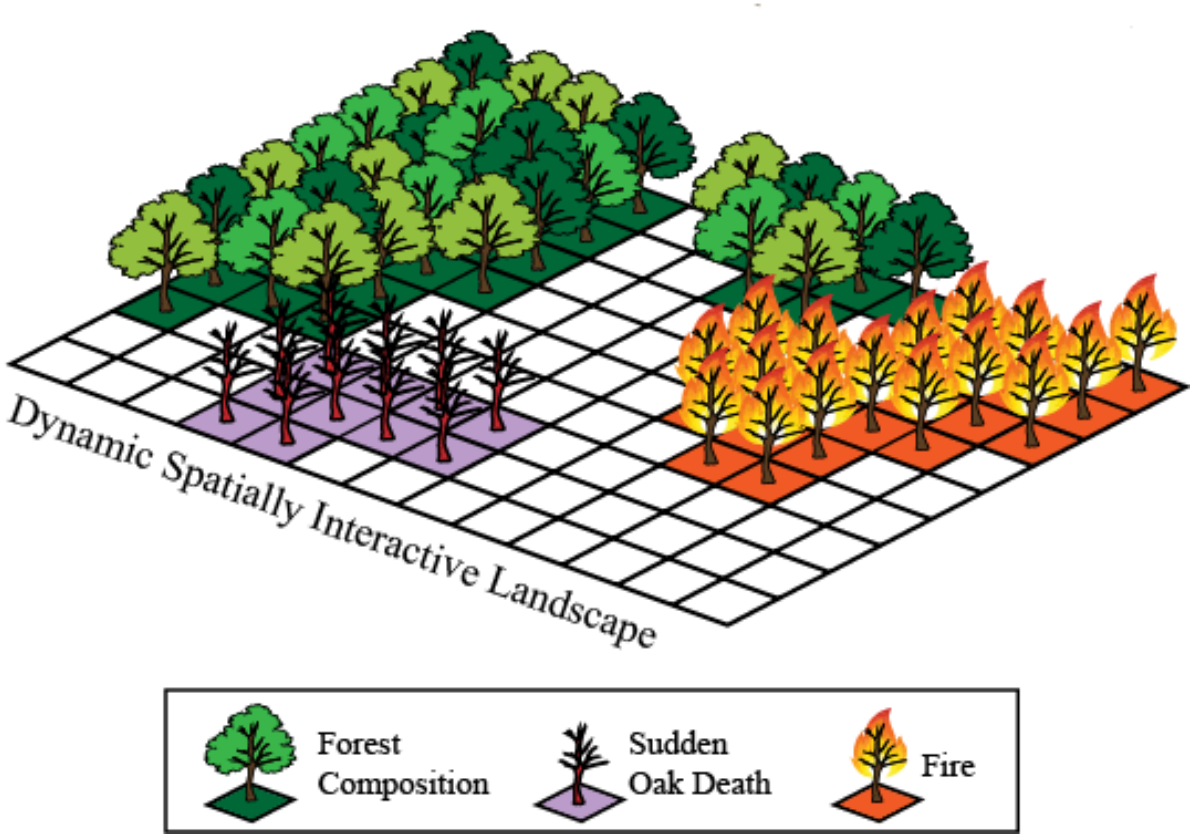

Figure 17: Spatial modeling framework showing fire, disease, and forest composition. These three components of the interactive landscape change over time and space, and interact with each other within and across time-steps. Sites also interact with each other within a time step.

Disturbance plays an important role in both the maintenance of and the transition of ecosystems (Brian Buma, Poore, and Wessman 2014). Many disturbance regimes are being altered by climate change and other anthropogenic factors such as introduced species (M. G. Turner 2010), and multiple disturbances can interact to produce unexpected changes in community composition or ecosystem state as compared to individual disturbance effects (Foster et al. 2015). Bender, Case, and Gilpin (1984) define two types of disturbance: pulse, which are short time frame (days to a couple months) events often with significant effects, i.e. fire; and

persistent, which are maintained over long time periods (months to many years), i.e. disease. These two types of disturbance can interact and affect each other in often unpredictable ways due to non-linear dynamics and interactive effects. Interactions between fire and disease can modify the other's likelihood, intensity or spatial distribution. Additionally, the interacting effects can combine to modify the ecosystem. Based on the "additive" model of disturbance interactions (Crain, Kroeker, and Halpern 2008), if the combined effects of two disturbances is greater than (synergism) or less than (antagonism) the sum of their individual effects then interacting effects occur. Recent advances in this theory allow for the characterization of mechanistic pathways driving interactions and acknowledging that the effects are often non-linear. Under this theory disturbance interactions can be of two types: (1) interaction chain effects where one disturbance influences the occurrence or magnitude of the second disturbance and both disturbances have a direct impact on the variable being tested (in this case forest composition) and (2) interaction modification effects where the effect of one disturbance on the response variable (forest composition) depends on the environmental conditions and time since the other disturbance (Figure 18) (B. Buma and Wessman 2011; Foster et al. 2015).

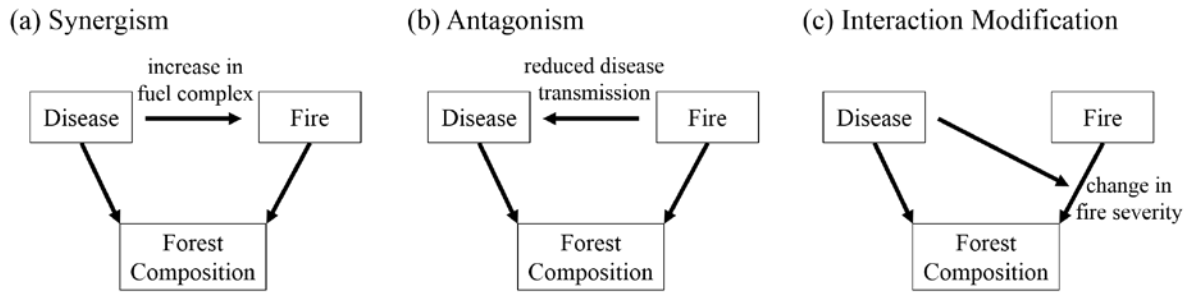

Figure 18: Disturbance interaction theory and associated mechanism. Arrows indicate direction of effect, top boxes are the disturbances, and bottom box is the response variable of interest, in this case forest composition. (a) and (b) are interaction chain which modify the likelihood of occurrence, while, (c) interaction modification modifies the magnitude or severity of the other disturbance. Figure modified from Foster et al. 2015.

Invasive forest pathogens tend to be persistent in nature and can dramatically alter forest composition due to many host species having no natural resistances (Cobb, Filipe, et al. 2012; Meentemeyer, Anacker, et al. 2008). For example, chestnut blight brought over through the nursery trade in the early 1900's wiped out most American chestnuts. American chestnut dominated forests were replaced by oak-hickory dominated forests (Prospero and Cleary 2017). *Phytophthora ramorum*, the causal agent of sudden oak death (SOD) and ramorum blight, is an invasive pathogen introduced in California in the early 1990s that can infect over a hundred plant species (Rizzo, Garbelotto, and Hansen 2005; Davidson, Patterson, and Rizzo 2008). Disease symptoms are expressed in two forms: lethal canker infections and non-lethal foliar infections. The lethal form of the disease infects stems and branches of several ecologically important tree species, such as, tanoak (*Notholithocarpus densiflorus*), coast live oak (*Quercus agrifolia*), canyon live oak (*Quercus chrysolepsis)*, California black oak (*Quercus* kelloggii), and Shreve's oak (*Quercus parvula var. shrevei*). These canker hosts are epidemiological dead ends with the exception of tanoak (Kovacs et al. 2011; Davidson et al. 2005). The foliar hosts can transmit the disease through inoculum produced on leaves and stems. California Bay Laurel produces the most inoculum of all infected species and as such is consider the reservoir host with other foliar hosts considered alternative hosts (Figure 1) (Kelly and Meentemeyer 2002; Meentemeyer, Rank, et al. 2008; Václavík et al. 2010).

Fire is a natural part of the ecosystem dynamics in Big Sur, CA. Many species have evolutionary adaptations that make fire an important part of their life cycle. In the Big Sur, CA there were a total of 69 fires during the 100-year period between 1912 and 2012 larger than 10000 m^2 (CAL FIRE 2014). Fire has been shown to reduce the likelihood of *P. ramorum* infection, with *P. ramorum* 29 times more likely to be recovered in unburned compared to

burned plots, however, the number of symptomatic bay laurels increased the likelihood of the pathogen being found at a post burn site (Beh et al. 2012). Most likely due to the increased likelihood that one of these symptomatic trees survived the fire. *P. ramorum* influences fire primarily by changing the fuel composition through species decline and mortality in canker hosts, however, over long-time periods the disease can lead to changes in species composition which can also change fuel loads. The effects of fire and disease on forest composition takes place over the course of multiple decades. Process-based models of fire and disease coupled together with a forest composition model provide a means to analyze projected changes in forest composition by fire and disease interactions.

Methods

Study System

In 2006-2007, a network of 280 plots throughout the Big Sur were created; 121 were located within the 2008 Basin Complex and Chalk fires creating a full factorial design across the 2 disturbances with unburned and burned, and infected and uninfected. The plots are 500 m^2 and distributed in a stratified-random design across redwood and mixed evergreen forest types, as well as in areas with and without *P. ramorum* (Haas et al. 2011). Within each plot, all stems ≥ 1 cm diameter at breast height (dbh) are measured, *P. ramorum* symptoms at leaf, stem and twig are recorded for each tree and sent to the lab for pathogen identification, cover class by species is estimated, cylindrical volume of logs ≥ 20 cm is measured, and soil data is collected using the browns-transect method. This data is used for model calibration and validation.

Modeling Framework

LANDIS-II is a process-based raster modeling framework consisting of a model core that links, parses, and validates data from multiple extensions (models) and allows the user to "plug in" a forest succession extension and any number of optional disturbance extensions. Forests are represented as tree species-age cohorts (i.e. tanoak 100 for all tanoaks between 91-100 years) within raster cells across the landscape (Scheller et al. 2007). The NECN succession extension (version 4.1), EDA extension (version 1.1), and Dynamic Fuel and Fire extension (version 2.0.5) are utilized in this study.

Succession Extension

The NECN succession extension, originally developed as the Century Succession extension (Scheller et al. 2011), is a combination of the original LANDIS biomass extension and the CENTURY Soil Organic Matter model (Parton et al. 1983). It simulates cohort growth, mortality, and regeneration based on life history and physiological attributes. Species compete for resources within a grid cell and spatially disperse across cells within the landscape. This allows for species range shifts and the effects of the disease-fire interaction on species composition to be simulated. Additionally, the model estimates above- and below-ground NPP, NEE, multiple pools of live and dead tree biomass (including leaf, wood, fine root, course root, and course woody debris) and active, passive, and slow soil organic matter pools (Parton et al. 1983; Scheller et al. 2011). NECN incorporates a climate library that allows all extensions to utilize the same climate information. The climate data influences soil water content and nitrogen available for tree growth. Growth and competition are simulated based on limitation imposed by

temperature, water, nitrogen, leaf area, and light availability instead of operating at a photosynthetic level (Scheller et al. 2011).

Dynamic Epidemiological Extension

The EDA extension simulates disease spread and using dynamic spatially explicit processes based on disease data. The model simulates *P. ramorum* infection and disease related mortality. It is based on a spatial susceptible-infected-recovered model but modified so that recovered becomes diseased. This is done to indicate when a grid cell goes from being cryptically infected (non-detectable in the field) to symptomatic (visually identifiable in the field). Currently only whole cohorts are infected and diseased not individual trees or partial cohorts. This is a reasonable assumption given the 30-m resolution but should be adjusted when using larger resolutions.

Dynamic Fuel and Fire Extension

Fire is simulated within LANDIS-II using the Dynamic Fire extension (Sturtevant et al. 2009), which is designed to simulate landscape-scale fire regimes and stochastic behavior over long time scales. The Dynamic Fire extension simulates the general characteristics of a fire regime, including fire frequency, fire sizes and fire effects (mortality). Fire-induced cohort mortality is not mechanistically simulated but is class based. Cohort-based mortality depends on the cohort age, species fire tolerance, and the severity of the simulated fire. Young cohorts of a species with a low fire tolerance are the most susceptible, but mature fire tolerant cohorts can be killed by very severe fires. Reproduction following fire depends on species-specific reproductive rates either through resprouting or serotiny, seed release in response to fire occurrence, and is

controlled by the succession model. Additionally, species can disperse into a burned area from outside the burned area and will survive if site conditions are favorable (Sturtevant et al. 2009).

In the Dynamic Fire extension, fire spread rate and direction are a function of fuel type, weather, topography, and ignition rate. Fuel types represent fuel conditions of both the fuel bed and standing dead biomass with unique spread parameters, ignition probability and the base height of the crown (CBH: the height above ground that the live crown begins) (Sturtevant et al. 2009). Temperature, wind speed, wind azimuth, relative humidity and precipitation are inputs into the model. The fine fuel moisture conditions and wind speed velocity determine the Initial Spread Index (ISI), which is combined with larger fuel moisture into the Fire Weather Index (FWI) (Sturtevant et al. 2009).

The Dynamic Fire extension calculates fire severity potential as a function of crown fraction burned and fire spread rate. Crown-fraction burned is a function of foliar moisture content (FMC), CBH and surface fuel consumption. Simulated fires generally have a wide range of fire severity potentials (Sturtevant et al. 2009). Actual severity can be mixed as well depending on the cohorts present in the burn area.

We use the Dynamic Fuels extension (Sturtevant et al. 2009) to assign fuel types. The extension assigns a fuel type to each cell within the study area for each time step based on species and cohort ages in the cell at that time step. These fuel types change based on succession or disturbance. The fuel type following a fire will not be the same as that before the fire due to the change in cohort species and ages present after fire.

Model Inputs

LANDIS-II model inputs include initial vegetation data, ecoregion data, species and functional-group trait data, epidemiological data, fuel and fire data, and climate data (Table 5).

See Appendix 1 for all tables with NECN and EDA and Dynamics Fuel and Fire extension data parameters.

Table 5: Data and Sources.

Parameter Groups	Source	Data
Species Specific	Silvics Manual, Literature, LEMMA GNN	Seed dispersal; fire regen; resprout probability; resprout age limits; shade, fire, and drought tolerance; sexual maturity; longevity; min temp; GDD min and max; leaf, wood, and root lignin and C/N ratios.
Functional Groups	Silvics Manual and previous Century models	Mortality shape curves; max LAI; growth parameters; leaf drop month; and fraction of carbon in fine and course roots.
Ecoregion Types	LandFire Biophysical Regions	Groups regions with similar climate, topography, and soil
Ecoregion Parameters	SSURGO, NADP	Soil depth; percent clay; percent sand; field cap; wilting point; drainage; nitrogen
Climate (Daily)	CA-BCM 2014	Precipitation, TMIN, TMAX, Wind
Fire	CAL FIRE, Literature	Ignition events, Max Size, Fuel moisture mins and max per season.

Acronyms: LEMMA = Landscape Ecology, Modeling, Mapping & Analysis, GNN = Gradient Nearest Neighbor, GDD = growing degree days, C/N = Carbon/Nitrogen, LAI = Leaf Area Index, SSURGO = Soil Survey Geographic Database, NADP = National Atmospheric Deposition Program, CA-BCM 2014 = California Basin Characterization Model Downscaled Climate and Hydrology, CAL FIRE = California Department of Forestry and Fire Protection.

Vegetation Data

Initialization of the current vegetation on the simulated landscape, used the gradient nearest neighbor (GNN) map for the California Southern Coastal Range (map region 233) produced by the Landscape Ecology, Modeling, Mapping and Analysis (LEMMA) group for the Northwest Forest Plan Effectiveness Monitoring (Ohmann et al. 2011; Ohmann and Gregory

2002). The GNN method imputes forest inventory plot data at every pixel, characterizing tree species composition, age, biomass, and other variables. The inventory plots come from various sources, with the predominant ones being the US Forest Service Forest Inventory and Analysis (FIA) and Current Vegetation Survey (CVS) programs (Ohmann et al. 2011). Age information for each individual tree within the imputed forest inventory plots was obtained from the supplemental TREE_LIVE database provided by the LEMMA group. These data were used to classify species-age cohorts at 10-year intervals to match the succession time-step. Age cohorts range from 10 to the maximum age of the species.

Ecoregions

LANDIS-II uses ecoregions to divide the study area into regions that have homogeneous soils and climate. For this study, LANDFIRE biophysical regions for the California Southern Coastal Range (map region 4) are utilized. LANDFIRE biophysical regions are classified based on topography, soil, and climate data and were developed by the LANDFIRE group of the Nature Conservancy (Rollins 2009). There are 17 ecoregions in the study area: Water, Barren, Southern California Coastal Scrub, Northern California Coastal Scrub, Northern and Central California Dry-Mesic Chaparral, Mediterranean California Lower Montane, Black Oak-Conifer Forests and Woodland, Mediterranean California Dry-Mesic Mixed Conifer Forest and Woodland, Central and Southern California Mixed Evergreen Woodland, California Northern Coastal Grassland, California Montane Woodland and Chaparral, California Montane Riparian Systems, California Mesic Chaparral, California Coastal Redwood Forest, California Coast Live Oak Woodland and Savanna, California Coastal Closed-Cone Conifer Forest and Woodland, California Central Valley and Southern Coastal Grassland. Ecoregion parameters include soil properties such as percent clay and sand, SOC decomposition rates, drainage class, and pools of

nitrogen and carbon. SSURGO National Soil Survey data for Monterey County, California ("Web Soil Survey" 2014) was spatially averaged to a depth of 1 m across the ecoregions to obtain the necessary data at the ecoregion level. Percent clay and sand, field capacity, and drainage class were calculated directly from the SSURGO data, while wilting point was calculated as field capacity minus available water content. Soil organic carbon and nitrogen pools were calculated using soil data collected across the 280 plots in the Big Sur plot network using the browns-transect method (Cobb and Metz 2017; Cobb, Chan, et al. 2012). Assumption for nitrogen inputs were that they come from primarily from wet and dry deposition, biological fixation, soil, and decaying logs (Zhang et al. 2012; Fenn et al. 2003). Wet and dry deposition were calculated from National Atmospheric Deposition Program (NADP) data across the study system (NADP Program Office 2017).

Species and Functional Group Parameters

I simulated 27 tree species based on the data from LEMMA GNN: bristlecone fir, grand fir, bigleaf maple, California buckeye, white alder, red alder, pacific madrone, tanoak, knobcone pine, Coulter pine, sugar pine, singleleaf pinyon, ponderosa pine, Monterey pine, gray pine, California sycamore, balsam poplar, big-cone Douglas fir, Douglas fir, California live oak, canyon live oak, blue oak, Oregon white oak, California white oak, interior live oak, redwood, California bay laurel. These 27 species were grouped into 5 functional groups: Redwood, Evergreen-Conifer, Deciduous Conifer, Evergreen Broadleaf, Deciduous Broadleaf, see Appendix 1 for data tables containing species and functional group parameters.

Epidemiological Data

The model is initialized at the best known location of initial infection based on the best knowledge of invasion history in central coastal California (Rizzo, Garbelotto, and Hansen 2005; Mascheretti et al. 2008; Meentemeyer et al. 2011). Data on host species vulnerability were utilized based on species mortality within both the Big Sur plot network as well as Sonoma County plot data. Host Index is the measure of the host ability to produce inoculum and to become infected (Davidson et al. 2005; Davidson, Patterson, and Rizzo 2008) and is derived from information from the plot network (Meentemeyer et al. 2011; Meentemeyer, Anacker, et al. 2008). The dispersal kernel utilizes the power law distribution in order to account for long-distance dispersal events. The effect of precipitation is simulated by summing the previous 5 days and temperature effects are simulated using a polynomial transformation of the daily temperature using parameters in Table 4.

Climate Data

The NECN Succession extension utilizes monthly temperature and precipitation data for model spin-up and future projections, however, the EDA extension requires daily data. We modified the climate library to take in daily data and apply the proper temporal scaling for each extension and were able to supply daily data to the model while still having the ability to provide monthly data to the NECN succession extension. Climate data was obtained from the US Geological Survey GeoData Portal (https://cide.usgs.gov/gdp/) as an area weighted average for each ecoregion. Climate data is from the Western US Hydroclimate Scenarios Project Observations and Statistically Downscaled Data at 1/16th degree resolution (Hamlet, Salathé, and Carrasco 2010). This method uses the Modified Delta approach (Littell et al. 2011), based on 10

models from Phase 3 of the Coupled Model Intercomparison Project to create daily temperature and precipitation values for historical and future climate (1950-2099). The model only uses the 10 best performing GCMs for a given area in this case the California Basin. Future climate data is also an average of the 10 best performing GCMs as well. Data from 1950 to 1990 was used for model spin-up, while 1990 to 2090 data was used for model projections. Simulating from 1990 to 2090 was necessary to be able to recreate the disease dynamics during the early stage of infection.

Fire Data

The number of ignition events for a given time step is randomly drawn from a Poisson distribution based on the average number of lightning strikes for the historical fire regime, 2.97 per year per 100 km^2 in California's central coast (Van Wagtendonk and Cayan 2008). This scales to 23 ignition events per year for the entire study area, ignition occurs if the fuel index is high enough. This ignores data on human ignition events due to lack of good data on number of human ignition events. It also assumes that all lighting strikes hit land rather than water so these two assumptions should offset. Fire size is based on connectivity of the fuel system, local weather, wind, and topography. This led to an average number of fires of ~71 across the 30 simulations which is in line with the historical fire data from CALFIRE of 69 fires.

Model Calibration

The NECN succession was calibrated using literature review and data for central coastal California. Expected patterns of growth, NEE, carbon accumulation, and stand age were determine from literature review (Henson 1996; D. P. Turner et al. 1995; Vogt 1991; Waring 1983; Noss 1999; Johnson, Shifley, and Rogers 2009; Callaway and D'Antonio 1991; Battles et

al. 2008; Pelt and Franklin 2000; Smith, Rizzo, and North 2005; Waring and Running 2010). Calibration of the NECN Succession extension began with single-cell simulations, adjusting parameters (e.g. temperature response and moisture sensitivity shape parameters) to match patterns of growth and NEE in literature (Ewing et al. 2009; G. Turner 2008; D. P. Turner et al. 1995; Waring and Running 2010). The other parameters (e.g. soil organic carbon decay rates and shade tolerance) were calibrated across the entire Big Sir to ensure that starting conditions matched input data and landscape-scale processes were simulated correctly. Biomass estimates from the LEMMA GNN maps were created using the component ratio method (CRM) (Heath et al. 2009). The CRM computes aboveground biomass as the sum of three components: bole of the tree, stump of the tree, and the top of the tree. The biomass of the tree bole is calculated using regional volume equations, while the biomass of additional tree components is calculated using a series of ratios established by Jenkins et. al. (2003). The GNN biomass estimates were used to calibrate the initial aboveground biomass for model spin-up (Figure 14). Final calibration was assessed based on the following criteria: (1) initial aboveground carbon was within 10% of GNN estimates across all ecoregions (Figure 14), (2) projected aboveground NPP and carbon matched trends in literature, and (3) soil organic carbon accumulated 5-20% in all pools over the 100-year simulation.

Simulation Model Runs

The model simulated from 1990-2090 using 10-year time steps for NECN and a 1-year time step for EDA and Dynamic Fuel and Fire. The model was replicated 30 times using different random seeds for each simulation in order to account for stochastic variability in climate, disease spread, fire ignition locations, and seedling establishment. Three disturbance scenarios were utilized: fire, disease, and fire and disease. This allowed for the comparison of

species composition considering each disturbance in the absence of the other, as well as the interacting effects of the two disturbance types together.

Analysis and Results

Effects on Fire Regime

I calculated the size, average severity, and number of cohorts killed for each fire that occurred during the 100-year simulation for all 30 simulations and then averaged all three of these variables across an entire simulation. I then averaged the number of fires, number of cohorts killed, average fire size, and average fire severity from the thirty runs for each of the 2 disturbance scenarios (fire, and fire and disease). Across the entire landscape only fire severity is significantly different between the two disturbance scenarios, however, the variability in the number of fires with disease increases with disease, despite the average number of fires being almost identical (Figure 19). The fire data used for this analysis account for every pixel including those outside of the fire perimeter. We analyzed fire severity across the ecoregions for both disturbance scenarios to see if all ecoregions show the same decrease in fire severity with disease or if they differ in this effect. Of the 17 ecoregions, only mixed evergreen, redwood, and oak woodlands had statistically significant decreases in fire severity at 95% confidence (Figure 20).

Fire severity was analyzed by disease stage to assess whether changes in fire severity depended on disease stage. I created four categories of disease stage to capture the effect of disease stage on fuel conditions. The four categories are: 1) uninfected; 2) infected = no disease effects only non-symptomatic hosts are present; 3) diseased with mortality occurring less than or equal to 3 years prior to the fire; and 4) diseased with mortality occurring more than three years before the fire. I used three years as the cutoff for early to late stage of disease progression as the

majority of trees experiencing disease related mortality have lost all of their branches and/or have fallen within 4 years of mortality. Fire severity for the disease stage analysis was averaged over each 100-year simulation and then averaged across all 30 simulations. Stage of disease appears to affect average fire severity especially but the only statistically significant difference occurred in diseased plots with mortality occurring 3 years or less prior to a fire (Figure 21).

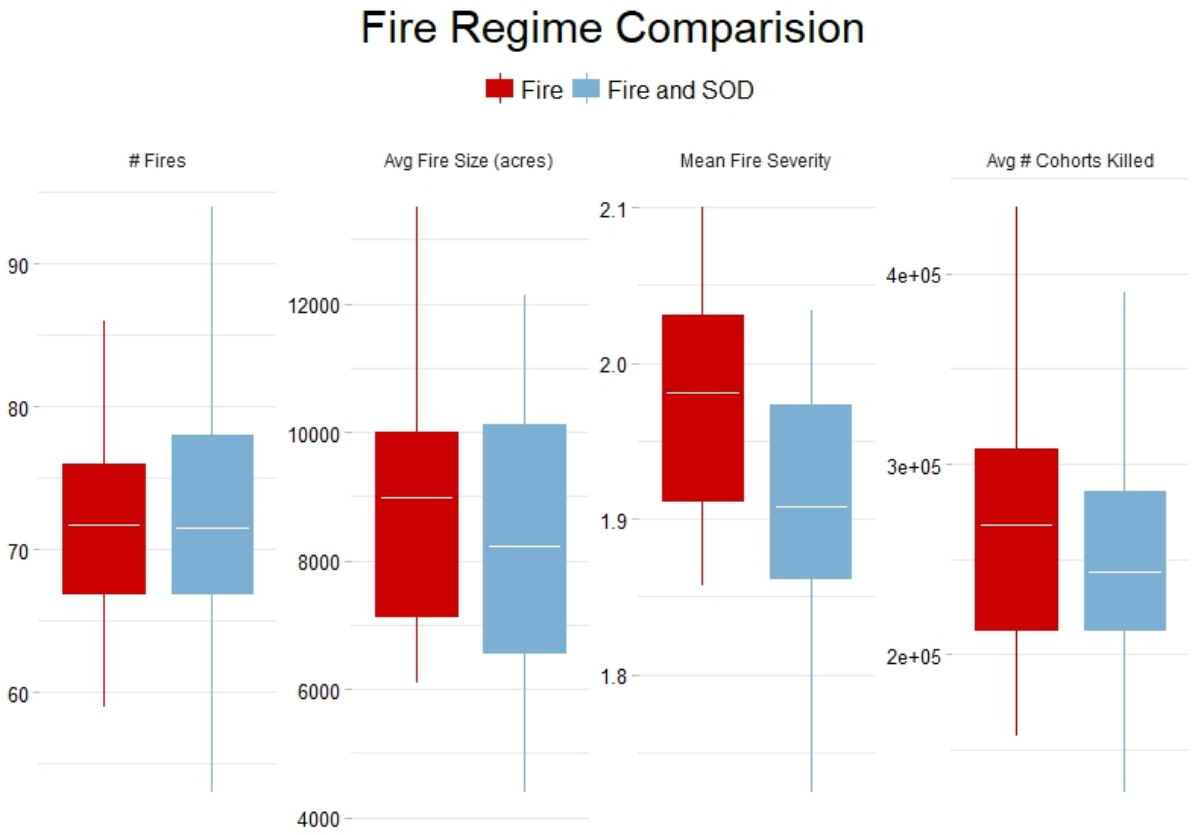

Figure 19: Average # of fires, average fire size, average fire severity, and average # of cohorts killed across the 30 simulations using the two disturbance scenarios with fire (fire, and fire and disease). Only fire severity is significant at a 0.05 confidence interval, p-value < 0.001. Both number of fires and average fire size show greater variability between simulations for fire and disease scenarios.

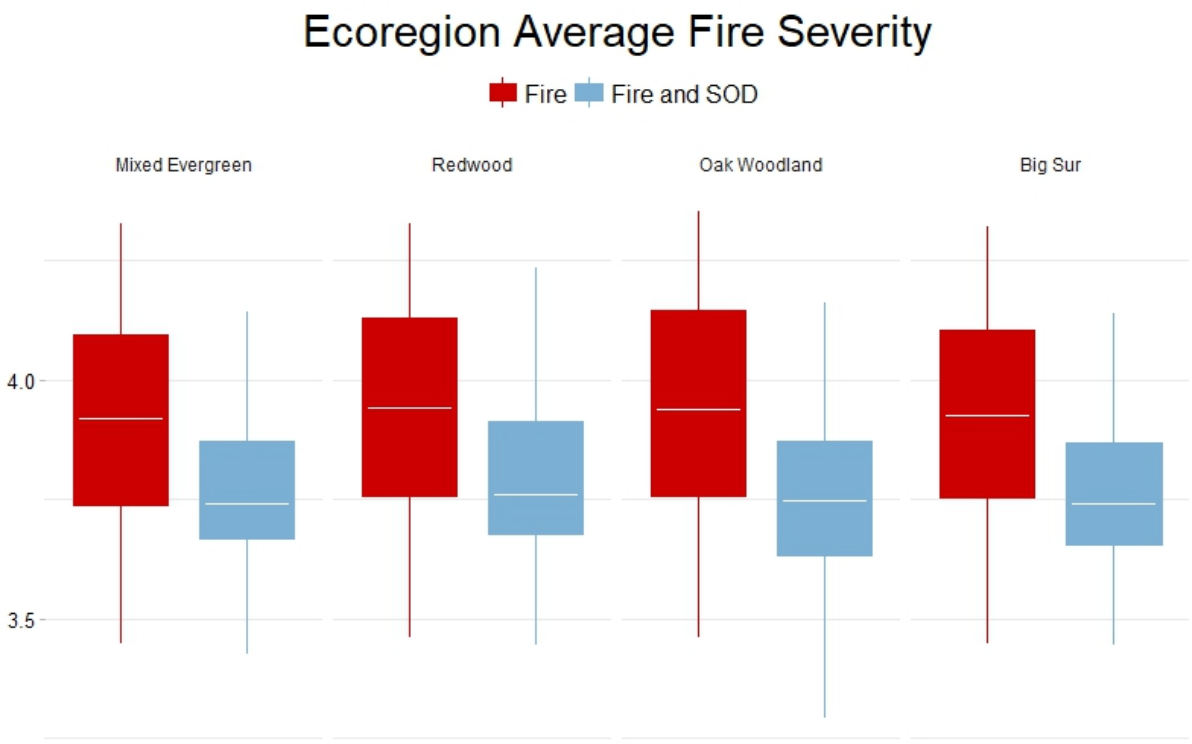

Figure 20: Average Fire Severity across ecoregions and entire landscape only accounting for pixels within the fire perimeter. The p-values for each ecoregion shown are significant at 95% confidence using a t-test with a Bonferroni p-value adjustment: Mixed Evergreen = 0.0067, Redwood = 0.0071, Oak Woodland = 0.0045, and the entire Big Sur = 0.0039, however, the other ecoregions were not statistically significant compare across the 2 disturbance regimes.

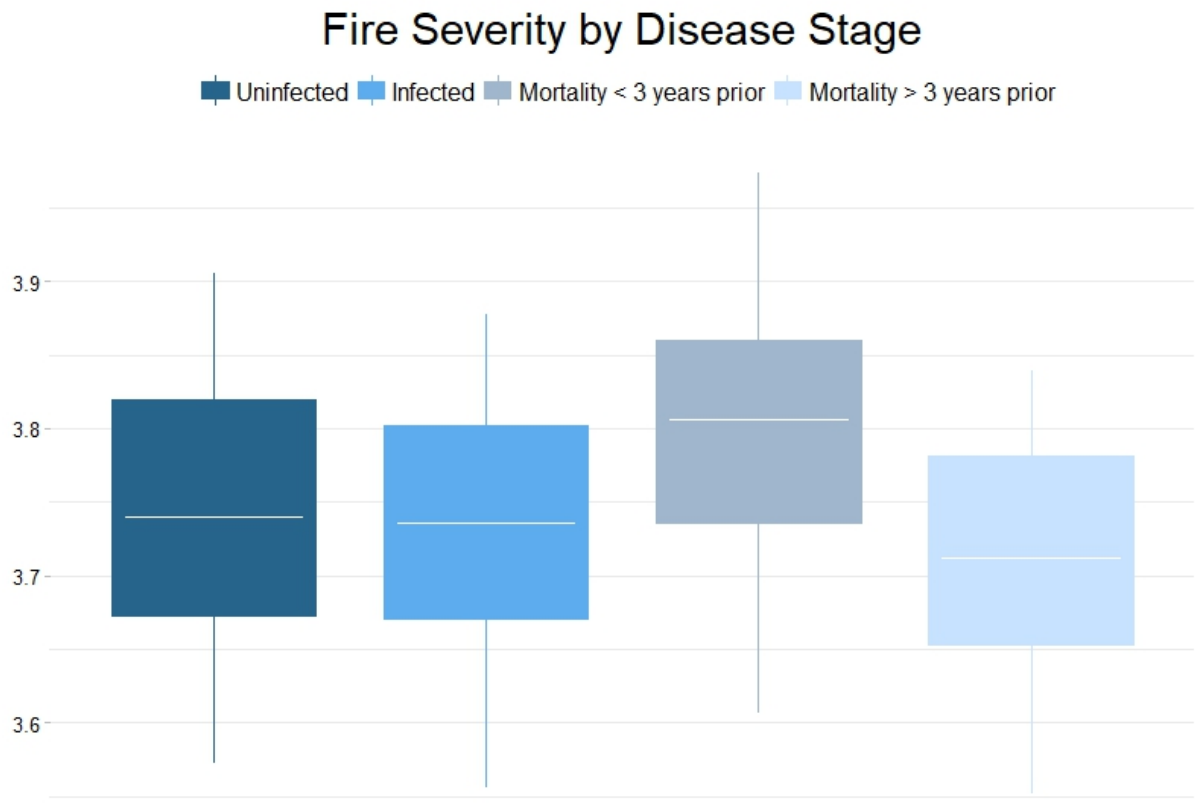

Figure 21: Fire severity based on disease stage. Diseased with Mortality ≤ 3 is statistically different from the other disease states p-values =0.044, 0.021, and 0.006 for Infected, Uninfected, and Mortality greater than three years prior to fire, while other disease stages are not significantly different from each other using a pairwise non-paired t-test with non-pooled standard deviation, and a Bonferroni p-value adjustment.

Ecosystem Effects

In order to analyze the ecosystem effects of fire and disease, we analyze changes in species composition specifically the ratios of bay laurel to tanoak, bay laurel to coast live oak, and bay laurel to California black oak for the three disturbance scenarios. These ratios were chosen as these species are relatively abundant in our study area and epidemiologically/culturally important, with bay laurel being the reservoir host, tanoak being both a capable alternative host and the most susceptible host, and both oak species being canker hosts and endemic to the region. I averaged the biomass for each species for the 30 simulations for each disturbance

scenario for each time step at both the landscape level and the ecoregion level. I then calculated the three ratios: bay laurel/tanoak, bay laurel/coast live oak, and bay laurel/California black oak. The ratio of bay laurel to tanoak increased over time in the SOD only scenario and decreased in both the fire and fire + disease scenarios (Figure 22). The difference in the bay laurel to tanoak ratio between the disturbance scenarios holds across ecoregions, however, the magnitude varies greatly across the ecoregions (Figure 23).

The ratio of bay laurel to coast live oak increased over time in the SOD only scenario and decreased in both the fire and fire + disease scenarios (Figure 24). The magnitude of this change is much smaller than the change in the ratio of bay laurel to tanoak. The bay laurel to coast live oak ratio also holds across all ecoregions, however, the magnitude varies greatly across the ecoregions with some experiencing little to no change between scenarios (Figure 25).

The ratio of bay laurel to California black oak increased over time in the SOD only scenario and decreased in both the fire and fire + disease scenarios and starts out much larger than either the ratio of bay laurel to tanoak or bay laurel to coast live oak (Figure 26). The magnitude of this change is much smaller than the change in the ratio of bay laurel to tanoak. The changes in the ratio of bay laurel to California black oak show little to no change across four of our ecoregions and the magnitude varies greatly across the ecoregions (Figure 27). It is important to note that the redwood and mixed evergreen ecoregions make up greater than 50% of our study area and will have a disproportionately large effect at the landscape level compared to other ecoregions. Bay laurel abundance represented as a percent of total biomass increases in the SOD only scenario and decreases in both scenarios involving fire (Figure 28). Tanoak abundance as a percent of total biomass increases in the fire only scenario but decreases in both scenarios involving SOD (Figure 29). Coast live oak as a percent of total biomass increases in all 3

disturbances scenarios, however, to a much lesser degree in the SOD only scenario (Figure 30). California black oak as a percent of total biomass is flat to increasing in all 3 disturbance scenarios, however, the variability between simulations is much greater than the differences between disturbance scenarios (Figure 31). Redwood as a percent of total biomass decreases dramatically in all 3 disturbance scenarios with little to no difference between scenarios (Figure 32).

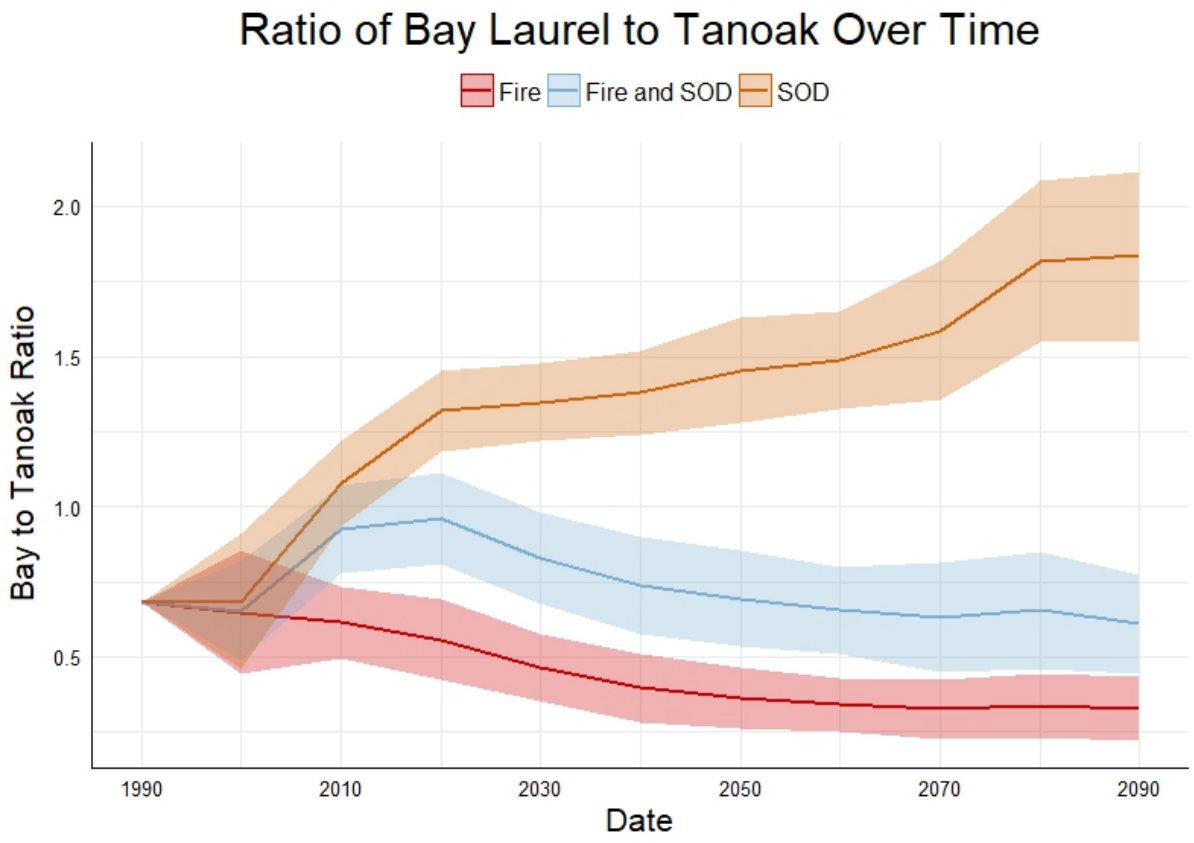

Figure 22: Ratio of bay laurel to tanoak over the course of the 100-year simulation for all 3 disturbance scenarios: fire, disease, and fire and disease. Solid line indicates the average and the shaded region is the standard deviation for the 30 simulations.

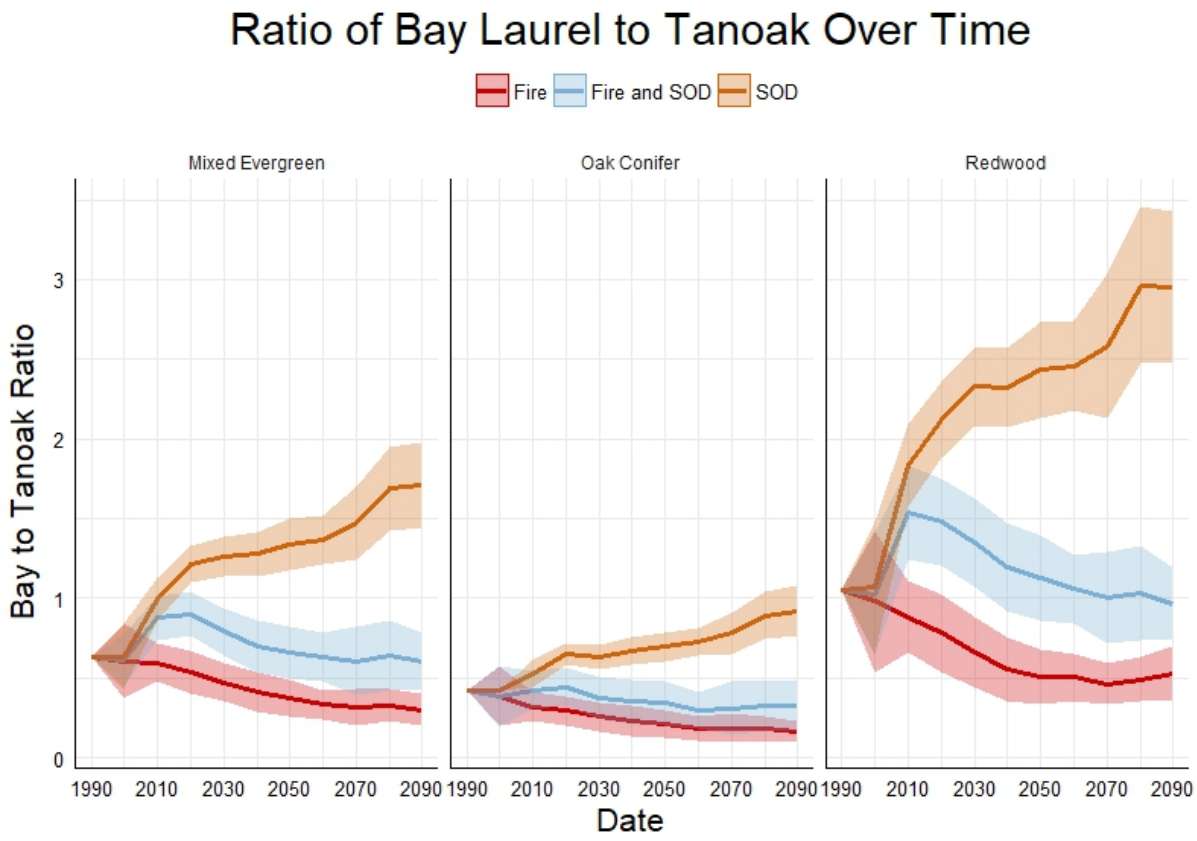

Figure 23: Ratio of bay laurel to tanoak over the course of the 100-year simulation for 3 ecoregions for all 3 disturbance scenarios: fire, disease, and fire and disease. Solid line indicates the average and the shaded region is the standard deviation for the 30 simulations.

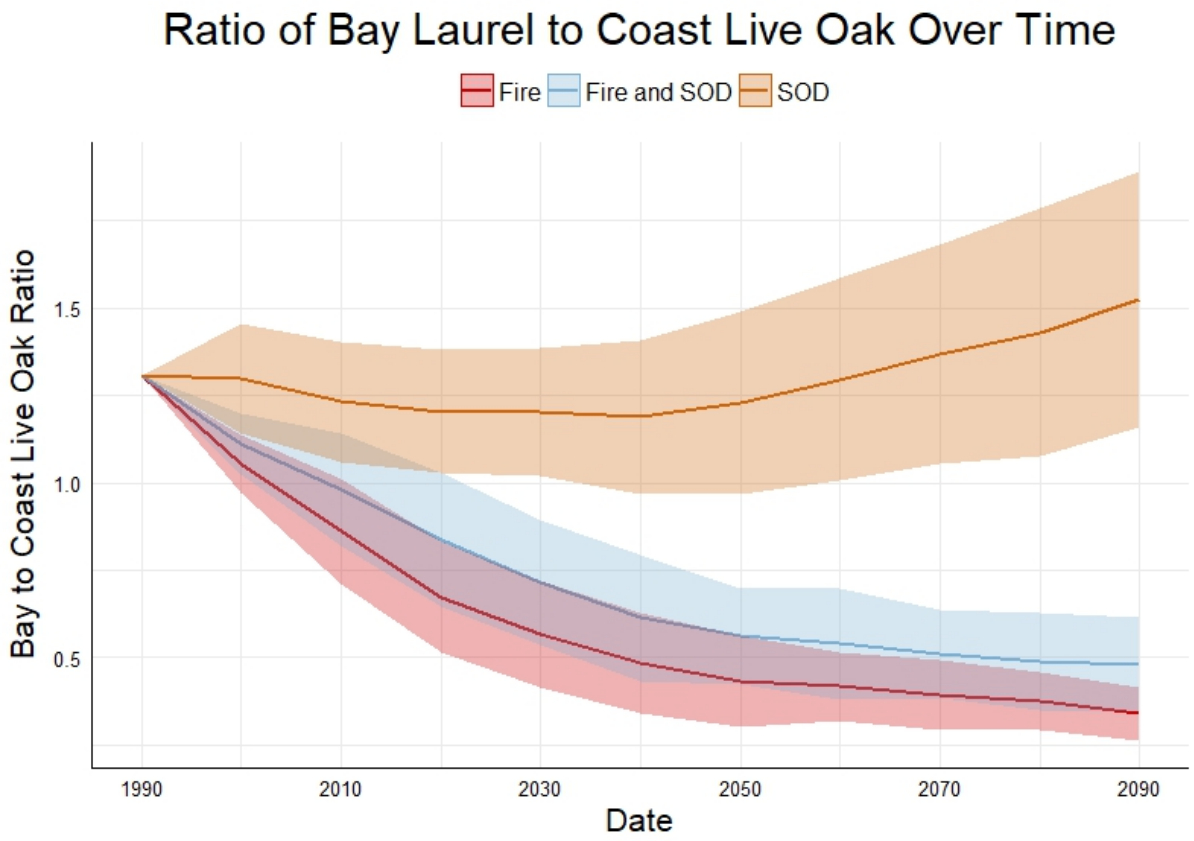

Figure 24: Ratio of bay laurel to coast live oak over the course of the 100-year simulation for all 3 disturbance scenarios: fire, disease, and fire and disease. Solid line indicates the average and the shaded region is the standard deviation for the 30 simulations.

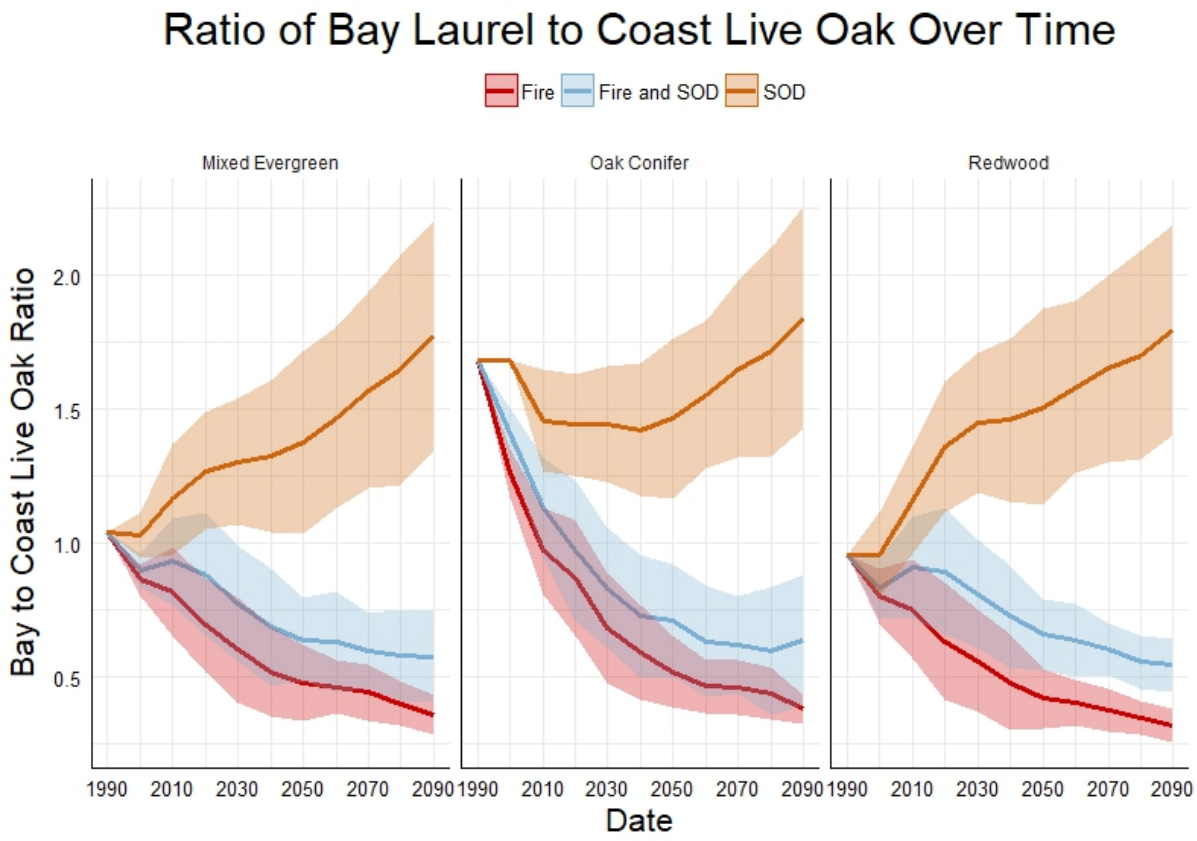

Figure 25: Ratio of bay laurel to coast live oak over the course of the 100-year simulation for 3 ecoregions for all 3 disturbance scenarios: fire, disease, and fire and disease. Solid line indicates the average and the shaded region is the standard deviation for the 30 simulations.

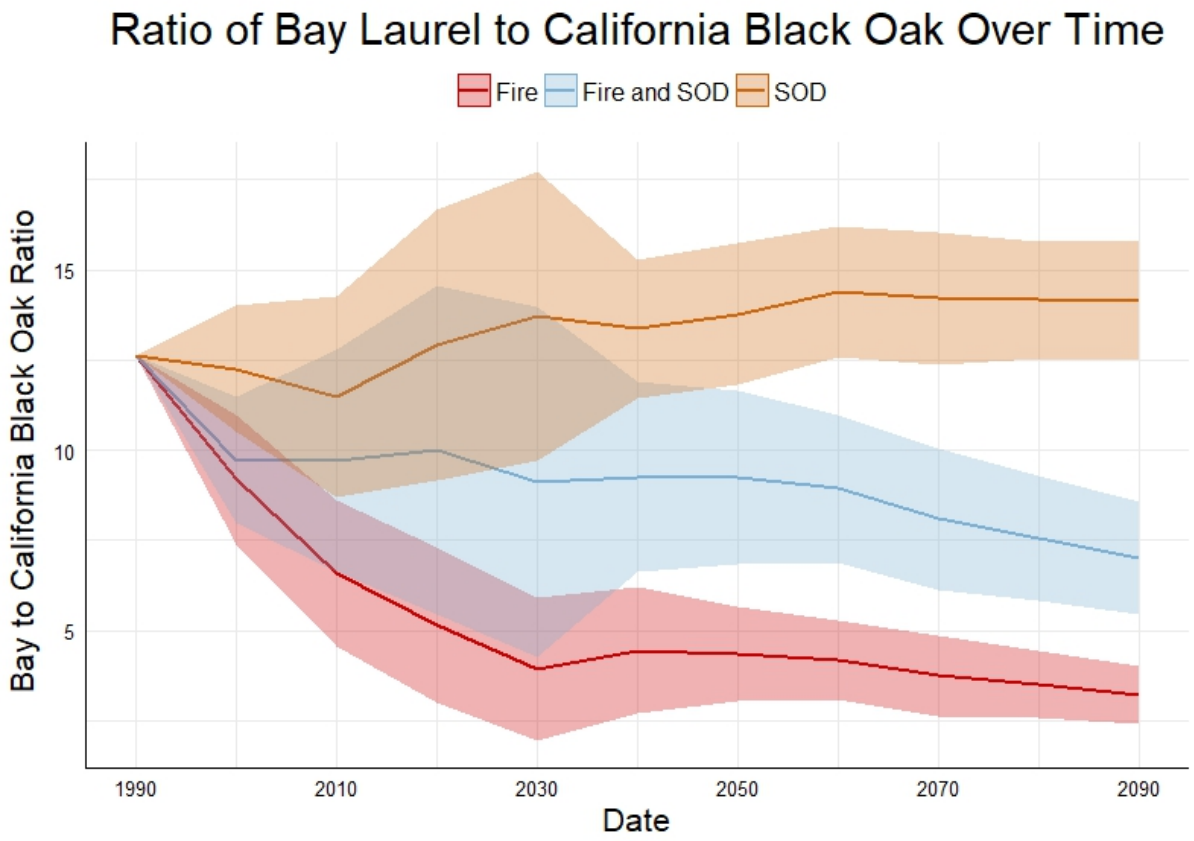

Figure 26: Ratio of bay laurel to California black oak over the course of the 100-year simulation for all 3 disturbance scenarios: fire, disease, and fire and disease. Solid line indicates the average and the shaded region is the standard deviation for the 30 simulations.

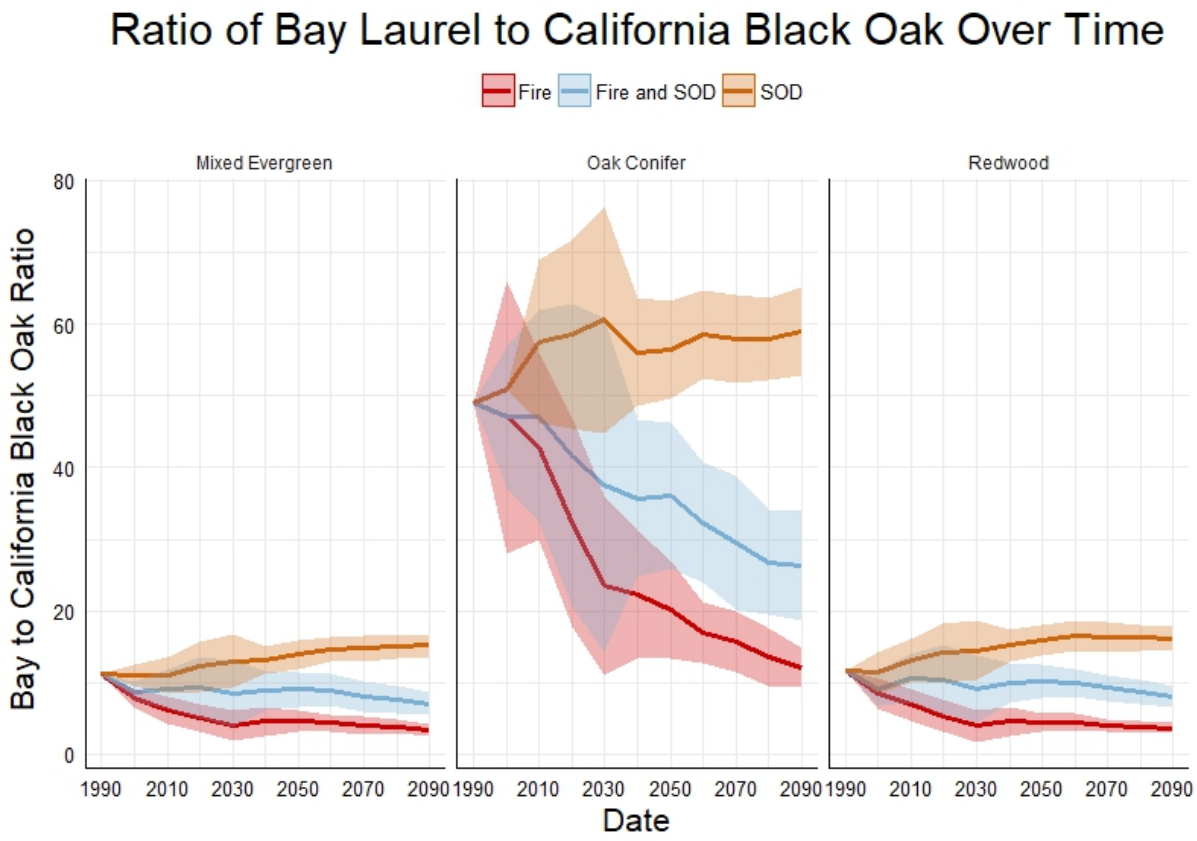

Figure 27: Ratio of bay laurel to California black oak over the course of the 100-year simulation for 3 ecoregions for all 3 disturbance scenarios: fire, disease, and fire and disease. Solid line indicates the average and the shaded region is the standard deviation for the 30 simulations.

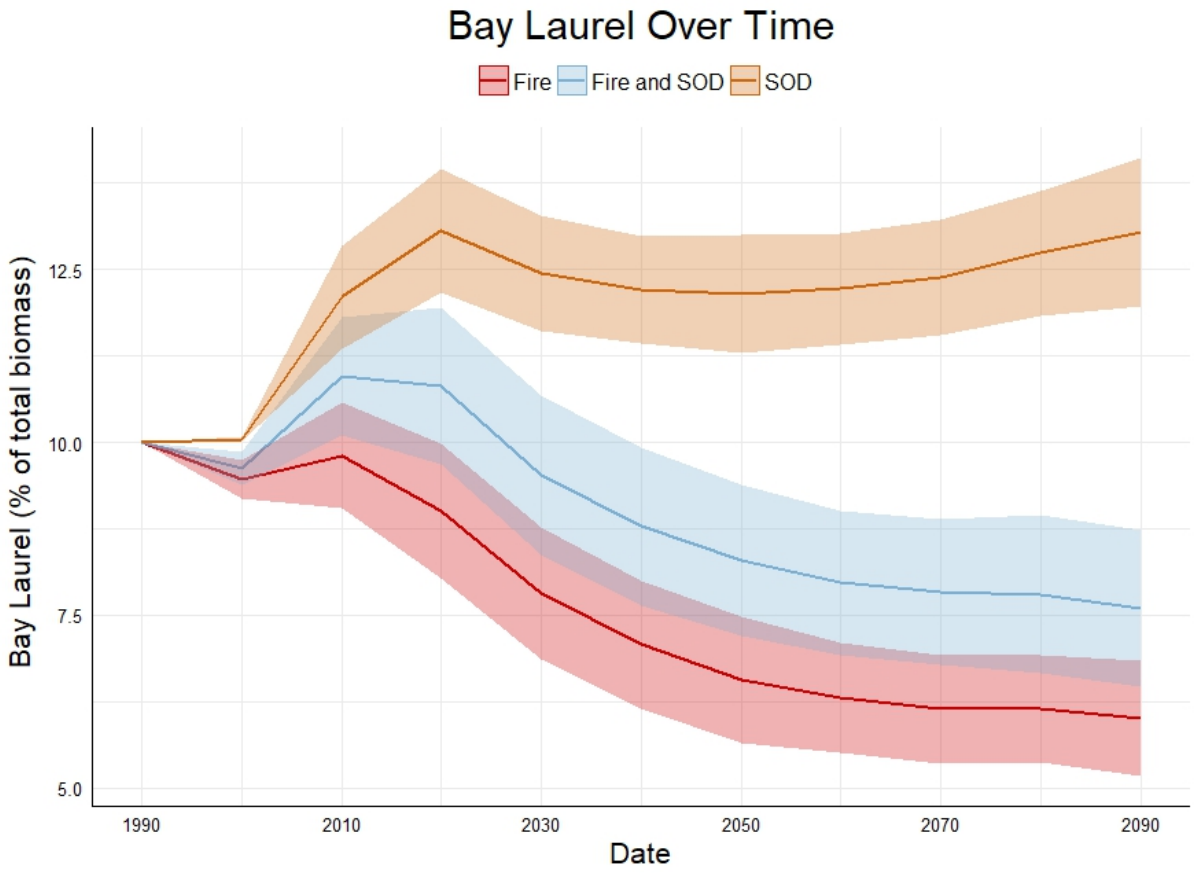

Figure 28: Bay Laurel over the course of the 100-year simulation for all 3 disturbance scenarios: fire, disease, and fire and disease. Solid line indicates the average and the shaded region is the standard deviation for the 30 simulations.

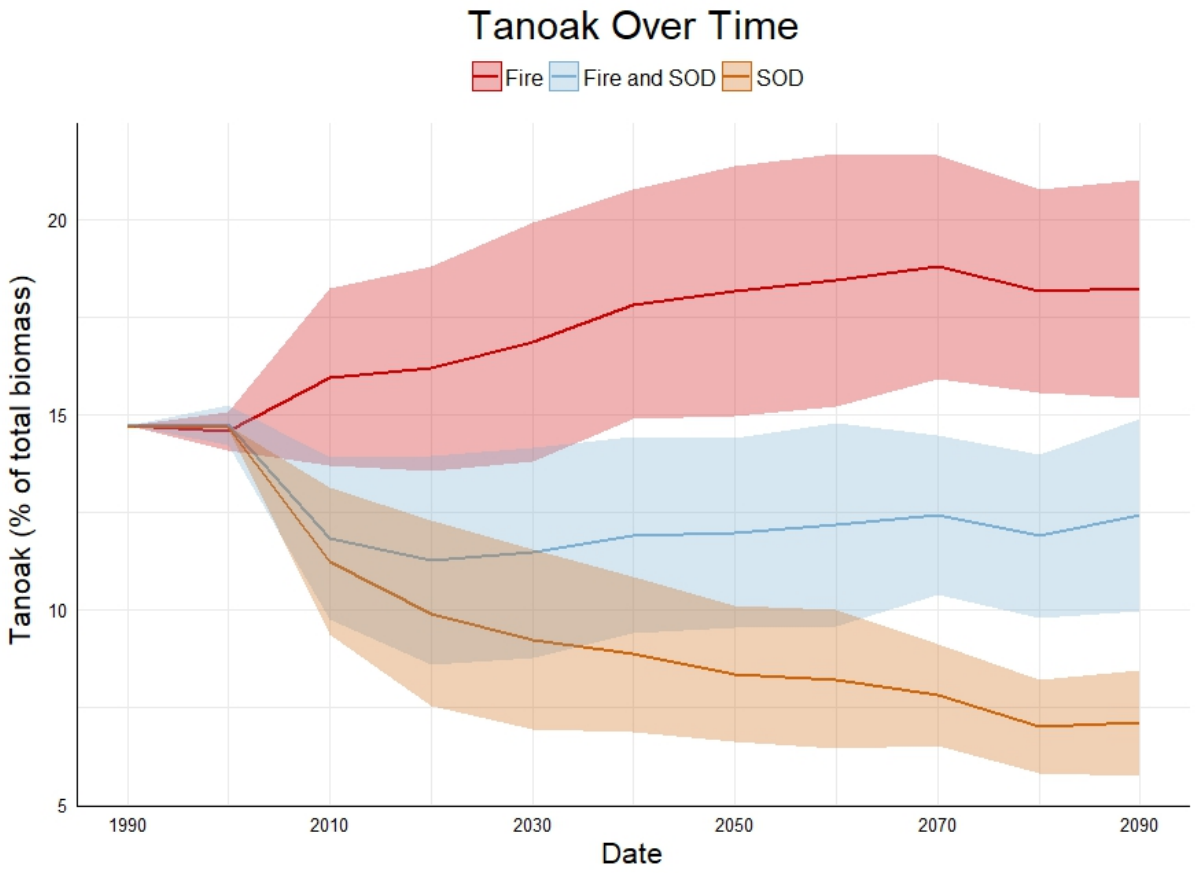

Figure 29: Tanoak over the course of the 100-year simulation for all 3 disturbance scenarios: fire, disease, and fire and disease. Solid line indicates the average and the shaded region is the standard deviation for the 30 simulations.

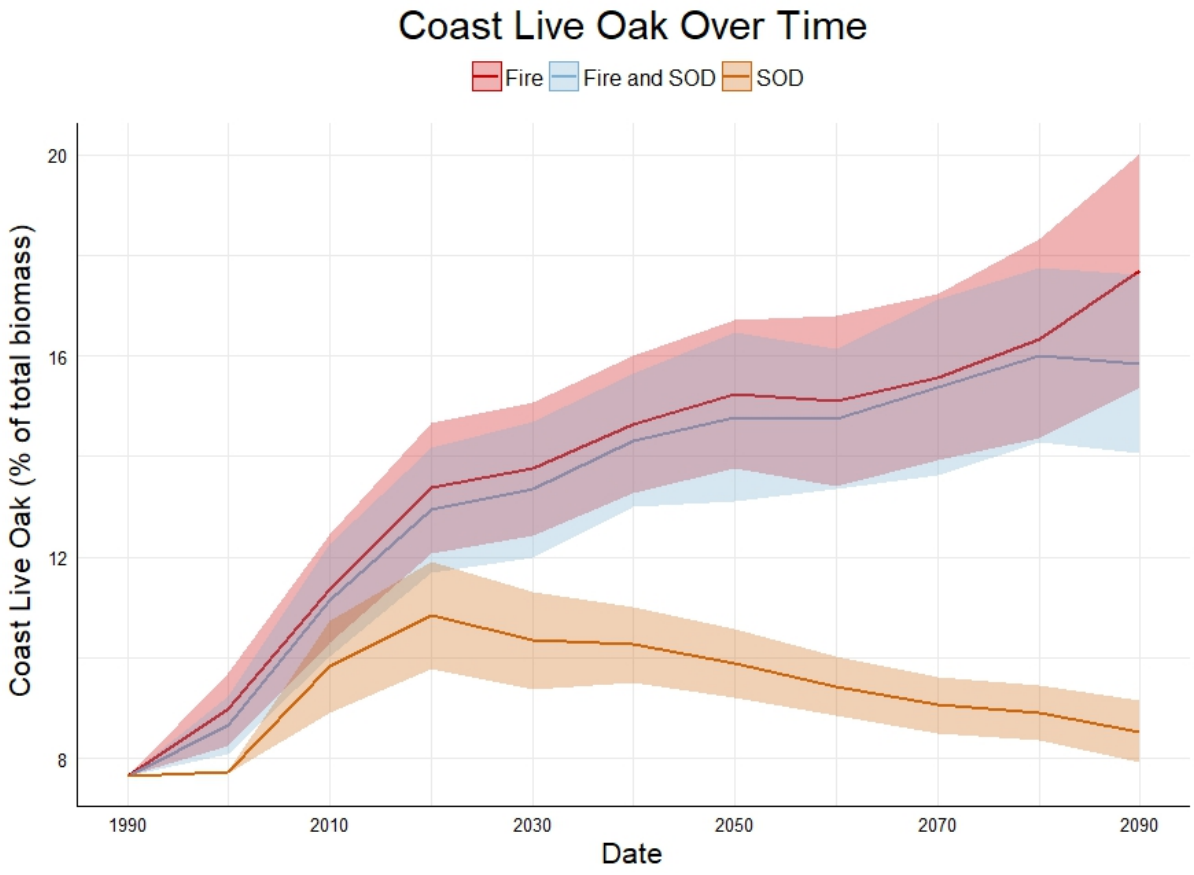

Figure 30: Coast live oak over the course of the 100-year simulation for all 3 disturbance scenarios: fire, disease, and fire and disease. Solid line indicates the average and the shaded region is the standard deviation for the 30 simulations.

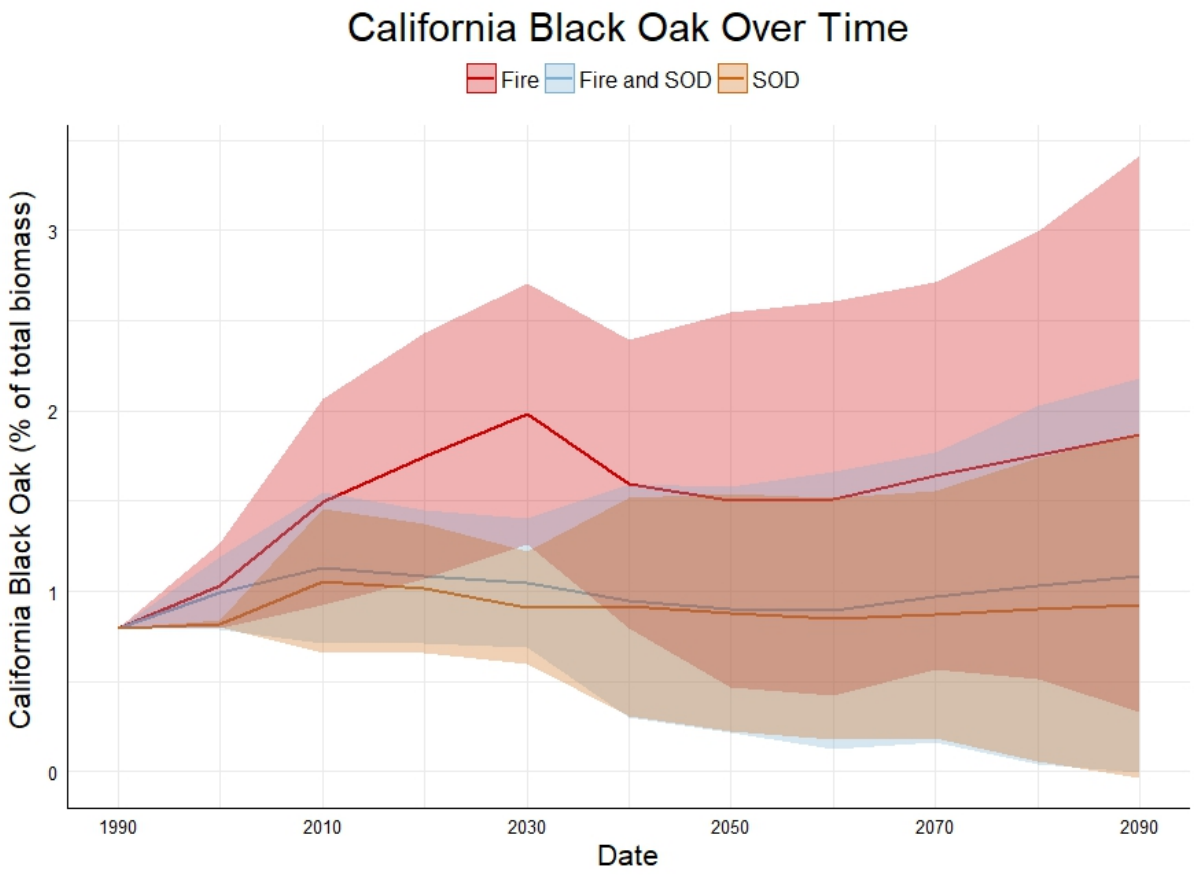

Figure 31: Bay Laurel over the course of the 100-year simulation for all 3 disturbance scenarios: fire, disease, and fire and disease. Solid line indicates the average and the shaded region is the standard deviation for the 30 simulations.

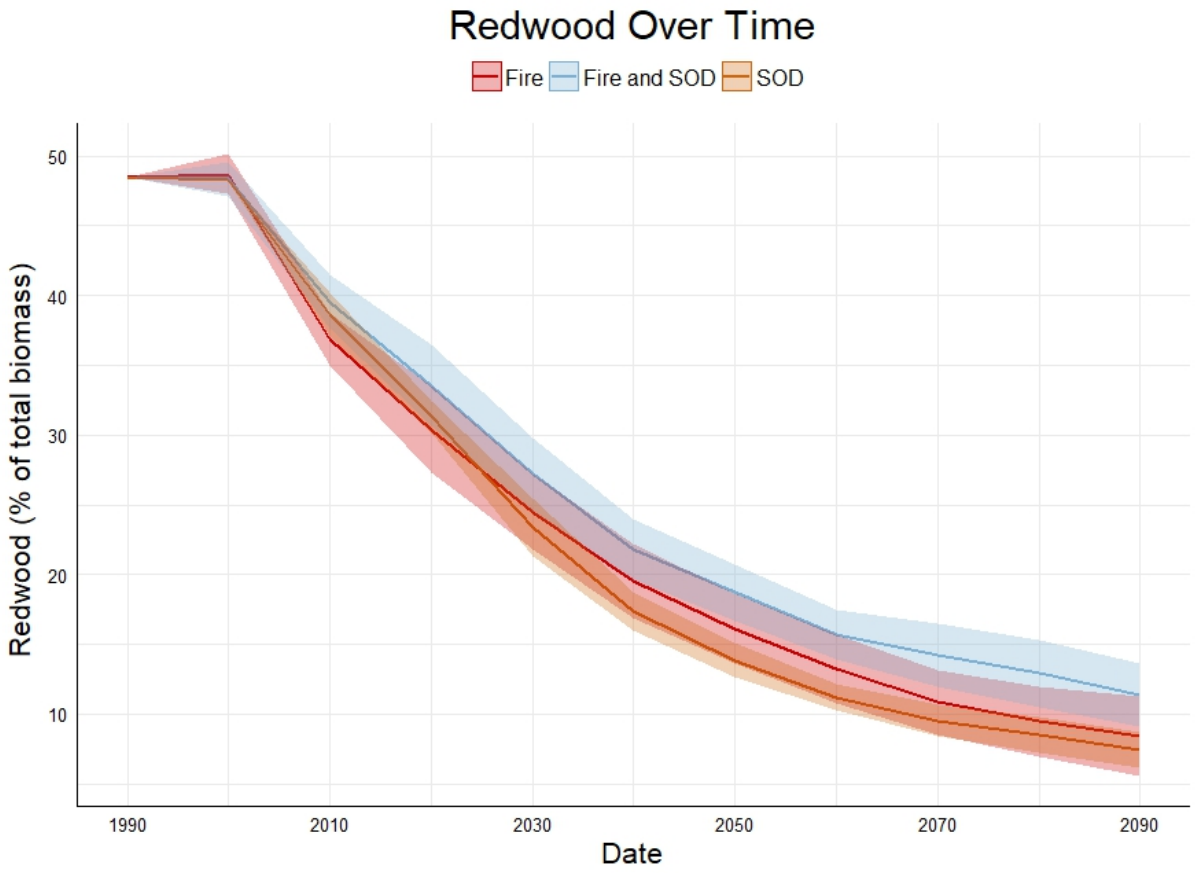

Figure 32: Redwood over the course of the 100-year simulation for all 3 disturbance scenarios: fire, disease, and fire and disease. Solid line indicates the average and the shaded region is the standard deviation for the 30 simulations.

Conclusions

Forest pests and pathogens can interact with fire regime through changes in fuel load due to disease/pest related decline and mortality. These interactions often involve non-linear dynamics, resulting in different outcomes depending on time since disturbance and environmental conditions. For example, empirical analysis of the effect of disease on fire severity after the 2008 chalk and basin complex fires in Big Sur, CA revealed that disease had no significant effect on fire severity unless stage of disease was taken into account. In this analysis they discovered that plots in the early stage of disease had a higher fire severity than other

disease stages and non-infected plots that were located within the fire perimeters (Metz et al. 2010). Empirical and modeling studies in bark beetle systems have shown no relationship between bark beetle outbreaks and fire severity and area burned even though there are occasional very large high severity fires that occur (M. J. Jenkins et al. 2008; Hart et al. 2015).

Our results suggest that at both the landscape- and ecoregion-level average fire size and fire severity decrease compared to a natural fire regime without disease present. The patchy nature of the disease and the mortality associated with it are possible reasons for this difference (Cobb, Filipe, et al. 2012; Meentemeyer et al. 2011). This may also explain why there is more variability in the number of fires in the fire and disease scenario compared to fire only. While there is a change in fuel load when disease mortality occurs, the patchy nature of the disease makes the fuel less continuous compared to other disturbances and thus timing and location of fire events relative to disease related mortality are important factors to consider. The fire severity by disease stage analysis reveals that time since disturbance is an important factor in fire severity over long time periods. These results match those found by Metz et al. (2010) that found that fire severity increased during the early stage of disease. Linking this back to our additive theory of disturbance, the effect of disease on fire appears to be both an interaction modification and interaction chain. Here the interaction chain effect is shown through the increased variability in number of fires in the simulations. The interaction modification effects are shown in the fire disease dynamics where time since disturbance makes the modification either a synergism in early stages of the disease or an antagonism when disease mortality has occurred more than 4 years prior to fire occurrence.

Interacting disturbances often shape the landscape in unexpected ways even when the magnitude of one disturbance isn’t increased due to the presence of the other. This can result

from lack of recovery of the system between disturbances (Brian Buma, Poore, and Wessman 2014; B. Buma and Wessman 2011, 2013) or species specific resilience mechanisms making certain species better suited for multiple disturbances (B Buma and Wessman 2012). Empirical data suggests that occurrence of fire in areas affected by SOD increases the ability of oaks and tanoak to maintain roughly their current level of abundance on the landscape despite the negative effects of SOD, however, the structure of these forests will change due to the loss of large trees. This is primarily due to their ability to regenerate more readily post-fire than bay laurel, fire killing the pathogen, and older trees being more susceptible to disease than younger trees.

The changes in forest composition across the modeled disturbance scenarios suggest that oaks and tanoaks would increase relative to bay laurel in a fire only scenario and decrease relative to bay laurel in the SOD only scenario. Both of these results are expected based on disease dynamics, fire-tolerance, and post-fire regeneration. Oaks and tanoaks have a higher fire tolerance and grow more rapidly after resprouting than bay laurel. The ratio of bay laurel to tanoak in the fire + SOD scenario initially increases along with the SOD only scenario, but then decreases along with the fire only scenario. The final ratio is between the two disturbance scenarios of the individual disturbances. The ratio of bay laurel to coast live oak in the fire and SOD scenario trends more toward the fire only scenario suggesting fire has a greater effect on this interaction than disease. The ratio of bay laurel to California black oak in the fire and SOD scenario is roughly between the 2 individual disturbance scenarios. These ratios are likely shaped by the individual species responses to the multiple disturbance.

Results suggest that both bay laurel and coast live oak abundance at a landscape level respond more to fire than to SOD. California black oak seems to respond more to SOD than fire but variability between simulations is much greater than between disturbance differences.

Tanoak appears to initially respond more to SOD than to fire but over time the effect of both disturbances equalizes.

Another factor affecting these results is the response of redwood to warming temperatures during the simulation. There is a large decrease in redwood abundance in our study area over the course of the simulations. The relative lack of response to the disturbance scenarios and small variance between simulations relative to the magnitude of the loss in redwood biomass suggests that this change is driven by a change in climate. A modeling study by Fernandez et al. (2015) suggests that as much as 80% of redwoods would be lost by 2030 in the southern portion of the redwood range if temperatures were to increase in the future. The Big Sur is in the southern portion of the redwood range. The loss of redwood opens up large areas of potential habitat for other species and creates a shift in ecosystem type. Our results suggest that a combination of canyon live oak, coulter pine, sycamore, tanoak, interior live oak, and coast live oak will benefit most from the decline in redwood, however, there is variation in which species benefits most based on the disturbance scenario. Under a fire only scenario the model projects that oak species would primarily replace redwoods. While under a SOD only scenario coulter pines, sycamore and non-susceptible oak species would benefit most. These results suggest that depending on environmental conditions, timing and type of disturbance events, and future climatic conditions, forests in the Big Sur will likely experience a shift away from the redwood dominant forests to a combination of oak woodlands and mixed evergreen forests.

This work highlights the complex nature of disease dynamics and interacting disturbances. Future work will explore changes in forest age structure, management scenarios based on goals of stakeholders in the area, and exploration of the biodiversity disease risk hypothesis during multiple disturbances. In order to explore these questions, the EDA model will

be further improved to include disease build-up in a site over-time and an adaptive management extension will be developed.

CHAPTER 5: CONCLUSIONS

Human activity is causing large-scale changes to forested ecosystems due to a combination of introduced forest pests and pathogens and climate change. The changes caused by many of these invasive forest pests and pathogens over long time periods is unknown due to the relatively recent introduction of many of them. However, evidence points to dramatic shifts in forest composition for pathogens that selectively remove hosts and potentially compound interactions with natural disturbances (Brian Buma, Poore, and Wessman 2014; Prospero and Cleary 2017). In this dissertation, I co-developed a dynamic epidemiological model for the LANDIS-II FLSM and used it to explore changes in forest composition and fire regime in Big Sur, CA under three disturbance scenarios: fire, disease, and fire and disease.

In chapter 2, I show that utilizing parallelization in forest landscape simulation models can mitigate the necessity for the tradeoff in spatial resolution and spatial extent. In chapter 3, I developed a dynamic epidemiological model that interacts with a FLSM and examined accuracy in a highly heterogeneous environment, Big Sur, CA. In chapter 4, I used the dynamic epidemiological model coupled with a FLSM and fire model to examine the effects of a novel disease on the natural fire regime and the effects of interacting disturbances on forest composition over the course of a century.

This research makes three primary contributions to the fields of landscape ecology, physical geography, and disease/disturbance ecology.

(1) Improvements in forest landscape simulation modeling. Forest landscape simulation models (FLSMs) often require tradeoffs between spatial resolution and extent, due to the computational complexity of these models. By introducing parallelization to the FLSM modeling framework I was able to reduce the need for this tradeoff. This allows for smaller spatial resolutions to be used to further increase understanding of processes in highly heterogeneous environments.

(2) Improving forest epidemiological modeling. The dynamic epidemiological model presented in chapter 3 achieves several advances compared to other forest epidemiological models: (1) separates host competency from host susceptibility, (2) includes disease related mortality, (3) includes link to model of species composition due to forest growth, succession, and regeneration, (4) includes asymmetries in host competency and susceptibility by species and age classes. Separating host competency from host susceptibility allow us to more accurately capture disease dynamics. For instance, oaks play no role in the spread of *P. ramorum* (no competency) but experience disease related decline and mortality (high susceptibility). Previous models (Meentemeyer et al. 2011) have included asymmetries in host competency by species but not by age class. This distinction allows for increased inoculum production as trees age, grow, and have more leaf area for spore production. Despite these advances the model could be improved by: (1) allowing disease build up in a site over time, (2) include an option for anisotropic spread (3) include an option for inoculum production based on leaf biomass within a site rather than by age class.

(3) Understanding the impacts of novel disease on natural fire regime and forest composition. This work offers insights into how forests will respond to the introduction of a novel disease with asymmetric host competency and susceptibility. This includes interactions

with the natural disturbance regime. Interactions between disturbances can often have synergistic or antagonistic effects on forest composition. The results of our model suggest that the timing of these two disturbance events relative to each other largely determines the nature of the interaction. During the early stage of the disease, when tree decline and mortality have happened recently fire severity is increased, however, the temporal window for this synergistic interaction is small. During other stages of disease fire severity is decreased and this interaction dominates at a landscape level over long-time periods due to a higher frequency of occurrence. Individual tree species respond differently to the interaction between fire and SOD and this is largely driven by their susceptibility to disease and adaptations to fire (i.e. fire-tolerance and post fire regeneration strategy).

In summary, this dissertation seeks to connect plant epidemiology and forest modeling in order to understand how invasive forest diseases alter natural disturbance regimes and potential change forest composition over the course of a century. In this research, I show that linking models of epidemiology, fire, and forest composition can aid in our understanding of interacting disturbances and their effects of forest ecosystems. The results of this work support existing theories on forest composition changes due to disease dynamics, that tanoak and oak species will survive in the ecosystem but at lower levels. The results of this modeling work also support the idea that time since disturbance is equally/more important than the actual disturbance in determining the effect on subsequent disturbances.

APPENDIX 1: SUPPLEMENTAL TABLES

Tables A1-A10, A11-A12, and A13-A15 contain all parameter values used to run the LANDIS-II NECN extension (version 4.1), EDA extension (version 1.1), and Dynamic Fuel and Fire extension (version 2.0.5) for Big Sur, CA. Values were averaged where multiple sources were available. Where no literature was available, values were approximated from similar species or previous studies, or were adjusted during calibration. Species are bristlecone fir (Abiebrac), grand fir (Abiegran), bigleaf maple (Acermacr), California buckeye (Aesccali), white alder (Alnurhom), red alder (Alnurubr), pacific madrone (Arbumenz), tanoak (Lithdens), knobcone pine (Pinuatte), Coulter pine (Pinucoul), sugar pine (Pinulamb), singleleaf pinyon (Pinumono), ponderosa pine (Pinupond), Monterey pine (Pinuradi), gray pine (Pinusabi), California sycamore (Platrace), balsam poplar (Popubals), big-cone Douglas fir (Pseumacr), Douglas fir (Pseumenz), California live oak (Queragri), canyon live oak (Querchry), blue oak (Querdoug), Oregon white oak (Quergarr), California white oak (Querloba), interior live oak (Querwisl), redwood (Sequsemp), California bay laurel (Umbecali). If all parameters were set the same across ecoregions, the ecoregion name is shown as "All ecoregions".

Species Shade Class	Probability by actual shade					
	0	1	2	3	4	5
1	1	1	0.5	0.1	0	0
2	0.75	1	1	0.5	0.1	0
3	0.25	0.75	1	1	0.5	0.1
4	0.25	0.5	0.75	1	1	0.5
5	0.1	0.25	0.5	0.75	1	1

Table A1: Light establishment table.

Shade Class	All Ecoregions
1	15%
2	25%
3	45%
4	55%
5	75%

Table A2: Available light biomass.

Active	MapCode	Name	Description
no	0	BS0	None
yes	1	BS1	Water
yes	2	BS2	Barren
yes	3	BS3	Mixed Evergreen
yes	4	BS4	California Coastal Redwood Forest
yes	5	BS5	Dry Mesic Mixed Conifer Forest
yes	6	BS6	Lower Montane Black Oak Conifer Forest
yes	7	BS7	Southern California Coastal Scrub
yes	8	BS8	California Maritime Chaparral
yes	9	BS9	California Mesic Chaparral
yes	10	BS10	California Montane Woodlandand
yes	11	BS11	Central California Dry Mesic Chaparral
yes	12	BS12	California Coastal Live Oak Woodland
yes	13	BS13	Northern California Coastal Scrub
yes	14	BS14	California Southern Coastal Grassland
yes	15	BS15	California Northern Coastal Grassland
yes	16	BS16	California Montane Riparian
yes	17	BS17	California CoastalConifer Forest

Table A3: Ecoregions

Species	Longe-vity	Sexual maturity	Shade tolerance	Fire tolerance	Seed dispersal distance effective	Seed dispersal distance Max	Vegetative Rep prob	Sprout age Min	Sprout age Max	Post-fire regeneration
Abiebrac	300	20	4	1	60	100	0	0	0	none
Abiegran	325	20	4	3	120	400	0	0	0	none
Acermacr	200	10	4	2	54	150	0.7	1	150	resprout
Aesccali	300	10	2	1	14	40	0.8	1	300	resprout
Alnurhom	160	10	2	1	100	1000	0	0	0	none
Alnurubr	120	10	2	2	250	1000	0.2	2	15	resprout
Arbumenz	400	6	3	1	50	100	0.2	5	400	resprout
Lithdens	400	5	3	3	48	1000	0.7	0	400	resprout
Pinuatte	120	10	1	1	48	1000	0	0	0	none
Pinucoul	160	10	1	3	50	100	0	0	0	serotiny
Pinulamb	550	20	3	3	30	1000	0	0	0	none
Pinumono	1000	20	1	1	24	1000	0	0	0	none
Pinupond	929	7	2	4	140	1000	0	0	0	none
Pinuradi	120	5	3	3	70	1000	0	0	0	serotiny
Pinusabi	200	10	2	2	40	1000	0	0	0	none
Platrace	160	6	1	1	70	225	0.4	5	150	resprout
Popubals	200	8	1	2	400	3000	0.5	0	200	resprout
Pseumacr	700	20	2	4	60	600	0	0	0	none
Pseumenz	1350	15	2	4	140	1400	0	0	0	none
Queragri	300	10	2	5	50	2000	0.6	1	250	resprout
Querchry	310	20	2	2	60	2000	0.6	1	300	resprout
Querdoug	400	10	2	4	40	2000	0.25	1	200	resprout
Quergarr	500	10	2	5	60	2000	0.6	1	500	resprout
Querkell	500	30	2	4	50	2000	0.6	1	400	resprout
Querloba	600	10	2	4	90	2000	0.6	1	200	resprout
Querwisl	400	10	2	3	30	2000	0.6	1	200	resprout
Sequsemp	2200	10	5	5	200	1000	0.8	1	2000	resprout
Umbecali	200	30	3	1	36	120	0.6	1	200	resprout

Table A4: General species parameters

Species	Functional Type	N Fixer	GDD Min	GDD Max	Min January Temperature	Drought Tolerance	Leaf Long	Epicormic Resprout
Abiebrac	2	N	500	2450	-17	0.5	6	N
Abiegran	2	N	500	2450	-14	0.5	7	N
Acermacr	5	N	550	3600	-8	0.45	1	N
Aesccali	5	N	1400	4400	2	0.6	1	N
Alnurhom	5	Y	800	2950	-9	0.4	1	N
Alnurubr	5	Y	400	2950	-15	0.4	1	N
Arbumenz	5	N	900	3700	-4	0.5	1	N
Lithdens	4	N	1200	3400	-2	0.6	4	N
Pinuatte	2	N	1200	3600	-3	0.6	5	N
Pinucoul	2	N	1800	4200	5	0.6	3.5	N
Pinulamb	2	N	600	3600	-4	0.6	3	N
Pinumono	2	N	1000	4000	-8	0.6	7	N
Pinupond	2	N	400	2800	-15	0.6	5	N
Pinuradi	2	N	815	2866	-4	0.6	4	N
Pinusabi	2	N	1200	4400	0	0.6	4	N
Platrace	5	N	1500	5000	7	0.5	1	N
Popubals	5	N	200	2491	-30	0.267	1	N
Pseumacr	2	N	1200	3600	5	0.6	5	Y
Pseumenz	2	N	200	2800	-17	0.6	5	N
Queragri	4	N	1800	4800	5	0.6	2	Y
Querchry	4	N	900	4000	-3	0.6	2	Y
Querdoug	5	N	2000	4600	2	0.6	1	N
Quergarr	5	N	900	3400	-4	0.6	1	Y
Querkell	5	N	1100	3800	-4	0.6	1	Y
Querloba	5	N	2000	4800	4	0.6	1	Y
Querwisl	4	N	800	4200	-1	0.6	1	N
Sequsemp	1	N	400	4000	5	0.25	10	Y
Umbecali	4	N	1100	4200	-1	0.5	2	Y

Table A5.1: NECN succession species parameter

Species	Lignin Content				C:N Ratio				
	Leaf	Fine Root	Wood	Coarse Root	Leaf	Fine Root	Wood	Coarse Root	Litter
Abiebrac	0.25	0.22	0.35	0.35	42	27	500	170	77
Abiegran	0.25	0.22	0.35	0.35	42	27	500	170	77
Acermacr	0.18	0.22	0.26	0.26	24	31	444	90	62
Aesccali	0.18	0.23	0.23	0.21	27	48	352	200	40
Alnurhom	0.22	0.15	0.26	0.26	22	25	246	90	28
Alnurubr	0.22	0.15	0.26	0.26	22	25	246	90	28
Arbumenz	0.22	0.26	0.26	0.26	25	45	412	90	100
Lithdens	0.21	0.25	0.25	0.25	41	42	352	200	72
Pinuatte	0.17	0.20	0.25	0.25	53	53	250	170	100
Pinucoul	0.17	0.20	0.25	0.25	53	53	250	170	100
Pinulamb	0.17	0.20	0.25	0.25	53	53	278	185	100
Pinumono	0.17	0.20	0.25	0.25	53	53	250	170	100
Pinupond	0.28	0.20	0.26	0.26	48	48	250	170	100
Pinuradi	0.28	0.02	0.25	0.25	48	48	250	170	100
Pinusabi	0.28	0.20	0.25	0.25	48	48	250	170	100
Platrace	0.26	0.22	0.20	0.20	22	25	336	49	65
Popubals	0.26	0.23	0.2	0.2	22	25	336	49	65
Pseumacr	0.20	0.25	0.26	0.34	42	52	455	200	77
Pseumenz	0.20	0.25	0.26	0.34	42	52	455	200	77
Queragri	0.18	0.21	0.21	0.21	27	48	352	200	33
Querchry	0.18	0.21	0.21	0.21	27	48	352	200	33
Querdoug	0.18	0.23	0.23	0.23	27	48	352	200	33
Quergarr	0.18	0.23	0.23	0.23	27	48	352	200	33
Querkell	0.18	0.23	0.23	0.23	27	48	352	200	33
Querloba	0.18	0.23	0.23	0.21	27	48	352	200	33
Querwisl	0.18	0.21	0.21	0.21	27	48	352	200	33
Sequsemp	0.28	0.35	0.35	0.35	49	82	455	214	100
Umbecali	0.18	0.21	0.21	0.21	29	41	352	200	61

Table A5.2: NECN succession species parameters continued

Name	Index	Temperature Parameters				Leaf	Leaf Area Index Parameters		
		Mean PDDF1	Max PPDF2	PPDF3	PPDF4	Fraction	BTOLAI	KLAI	MAXLAI
Redwood	1	23	40	1.4	4.6	0.3	0.01	1000 0	15
Conifer	2	27	42	1.3	4.4	0.3	0.01	8000	12
Broad Leaf Evergreen	4	30	45	1	3.5	0.32	0.0001	2000	9
Broad Leaf Deciduous	5	30	45	1	3.5	0.32	0.0001	2000	8

Table A6.1: NECN succession functional group parameters.

Name	Drought Parameters		Wood	Monthly	Age Mortality	Drop	Coarse Root	Fine Root
	PPRPTS2	PPRPTS3	Decay Rate	Wood Mortality	Shape	Month	Fraction	Fraction
Redwood	0.1	0.4	0.05	0.0008	15	9	0.18	0.29
Conifer	0.1	0.2	0.05	0.0008	15	9	0.23	0.2
Broad Leaf Evergreen	0.1	0.2	0.05	0.0008	15	10	0.2	0.25
Broad Leaf Deciduous	0.1	0.1	0.05	0.0008	15	10	0.19	0.25

Table A6.2: NECN succession functional group parameters continued

Species	Soil Depth	Percent Clay	Percent Sand	Field Cap	Wilting Point	Storm Flow Fraction	Base Flow Fraction	Drainage Class
BS1	100	0.148	0.615	0.2229	0.092	0.2	0.2	0.8
BS2	100	0.169	0.549	0.246	0.098	0.2	0.2	0.8
BS3	100	0.207	0.514	0.263	0.111	0.2	0.2	0.8
BS4	100	0.21	0.496	0.267	0.112	0.2	0.2	0.8
BS5	100	0.198	0.489	0.265	0.107	0.2	0.2	0.8
BS6	100	0.177	0.52	0.253	0.101	0.2	0.2	0.8
BS7	100	0.195	0.526	0.257	0.107	0.2	0.2	0.8
BS8	100	0.141	0.563	0.236	0.089	0.2	0.2	0.8
BS9	100	0.2	0.52	0.26	0.108	0.2	0.2	0.8
BS10	100	0.208	0.504	0.265	0.111	0.2	0.2	0.8
BS11	100	0.203	0.519	0.261	0.11	0.2	0.2	0.8
BS12	100	0.201	0.521	0.26	0.109	0.2	0.2	0.8
BS13	100	0.202	0.524	0.26	0.109	0.2	0.2	0.8
BS14	100	0.223	0.461	0.277	0.116	0.2	0.2	0.8
BS15	100	0.179	0.564	0.246	0.102	0.2	0.2	0.8
BS16	100	0.199	0.526	0.259	0.108	0.2	0.2	0.8
BS17	100	0.171	0.533	0.249	0.099	0.2	0.2	0.8

Table 7.1: Ecoregion parameters. Soil organic matter (SOM) is divided into four pools (SOM1-surface, SOM1-soil, SOM2 and SOM3) based on the Century soil model (Parton et al. 1983). Data derived from ("Web Soil Survey" 2014; N. P. Office 2017; Zhang et al. 2012; Fenn et al. 2003).

Ecoregion	Nitrogen Inputs		Latitude		SOM Decay Rates			Denitrification
	Intercept	Slope		surf	SOM1	SOM2	SOM3	
BS1	0.0004	0.01	36	0.3	0.07	0.007	0.00005	0.001
BS2	0.0004	0.01	36	0.3	0.07	0.007	0.00005	0.001
BS3	0.0004	0.01	36	0.3	0.07	0.007	0.00005	0.001
BS4	0.0004	0.01	36	0.3	0.07	0.007	0.00005	0.001
BS5	0.0004	0.01	36	0.3	0.07	0.007	0.00005	0.001
BS6	0.0004	0.01	36	0.3	0.07	0.007	0.00005	0.001
BS7	0.0004	0.01	36	0.3	0.07	0.007	0.00005	0.001
BS8	0.0004	0.01	36	0.3	0.07	0.007	0.00005	0.001
BS9	0.0004	0.01	36	0.3	0.07	0.007	0.00005	0.001
BS10	0.0004	0.01	36	0.3	0.07	0.007	0.00005	0.001
BS11	0.0004	0.01	36	0.3	0.07	0.007	0.00005	0.001
BS12	0.0004	0.01	36	0.3	0.07	0.007	0.00005	0.001
BS13	0.0004	0.01	36	0.3	0.07	0.007	0.00005	0.001
BS14	0.0004	0.01	36	0.3	0.07	0.007	0.00005	0.001
BS15	0.0004	0.01	36	0.3	0.07	0.007	0.00005	0.001
BS16	0.0004	0.01	36	0.3	0.07	0.007	0.00005	0.001
BS17	0.0004	0.01	36	0.3	0.07	0.007	0.00005	0.001

Table 7.2: Ecoregion parameters continued.

	SOM1 C surface	SOM1 N surface	SOM1 C soil	SOM1 N soil	SOM3 C	SOM2 N	SOM3 C	SOM3 N	Mineral N
BS1	25	8	75	20	1250	200	1150	172	4
BS2	25	8	75	20	1250	200	1150	172	4
BS3	65	19	195	48	3250	474	2990	408	10
BS4	145	35	435	88	7250	874	6670	751	18
BS5	61	16	183	40	3050	399	2806	343	8
BS6	55	13	165	33	2750	324	2530	279	7
BS7	40	12	120	30	2000	300	1840	258	6
BS8	40	12	120	30	2000	300	1840	258	6
BS9	40	12	120	30	2000	300	1840	258	6
BS10	40	12	120	30	2000	300	1840	258	6
BS11	40	12	120	30	2000	300	1840	258	6
BS12	62	17	186	43	3100	424	2852	365	9
BS13	38	10	114	25	1900	250	1748	215	5
BS14	38	10	114	25	1900	250	1748	215	5
BS15	38	10	114	25	1900	250	1748	215	5
BS16	38	10	114	25	1900	250	1748	215	5
BS17	58	14	174	35	2900	349	2668	300	7

Table 8: Initial ecoregion parameters. SOM = soil organic matter, C = carbon, N = nitrogen. All values in units g/m^{-2}.

Species	BS1	BS2	BS3	BS4	BS5	BS6	BS7	BS8	BS9
Abiebrac	100	100	6238	2241	6238	100	2241	6238	6238
Abiegran	100	100	3877	3877	100	100	100	100	100
Acermacr	1163	100	14007	14007	14007	9221	9221	14007	14007
Aesccali	12258	100	12258	12258	12258	4903	3547	12258	12258
Alnurhom	100	100	5664	5664	5664	626	626	5664	5664
Alnurubr	100	1163	9013	1163	9013	9013	100	1163	1163
Arbumenz	27104	5820	31310	29235	31310	31310	27104	21522	27104
Lithdens	40559	100	65973	40559	65973	65973	28274	33458	40559
Pinuatte	100	100	4102	4102	4102	4102	4102	4102	4102
Pinucoul	16667	7310	16667	16667	16667	7310	16667	7770	16667
Pinulamb	100	1055	1055	100	1055	100	100	100	100
Pinumono	100	4343	8743	100	4240	100	100	100	4343
Pinupond	3167	100	13985	8401	13985	707	3167	13985	13985
Pinuradi	63516	7065	63516	63516	7065	63516	63516	7065	63516
Pinusabi	4809	9717	11782	11782	9717	9717	9717	11782	11782
Platrace	3207	100	10737	10737	10737	1042	5039	10737	10737
Popubals	100	100	8607	8607	8607	100	100	100	100
Pseumacr	100	6284	6284	100	6284	100	100	100	100
Pseumenz	4307	100	35916	35916	33789	33789	12579	6848	33789
Queragri	46689	45685	68788	68788	64080	45685	50384	64080	64080
Querchry	31704	33612	44072	33612	44072	44072	20648	44072	44072
Querdoug	100	6255	17676	17040	17040	6081	3248	12951	20207
Quergarr	100	100	31075	31075	12673	100	100	100	31075
Querkell	14248	100	18921	18921	18921	3547	14248	14248	14248
Querloba	100	100	15988	15988	15988	8420	15988	8420	15988
Querwisl	18057	8912	55159	55159	55159	15200	55159	55159	55159
Sequsemp	152535	100	152535	169535	152535	152535	152535	152535	152535
Umbecali	21383	10066	34912	34912	32012	23627	21383	32012	32012

Table 9.1: Maximum biomass. Values are in g m^{-2} and were estimated from the (GNN) database (http://lemma.forestry.oregonstate.edu/)

Species	BS10	BS11	BS12	BS13	BS14	BS15	BS16	BS17
Abiebrac	6238	6238	6238	2241	2241	2241	6238	100
Abiegran	100	100	100	100	100	100	3877	100
Acermacr	14007	14007	14007	14007	14007	14007	14007	100
Aesccali	3970	4903	12258	3970	12258	3964	12258	100
Alnurhom	5664	5664	5664	5664	5664	5664	5664	626
Alnurubr	1163	1163	9013	1163	1163	1163	9013	100
Arbumenz	27104	27104	27104	27104	23110	23110	27104	4657
Lithdens	33458	40559	40559	34604	33458	28274	65973	28274
Pinuatte	100	4102	4102	4102	4102	100	4102	100
Pinucoul	7310	16667	16667	16667	16667	7310	16667	16667
Pinulamb	1055	1055	1055	1055	100	1055	100	100
Pinumono	100	4343	2557	100	100	100	100	100
Pinupond	13985	13985	13985	3167	3167	3167	13985	100
Pinuradi	63516	63516	63516	63516	63516	63516	63516	63516
Pinusabi	4809	9717	11782	11782	11782	4809	9717	4809
Platrace	3207	10737	10737	10737	10737	10737	10737	3207
Popubals	100	100	8607	100	100	100	100	100
Pseumacr	6284	6284	6284	6284	100	6284	100	100
Pseumenz	3253	35916	35916	18453	18453	1182	35916	14957
Queragri	64080	64080	68788	64080	64080	64080	64080	49173
Querchry	44072	44072	44072	33612	44072	31675	44072	100
Querdoug	100	17040	20207	20508	17040	12951	5906	100
Quergarr	100	12673	31075	12673	31075	12673	31075	100
Querkell	12852	17187	18921	14248	14248	14248	14248	100
Querloba	8420	15081	20847	15988	15988	15081	8420	100
Querwisl	17829	55159	55159	55159	33771	32062	55159	11865
Sequsemp	152535	2E+05	152535	152535	152535	152535	152535	127835
Umbecali	32012	32012	34912	22216	32012	23183	32012	21383

Table 9.2: Maximum biomass continued.

Species	All Ecoregions
Abiebrac	250
Abiegran	250
Acermacr	175
Aesccali	175
Alnurhom	175
Alnurubr	150
Arbumenz	150
Lithdens	200
Pinuatte	250
Pinucoul	250
Pinulamb	250
Pinumono	250
Pinupond	250
Pinuradi	250
Pinusabi	250
Platrace	250
Popubals	250
Pseumacr	300
Pseumenz	300
Queragri	150
Querchry	150
Querdoug	150
Quergarr	150
Querkell	150
Querloba	150
Querwisl	150
Sequsemp	250
Umbecali	150

Table A10: Monthly maximum above-ground net primary productivity (ANPP) (g m^{-2}).

TransmissionRate	5
AcquisitionRate	0.45
DispersalType	STATIC
DispersalKernel	Power Law
DispersalMaxDist	37500
AlphaCoef	2.6

Table A11: EDA transmission parameters

SRD Modifer	Duration	Type
-0.25	5	Fire

Table 12: Disturbance modifiers for EDA site host index (SHI).

	Host Index (Competency)						Host Susceptibility						Change	Output
	Low		Medium		High		Low		Medium		High		Fuel	Mortality
Species	Age	Score	Age	Score	Age	Score	Age	Mort Prob	Age	Mort Prob	Age	Mort Prob		
Umbecali	5	3	15	6	25	10	999	0	999	0	999	0	no	no
Lithdens	5	2	20	5	60	8	5	0.14	15	0.25	30	0.3	yes	yes
Sequsemp	50	2	999	4	999	7	999	0	999	0	999	0	no	no
Acermacr	50	1	999	4	999	7	999	0	999	0	999	0	no	no
Aesccali	50	1	999	4	999	7	999	0	999	0	999	0	no	no
Arbumenz	50	1	999	4	999	7	999	0	999	0	999	0	no	no
Pseumenz	50	1	999	4	999	7	999	0	999	0	999	0	no	no
Querchry	999	1	999	4	999	7	20	0.01	25	0.05	50	0.1	yes	yes
Querkell	999	1	999	4	999	7	20	0.01	25	0.05	40	0.16	yes	yes
Queragri	999	1	999	4	999	7	20	0.01	25	0.05	50	0.1	yes	yes

Table A13: EDA species parameters.

Index	Base Type	Surface Type	Ignite Probability	a	b	c	q	BUI	maxBE	CBH
1	Conifer	C1	0.1	90	0.0649	4.5	0.9	72	1.076	2
2	Conifer	C2	0.1	110	0.0282	1.5	0.7	64	1.321	3
3	Conifer	C3	0.1	110	0.0444	3	0.75	62	1.261	8
4	Conifer	C4	0.1	110	0.0293	1.5	0.8	66	1.184	4
5	Conifer	C5	0.1	30	0.0697	4	0.8	56	1.22	18
6	Conifer	C6	0.1	30	0.08	3	0.8	62	1.197	62
7	Conifer	C7	0.1	45	0.0305	2	0.85	106	1.134	10
8	Deciduous	D1	0.1	30	0.0232	1.6	0.9	32	1.179	0
9	Conifer	M1	0.1	0	0	0	0.8	50	1.25	0
10	Conifer	M2	0.1	0	0	0	0.8	50	1.25	6
11	Conifer	M3	0.1	0	0	0	0.8	50	1.25	6
12	Conifer	M4	0.1	0	0	0	0.8	50	1.25	6
13	Slash	S1	0.1	75	0.0297	1.3	0.75	38	1.46	0
14	Slash	S2	0.1	40	0.0438	1.7	0.75	63	1.256	0
15	Slash	S3	0.1	55	0.0829	3.2	0.75	31	1.59	0
16	Open	O1a	0.1	190	0.031	1.4	1	1	1	0
17	Open	O1b	0.1	250	0.035	1.7	1	1	1	0

Table A14: Fuel type parameters.

Fuel Type	Base Fuel	Age Range	Species
5	Conifer	0 to 1000	Pi ıuatte Pinucoul Pinulamb Pinuradi Pinusabi
7	Conifer	100 to 1350	Abiebrac Abiegran Pinupond Pseumacr Pseumenz
8	Deciduous	0 to 600	Acermacr Aesccali Alnurhom Alnurubr Arbumenz Platrace Popubals Queragri Querchry Querdoug Quergarr Querkell Querloba Querwisl Umbecali
9	Conifer	0 to 1000	Sequsemp
10	Conifer	1000 to 2200	Sequsemp
16	Open	0 to 100	Abiebrac Abiegran Pinupond Pseumacr Pseumenz

Table A15: Species fuel type.

APPENDIX 2: SUPPLEMENTAL FIGURES/MOVIES

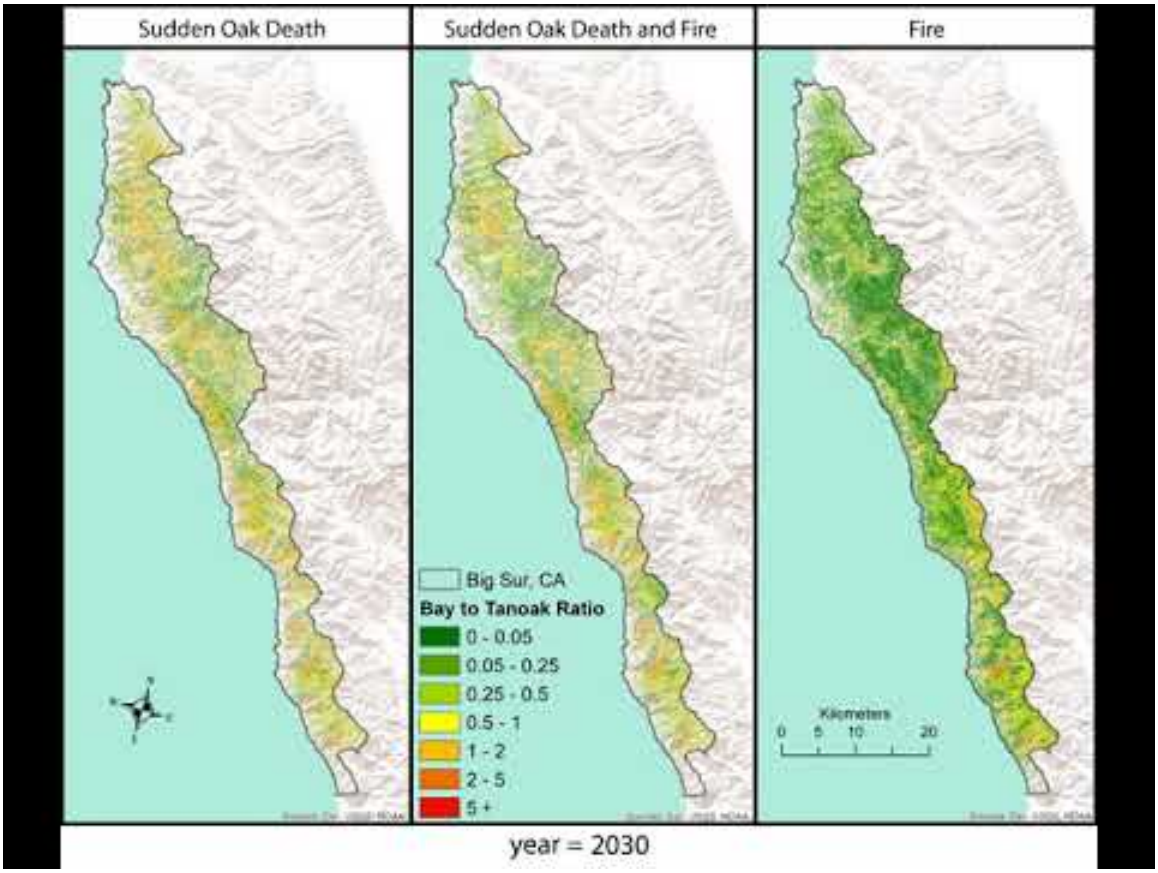

Figure A1: Bay laurel to tanoak ratio over time movie.

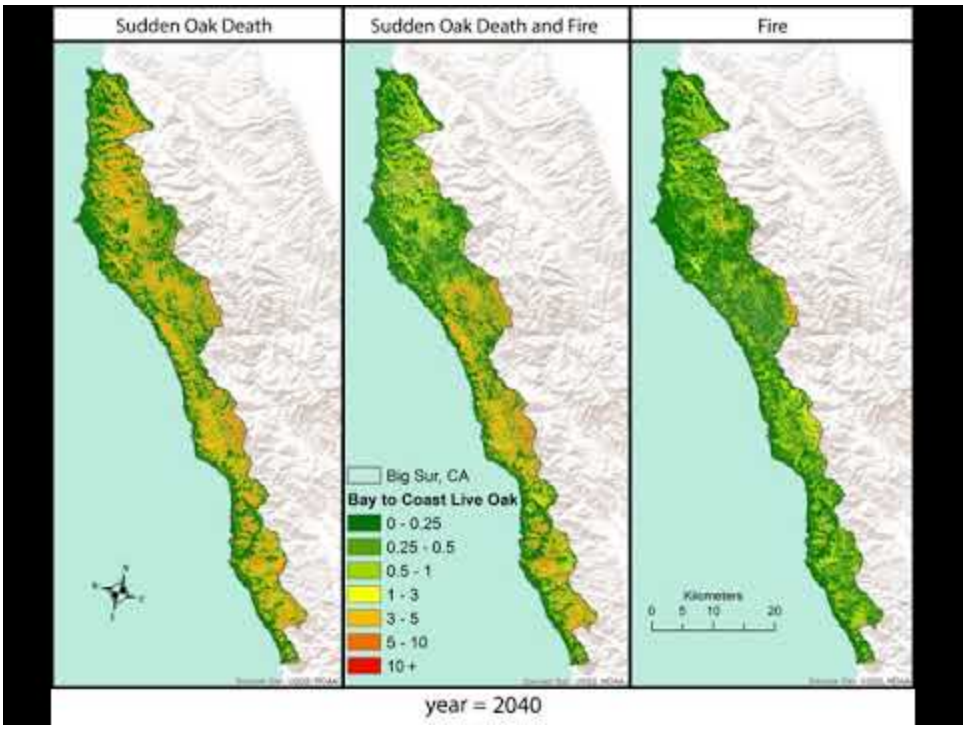

Figure A2: Bay laurel to coast live oak ratio over time movie.

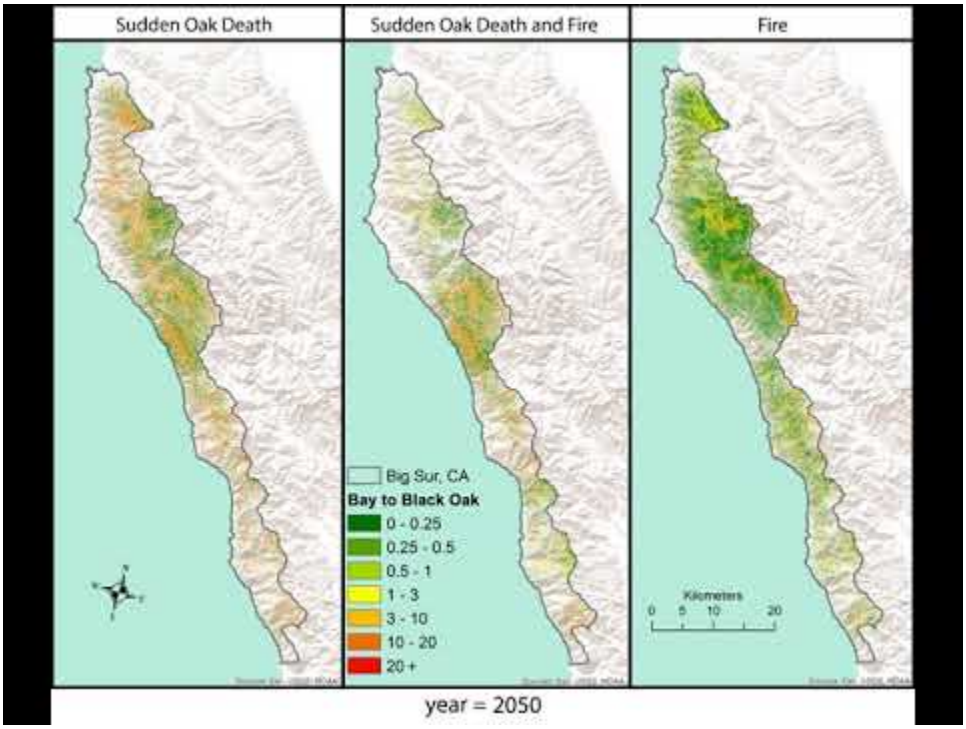

Figure A3: Bay laurel to California black oak ratio over time movie.

REFERENCES

Anderson, Pamela K, Andrew A Cunningham, Nikkita G Patel, Francisco J Morales, Paul R Epstein, and Peter Daszak. 2004. “Emerging Infectious Diseases of Plants: Pathogen Pollution, Climate Change and Agrotechnology Drivers.” *Trends in Ecology & Evolution* 19 (10): 535–44. doi:10.1016/j.tree.2004.07.021.

Aukema, J E, Brian Leung, Kent Kovacs, Corey Chivers, Kerry O Britton, Jeffrey Englin, Susan J Frankel, et al. 2011. “Economic Impacts of Non-Native Forest Insects in the Continental United States.” Edited by Brian Gratwicke. *PLoS ONE* 6 (9). Public Library of Science: e24587. doi:10.1371/journal.pone.0024587.

Aukema, J E, D G McCullough, B Von Holle, A M Liebhold, K Britton, and S J Frankel. 2010. “Historical Accumulation of Nonindigenous Forest Pests in the Continental United States.” *Bioscience* 60 (11): 886–97. doi:10.1525/bio.2010.60.11.5.

Battles, John J, Timothy Robards, Adrian Das, Kristen Waring, J Keith Gilless, Gregory Biging, and Frieder Schurr. 2008. “Climate Change Impacts on Forest Growth and Tree Mortality: A Data-Driven Modeling Study in the Mixed-Conifer Forest of the Sierra Nevada, California.” *Climatic Change* 87. Springer: 193–213.

Beh, Maia M., Margaret R. Metz, Kerri M. Frangioso, and David M. Rizzo. 2012. “The Key Host for an Invasive Forest Pathogen Also Facilitates the Pathogen’s Survival of Wildfire in California Forests.” *New Phytologist* 196 (4): 1145–54. doi:10.1111/j.1469-8137.2012.04352.x.

Bender, Edward A, Ted J Case, and Michael E Gilpin. 1984. “Perturbation Experiments in Community Ecology: Theory and Practice.” *Ecology* 65 (1): 1–13.

Boer, Pieter J Den. 1968. “Spreading of Risk and Stabilization of Animal Numbers.” *Acta Biotheoretica* 18 (1–4). Springer: 165–94.

Bouchard, Mathieu, and David Pothier. 2008. “Simulations of the Effects of Changes in Mean Fire Return Intervals on Balsam Fir Abundance, and Implications for Spruce Budworm Outbreaks.” *Ecological Modelling* 218 (3). Elsevier: 207–18.

Buma, B., and C. A. Wessman. 2011. “Disturbance Interactions Can Impact Resilience Mechanisms of Forests.” *Ecosphere* 2 (5): art64. doi:10.1890/ES11-00038.1.

———. 2013. “Forest Resilience, Climate Change, and Opportunities for Adaptation: A Specific Case of a General Problem.” *Forest Ecology and Management* 306. doi:10.1016/j.foreco.2013.06.044.

Buma, B, and C A Wessman. 2012. “Differential Species Responses to Compounded Perturbations and Implications for Landscape Heterogeneity and Resilience.” *Forest Ecology and Management* 266: 25–33.

Buma, Brian, Rebecca E. Poore, and Carol A. Wessman. 2014. “Disturbances, Their Interactions, and Cumulative Effects on Carbon and Charcoal Stocks in a Forested

Ecosystem." *Ecosystems* 17 (6): 947–59. doi:10.1007/s10021-014-9770-8.

CAL FIRE. 2014. "California Fire Perimeters and Size." http://frap.fire.ca.gov/projects/fire_data/fire_perimeters_index.

Callaway, Ragan M, and Carla M D'Antonio. 1991. "Shrub Facilitation of Coast Live Oak Establishment in Central California." *Madrono*. JSTOR, 158–69.

Cobb, R C, Maggie N Chan, Ross K Meentemeyer, and David M Rizzo. 2012. "Common Factors Drive Disease and Coarse Woody Debris Dynamics in Forests Impacted by Sudden Oak Death." *Ecosystems* 15 (2). Springer: 242–55.

Cobb, R C, Joao A N Filipe, Ross K Meentemeyer, Christopher A Gilligan, and David M Rizzo. 2012. "Ecosystem Transformation by Emerging Infectious Disease: Loss of Large Tanoak from California Forests." *Journal of Ecology* 100 (3). Wiley Online Library: 712–22.

Cobb, R C, R K Meentemeyer, and D M Rizzo. 2010. "Apparent Competition in Canopy Trees Determined by Pathogen Transmission rather than Susceptibility." *Ecology* 91 (2): 327–33. http://www.scopus.com/inward/record.url?eid=2-s2.0-77949284497&partnerID=40&md5=e815c187128e3a46b0c5fac917610c38.

Cobb, R C, Ross K. Meentemeyer, and David M. Rizzo. 2016. "Wildfire and Forest Disease Interaction Lead to Greater Loss of Soil Nutrients and Carbon." *Oecologia* 182 (1): 265–76. doi:10.1007/s00442-016-3649-7.

Cobb, R C, and Margaret R Metz. 2017. "Tree Diseases as a Cause and Consequence of Interacting Forest Disturbances." *Forests* 8 (5). Multidisciplinary Digital Publishing Institute: 147.

Cobb, R C, David A Orwig, and Steve Currie. 2006. "Decomposition of Green Foliage in Eastern Hemlock Forests of Southern New England Impacted by Hemlock Woolly Adelgid Infestations." *Canadian Journal of Forest Research* 36 (5). NRC Research Press: 1331–41.

Crain, Caitlin Mullan, Kristy Kroeker, and Benjamin S Halpern. 2008. "Interactive and Cumulative Effects of Multiple Human Stressors in Marine Systems." *Ecology Letters* 11 (12). Wiley Online Library: 1304–15.

Dale, Virginia H., Linda A. Joyce, Steve McNulty, Ronald P. Neilson, Matthew P. Ayres, Michael D. Flannigan, Paul J. Hanson, et al. 2009. "Climate Change and Forest Disturbances." *BioScience* 51: 723–34. doi:10.1641/0006-3568(2001)051[0723:CCAFD]2.0.CO;2.

Davidson, J M, H A Patterson, and D M Rizzo. 2008. "Sources of Inoculum for Phytophthora Ramorum in a Redwood Forest." *Phytopathology* 98 (8): 860–66. doi:10.1094/PHYTO-98-8-0860.

Davidson, J M, David M Rizzo, Matteo Garbelotto, Steven Tjosvold, and Garey W Slaughter. 2002. "Phytophthora Ramorum and Sudden Oak Death in California: II. Transmission and Survival." In *Standiford, RB; McCreary, D.; and Purcell, KL, Technical Coordinators. Proceedings of the Fifth Symposium on Oak Woodlands: Oaks in California's Changing*

Landscape. Gen. Tech. Rep. PSW-GTR-184, Albany, CA: US Department of Agriculture, Forest Service, Pac, 741–49.

Davidson, J M, Allison C Wickland, Heather A Patterson, Kristen R Falk, and David M Rizzo. 2005. "Transmission of Phytophthora Ramorum in Mixed-Evergreen Forest in California." *Phytopathology* 95 (5). Am Phytopath Society: 587–96. doi:10.1094/PHYTO-95-0587.

Davis, Frank W., Mark Borchert, Ross K. Meentemeyer, Alan Flint, and David M. Rizzo. 2010. "Pre-Impact Forest Composition and Ongoing Tree Mortality Associated with Sudden Oak Death in the Big Sur Region; California." *Forest Ecology and Management* 259 (12). Elsevier B.V.: 2342–54. doi:10.1016/j.foreco.2010.03.007.

Doerr, S H, R A Shakesby, W H Blake, C J Chafer, G S Humphreys, and P J Wallbrink. 2006. "Effects of Differing Wildfire Severities on Soil Wettability and Implications for Hydrological Response." *Journal of Hydrology* 319 (1–4): 295–311. doi:http://dx.doi.org/10.1016/j.jhydrol.2005.06.038.

Elderd, B. D., B. J. Rehill, K. J. Haynes, and G. Dwyer. 2013. "Induced Plant Defenses, Host-Pathogen Interactions, and Forest Insect Outbreaks." *Proceedings of the National Academy of Sciences* 110 (37): 14978–83. doi:10.1073/pnas.1300759110.

Eviner, Valerie T, and Gene E Likens. 2008. "Effects of Pathogens on Terrestrial Ecosystem Function." *Infectious Disease Ecology: Effects of Ecosystems on Disease and of Disease on Ecosystems. RS Ostfeld, F. Keesing, and V. Eviner, Eds. Princeton University Press, Princeton, NJ*, 260–83.

Ewing, Holly A, Kathleen C Weathers, Pamela H Templer, Todd E Dawson, Mary K Firestone, Amanda M Elliott, and Vanessa K S Boukili. 2009. "Fog Water and Ecosystem Function: Heterogeneity in a California Redwood Forest." *Ecosystems* 12 (3). Springer: 417–33.

Fenn, Mark E, Richard Haeuber, Gail S Tonnesen, Jill S Baron, Susanne Grossman-Clarke, Diane Hope, Daniel A Jaffe, Scott Copeland, Linda Geiser, and Heather M Rueth. 2003. "Nitrogen Emissions, Deposition, and Monitoring in the Western United States." *AIBS Bulletin* 53 (4). American Institute of Biological Sciences: 391–403.

Fernández, Miguel, Healy H Hamilton, and Lara M Kueppers. 2015. "Back to the Future: Using Historical Climate Variation to Project Near-term Shifts in Habitat Suitable for Coast Redwood." *Global Change Biology* 21 (11). Wiley Online Library: 4141–52.

Filipe, João A N, Richard C Cobb, Ross K Meentemeyer, Christopher A Lee, Yana S Valachovic, Alex R Cook, David M Rizzo, and Christopher A Gilligan. 2012. "Landscape Epidemiology and Control of Pathogens with Cryptic and Long-Distance Dispersal: Sudden Oak Death in Northern Californian Forests." *PLoS Computational Biology* 8 (1). Public Library of Science: e1002328.

Fitzpatrick, M C, E L Preisser, A Porter, J Elkinton, and A M Ellison. 2012. "Modeling Range Dynamics in Heterogeneous Landscapes: Invasion of the Hemlock Woolly Adelgid in Eastern North America." *Ecological Applications* 22 (2): 472–86. http://www.scopus.com/inward/record.url?eid=2-s2.0-

84859532218&partnerID=40&md5=70427a1eb0e8eaa4f5eabf824a0db58e.

Foster, C N, C F Sato, D B Lindenmayer, and P S Barton. 2015. “Integrating Theory into Disturbance Interaction Experiments to Better Inform Ecosystem Management.” *Global Change Biology*.

GAO. 2006. “Invasive Forest Pests: Lessons Learned from Three Recent Infestations May Aid in Managing Future Efforts.” Edited by General Accounting Office. Washington DC.

Garbelotto, Matteo, David M Rizzo, and Lawrence Marais. 2002. “Phytophthora Ramorum and Sudden Oak Death in California : IV . Preliminary Studies on Chemical Control 1,” 811–18.

Haas, Sarah E., J. Hall Cushman, Whalen W. Dillon, Nathan E. Rank, David M. Rizzo, and Ross K. Meentemeyer. 2016. “Effects of Individual, Community, and Landscape Drivers on the Dynamics of a Wildland Forest Epidemic.” *Ecology* 97 (3). doi:10.1890/15-0767.1.

Haas, Sarah E., Mevin B. Hooten, David M. Rizzo, and Ross K. Meentemeyer. 2011. “Forest Species Diversity Reduces Disease Risk in a Generalist Plant Pathogen Invasion.” *Ecology Letters* 14 (11): 1108–16. doi:10.1111/j.1461-0248.2011.01679.x.

Haight, R G, F R Homans, T Horie, S V Mehta, D J Smith, and R C Venette. 2011. “Assessing the Cost of an Invasive Forest Pathogen: A Case Study with Oak Wilt.” *Environ Manage* 47 (3). U.S. Forest Service Northern Research Station, 1992 Folwell Avenue, St. Paul, Minnesota 55108, USA. rhaight@fs.fed.us: 506–17. doi:10.1007/s00267-011-9624-5.

Hamlet, Alan F, Eric P Salathé, and Pablo Carrasco. 2010. “Statistical Downscaling Techniques for Global Climate Model Simulations of Temperature and Precipitation with Application to Water Resources Planning Studies.”

Hansen, E M, and Ellen Michaels Goheen. 2000. “PHELLINUS WEIRII AND OTHER NATIVE ROOT PATHOGENS AS DETERMINANTS OF FOREST STRUCTURE AND PROCESS IN WESTERN NORTH AMERICA1.” *Annual Review of Phytopathology* 38 (1): 515–39. doi:doi:10.1146/annurev.phyto.38.1.515.

Hart, Sarah J., Tania Schoennagel, Thomas T. Veblen, and Teresa B. Chapman. 2015. “Area Burned in the Western United States Is Unaffected by Recent Mountain Pine Beetle Outbreaks.” *Proceedings of the National Academy of Sciences* 112 (14). doi:10.1073/pnas.1424037112.

He, Hong S, and David J Mladenoff. 1999. “SPATIALLY EXPLICIT AND STOCHASTIC SIMULATION OF FOREST-LANDSCAPE FIRE DISTURBANCE AND SUCCESSION.” *Ecology* 80 (1). Wiley Online Library: 81–99.

Heath, Linda S, Mark Hansen, James E Smith, Patrick D Miles, and Brad W Smith. 2009. “Investigation into Calculating Tree Biomass and Carbon in the FIADB Using a Biomass Expansion Factor Approach.”

Henson, Paul. 1996. *The Natural History of Big Sur*. Vol. 57. Univ of California Press.

Jactel, Hervé, Jérôme Petit, Marie Laure Desprez-Loustau, Sylvain Delzon, Dominique Piou,

Andrea Battisti, and Julia Koricheva. 2012. “Drought Effects on Damage by Forest Insects and Pathogens: A Meta-Analysis.” *Global Change Biology* 18 (1): 267–76. doi:10.1111/j.1365-2486.2011.02512.x.

Jasinski, J P Paul, and Serge Payette. 2005. “The Creation of Alternative Stable States in the Southern Boreal Forest, Quebec, Canada.” *Ecological Monographs* 75 (4): 561–83.

Jenkins, Jennifer C, John D Aber, and Charles D Canham. 1999. “Hemlock Woolly Adelgid Impacts on Community Structure and N Cycling Rates in Eastern Hemlock Forests.” *Canadian Journal of Forest Research* 29 (5). NRC Research Press: 630–45.

Jenkins, Jennifer C, David C Chojnacky, Linda S Heath, and Richard A Birdsey. 2003. “National-Scale Biomass Estimators for United States Tree Species.” *Forest Science* 49 (1). Society of American Foresters: 12–35.

Jenkins, Michael J, Elizabeth Hebertson, Wesley Page, and C Arik Jorgensen. 2008. “Bark Beetles, Fuels, Fires and Implications for Forest Management in the Intermountain West.” *Forest Ecology and Management* 254 (1). Elsevier: 16–34.

Johnson, Paul S, Stephen R Shifley, and Robert Rogers. 2009. *The Ecology and Silviculture of Oaks*. CABI.

Jules, Erik S., Allyson L. Carroll, Andrea M. Garcia, Christopher M. Steenbock, and Matthew J. Kauffman. 2014. “Host Heterogeneity Influences the Impact of a Non-Native Disease Invasion on Populations of a Foundation Tree Species.” *Ecosphere* 5 (9): art105. doi:10.1890/ES14-00043.1.

Kauffman, Matthew J, and Erik S Jules. 2006. “Heterogeneity Shapes Invasion: Host Size And Environment Influence Susceptibility To A Nonnative Pathogen.” *Ecological Applications* 16 (1): 166–75. doi:10.1890/05-0211.

Kelly, Maggi, and Ross K Meentemeyer. 2002. “Landscape Dynamics of the Spread of Sudden Oak Death.” *Photogrammetric Engineering and Remote Sensing* 68 (10). ASPRS AMERICAN SOCIETY FOR PHOTOGRAMMETRY AND: 1001–10.

Kovacs, Kent F, Robert G Haight, Deborah G McCullough, Rodrigo J Mercader, Nathan W Siegert, and Andrew M Liebhold. 2010. “Cost of Potential Emerald Ash Borer Damage in U.S. Communities, 2009–2019.” *Ecological Economics* 69 (3): 569–78. doi:10.1016/j.ecolecon.2009.09.004.

Kovacs, Kent F, Tomáš Václavík, Robert G Haight, Arwin Pang, Nik J Cunniffe, Christopher A Gilligan, and Ross K Meentemeyer. 2011. “Predicting the Economic Costs and Property Value Losses Attributed to Sudden Oak Death Damage in California (2010–2020).” *Journal of Environmental Management* 92 (4). Elsevier: 1292–1302.

Kulakowski, Dominik, and Thomas T Veblen. 2007. “Effect of Prior Disturbances on the Extent and Severity of Wildfire in Colorado Subalpine Forests.” *Ecology* 88 (3): 759–69.

Liebhold, A. M., W. L. MacDonald, D. Bergdahl, and V. C. Mastro. 1995. “Invasion by Exotic Forest Pests: A Threat to Forest Ecosystems.” *Forest Science, Monograph* 30: a0001–

z0001(1).

Littell, Jeremy S, Donald McKenzie, Becky K Kerns, Samuel Cushman, and Charles G Shaw. 2011. “Managing Uncertainty in Climate-driven Ecological Models to Inform Adaptation to Climate Change.” *Ecosphere* 2 (9). Wiley Online Library: 1–19.

Lovett, Gary M, Charles D Canham, Mary A Arthur, Kathleen C Weathers, and Ross D Fitzhugh. 2006. “Forest Ecosystem Responses to Exotic Pests and Pathogens in Eastern North America.” *BioScience* 56 (5): 395–405.

Lovett, Gary M, Kathleen C Weathers, Mary A Arthur, and Jack C Schultz. 2004. “Nitrogen Cycling in a Northern Hardwood Forest: Do Species Matter?” *Biogeochemistry* 67 (3). Springer: 289–308.

Lynch, Heather J, and Paul R Moorcroft. 2008. “A Spatiotemporal Ripley’s K-Function to Analyze Interactions between Spruce Budworm and Fire in British Columbia, Canada.” *Canadian Journal of Forest Research* 38 (12). NRC Research Press: 3112–19.

Mascheretti, S, P J P Croucher, A Vettraino, S Prospero, and M Garbelotto. 2008. “Reconstruction of the Sudden Oak Death Epidemic in California through Microsatellite Analysis of the Pathogen Phytophthora Ramorum.” *Molecular Ecology* 17 (11): 2755–68. http://onlinelibrary.wiley.com/doi/10.1111/j.1365-294X.2008.03773.x/abstract.

McCool, Michael D, Arch D Robison, and James Reinders. 2012. *Structured Parallel Programming: Patterns for Efficient Computation*. Elsevier.

McCullough, Deborah G, Richard A Werner, and David Neumann. 1998. “Fire and Insects in Northern and Boreal Forest Ecosystems of North America.” *Annual Review of Entomology* 43 (1). Annual Reviews 4139 El Camino Way, PO Box 10139, Palo Alto, CA 94303-0139, USA: 107–27.

Meentemeyer, R K., Nik J. Cunniffe, Alex R. Cook, Joao A. N. Filipe, Richard D. Hunter, David M. Rizzo, and Christopher A. Gilligan. 2011. “Epidemiological Modeling of Invasion in Heterogeneous Landscapes: Spread of Sudden Oak Death in California (1990-2030).” *Ecosphere* 2 (2). [Meentemeyer, Ross K.; Hunter, Richard D.] Univ N Carolina, Dept Geog & Earth Sci, Charlotte, NC 28223 USA. [Cunniffe, Nik J.; Filipe, Joao A. N.; Gilligan, Christopher A.] Univ Cambridge, Dept Plant Sci, Cambridge CB2 3EA, England. [Cook, Alex R.] Natl U: art17. doi:10.1890/es10-00192.1.

Meentemeyer, R K, B L Anacker, W Mark, and D M Rizzo. 2008. “Early Detection of Emerging Forest Disease Using Dispersal Estimation and Ecological Niche Modeling.” *Ecological Applications* 18 (2): 377–90. http://www.scopus.com/inward/record.url?eid=2-s2.0-54549112102&partnerID=40&md5=3122529a940f9a2e186c0f7310c8d05e.

Meentemeyer, R K, Sarah E Haas, and Tomáš Václavík. 2012. “Landscape Epidemiology of Emerging Infectious Diseases in Natural and Human-Altered Ecosystems.” *Annual Review of Phytopathology* 50 (1): 379–402. doi:10.1146/annurev-phyto-081211-172938.

Meentemeyer, R K, N E Rank, D A Shoemaker, C B Oneal, A C Wickland, K M Frangioso, and

D M Rizzo. 2008. “Impact of Sudden Oak Death on Tree Mortality in the Big Sur Ecoregion of California.” *Biological Invasions* 10 (8): 1243–55. http://www.scopus.com/inward/record.url?eid=2-s2.0-49449113654&partnerID=40&md5=7f26613524b7446c804a0fdc48ff5a92.

Metz, Margaret R., J. Morgan Varner, Kerri M. Frangioso, Ross K. Meentemeyer, and David M. Rizzo. 2013. “Unexpected Redwood Mortality from Synergies between Wildfire and an Emerging Infectious Disease.” *Ecology* 94 (10): 2152–59. doi:10.1890/13-0915.1.

Metz, Margaret R, Kerri M Frangioso, Ross K Meentemeyer, and David M Rizzo. 2010. “Interacting Disturbances: Wildfire Severity Affected by Stage of Forest Disease Invasion.” *Ecological Applications* 21 (2): 313–20. doi:10.1890/10-0419.1.

Mladenoff, David J. 2005. “The Promise of Landscape Modeling: Successes, Failures, and Evolution.” *Issues and Perspectives in Landscape Ecology*, no. March: 90–100. doi:10.1017/CBO9780511614415.011.

Mladenoff, David J. 2004. “LANDIS and Forest Landscape Models.” *Ecological Modelling* 180 (1): 7–19. doi:10.1016/j.ecolmodel.2004.03.016.

Neary, Daniel G, Kevin C Ryan, and Leonard F DeBano. 2005. “Wildland Fire in Ecosystems: Effects of Fire on Soils and Water.” *Gen. Tech. Rep. RMRS-GTR-42-Vol* 4: 250.

Noss, Reed F. 1999. *The Redwood Forest: History, Ecology, and Conservation of the Coast Redwoods*. Island Press.

Office, NADP Program. 2017. “National Atmospheric Deposition Program (NRSP-3).” http://nadp.isws.illinois.edu/nadp/.

Ohmann, Janet L, and Matthew J Gregory. 2002. “Predictive Mapping of Forest Composition and Structure with Direct Gradient Analysis and Nearest-Neighbor Imputation in Coastal Oregon, USA.” *Canadian Journal of Forest Research* 32 (4). NRC Research Press: 725–41.

Ohmann, Janet L, Matthew J Gregory, Emilie B Henderson, and Heather M Roberts. 2011. “Mapping Gradients of Community Composition with Nearest-neighbour Imputation: Extending Plot Data for Landscape Analysis.” *Journal of Vegetation Science* 22 (4): 660–76.

Orwig, David A, Richard C Cobb, Anthony W D’Amato, Matthew L Kizlinski, and David R Foster. 2008. “Multi-Year Ecosystem Response to Hemlock Woolly Adelgid Infestation in Southern New England Forests.” *Canadian Journal of Forest Research* 38 (4). NRC Research Press: 834–43.

Parker, Thomas J, Karen M Clancy, and Robert L Mathiasen. 2006. “Interactions among Fire, Insects and Pathogens in Coniferous Forests of the Interior Western United States and Canada.” *Agricultural and Forest Entomology* 8 (3). Wiley Online Library: 167–89.

Parton, W J, D W Anderson, C V Cole, and J W B Stewart. 1983. “Simulation of Soil Organic Matter Formations and Mineralization in Semiarid Agroecosystems.” *Special Publication-University of Georgia, Agriculture Experiment Stations (USA)*.

Pelt, Robert Van, and Jerry F Franklin. 2000. “Influence of Canopy Structure on the Understory Environment in Tall, Old-Growth, Conifer Forests.” *Canadian Journal of Forest Research* 30 (8). NRC Research Press: 1231–45.

Perles, Stephanie J, Kristina K Callahan, and Matthew R Marshall. 2010. “Condition of Vegetation Communities in Delaware Wate Gap National Recreation Area: Eastern Rivers and Maountains Network Summary Report 2007-2009.” Edited by National Park Service. University Park, PA: National Park Service.

Power, Alison G., and Charles E. Mitchell. 2004. “Pathogen Spillover in Disease Epidemics.” *The American Naturalist* 164 (S5): S79–89. doi:10.1086/424610.

Prospero, Simone, and Michelle Cleary. 2017. “Effects of Host Variability on the Spread of Invasive Forest Diseases.” *Forests*. doi:10.3390/f8030080.

Rizzo, D M, and Matteo Garbelotto. 2003. “Sudden Oak Death: Endangering California and Oregon Forest Ecosystems.” *Frontiers in Ecology and the Environment* 1 (4). Wiley Online Library: 197–204.

Rizzo, D M, Matteo Garbelotto, and Everett M Hansen. 2005. “Phytophthora Ramorum: Integrative Research and Management of an Emerging Pathogen in California and Oregon Forests.” *Annu. Rev. Phytopathol.* 43: 309–35.

Rizzo, D M, G W Slaughter, and Jr J R Parmeter. 2000. “Enlargement of Canopy Gaps Associated with a Fungal Pathogen in Yosemite Valley, California.” *Canadian Journal of Forest Research* 30 (10): 1501–10. doi:10.1139/x00-073.

Rollins, Matthew G. 2009. “LANDFIRE: A Nationally Consistent Vegetation, Wildland Fire, and Fuel Assessment.” *International Journal of Wildland Fire* 18 (3). CSIRO: 235–49.

Romme, William H, J Clement, J Hicke, D Kulakowski, L H MacDonald, T L Schoennagel, and T T Veblen. 2006. “Recent Forest Insect Outbreaks and Fire Risk in Colorado Forests: A Brief Synthesis of Relevant Research.” *Colorado Forest Research Institute*.

Ross, R M, R M Bennett, C D Snyder, J A Young, D R Smith, and D P Lemarie. 2003. “Influence of Eastern Hemlock (Tsuga Canadensis L.) on Fish Community Structure and Function in Headwater Streams of the Delaware River Basin.” *Ecology of Freshwater Fish* 12 (1). US Geol Survey, No Appalachian Res Lab, Leetown Sci Ctr, Wellsboro, PA 16901 USA. US Geol Survey, Aquat Ecol Lab, Leetown Sci Ctr, Kearneysville, WV 25430 USA. Ross, RM (reprint author), US Geol Survey, No Appalachian Res Lab, Leetown Sci Ctr, Wellsboro,: 60–65. doi:10.1034/j.1600-0633.2003.00006.x.

Ruess, Roger W, Jack M McFarland, Lori M Trummer, and Jennifer K Rohrs-Richey. 2009. “Disease-Mediated Declines in N-Fixation Inputs by Alnus Tenuifolia to Early-Successional Floodplains in Interior and South-Central Alaska.” *Ecosystems* 12 (3): 489–502.

Scheller, Robert M., James B. Domingo, Brian R. Sturtevant, Jeremy S. Williams, Arnold Rudy, Eric J. Gustafson, and David J. Mladenoff. 2007. “Design, Development, and Application

of LANDIS-II, a Spatial Landscape Simulation Model with Flexible Temporal and Spatial Resolution." *Ecological Modelling* 201 (3–4): 409–19. doi:10.1016/j.ecolmodel.2006.10.009.

Scheller, Robert M, Dong Hua, Paul V Bolstad, Richard A Birdsey, and David J Mladenoff. 2011. "The Effects of Forest Harvest Intensity in Combination with Wind Disturbance on Carbon Dynamics in Lake States Mesic Forests." *Ecological Modelling* 222 (1): 144–53.

Scheller, Robert M, and David J Mladenoff. 2004. "A Forest Growth and Biomass Module for a Landscape Simulation Model, LANDIS: Design, Validation, and Application." *Ecological Modelling* 180 (1): 211–29.

———. 2007. "An Ecological Classification of Forest Landscape Simulation Models: Tools and Strategies for Understanding Broad-Scale Forested Ecosystems." *Landscape Ecology* 22 (4): 491–505. doi:10.1007/s10980-006-9048-4.

Shakesby, R A, and S H Doerr. 2006. "Wildfire as a Hydrological and Geomorphological Agent." *Earth-Science Reviews* 74 (3). Elsevier: 269–307.

Simberloff, D. 2000. *Nature and Human Society : The Quest for a Sustainable World : Proceedings of the 1997 Forum on Biodiversity*. Edited by Peter H Raven. Washington, D.C.: National Academy Press. http://search.lib.unc.edu?R=UNCb3480060.

Smith, Thomas F, David M Rizzo, and Malcolm North. 2005. "Patterns of Mortality in an Old-Growth Mixed-Conifer Forest of the Southern Sierra Nevada, California." *Forest Science* 51 (3). Society of American Foresters: 266–75.

Sturtevant, Brian R., Brian R. Miranda, Douglas J. Shinneman, Eric J. Gustafson, and Peter T. Wolter. 2012. "Comparing Modern and Presettlement Forest Dynamics of a Subboreal Wilderness: Does Spruce Budworm Enhance Fire Risk?" *Ecological Applications* 22 (4): 1278–96. doi:10.1890/11-0590.1.

Sturtevant, Brian R, Robert M Scheller, Brian R Miranda, Douglas Shinneman, and Alexandra Syphard. 2009. "Simulating Dynamic and Mixed-Severity Fire Regimes: A Process-Based Fire Extension for LANDIS-II." *Ecological Modelling* 220 (23): 3380–93. doi:10.1016/j.ecolmodel.2009.07.030.

Thompson, Jonathan R., Erin Simons-Legaard, Kasey Legaard, and James B. Domingo. 2016. "A LANDIS-II Extension for Incorporating Land Use and Other Disturbances." *Environmental Modelling and Software* 75: 202–5. doi:10.1016/j.envsoft.2015.10.021.

Turner, David P, Greg J Koerper, Mark E Harmon, and Jeffrey J Lee. 1995. "A Carbon Budget for Forests of the Conterminous United States." *Ecological Applications* 5 (2). Wiley Online Library: 421–36.

Turner, G. 2008. "A Comparison of The Limits to Growth with 30 Years of Reality." *Global Environmental Change* 18 (3): 397–411. doi:10.1016/j.gloenvcha.2008.05.001.

Turner, Monica G. 2010. "Disturbance and Landscape Dynamics in a Changing World." *Ecology* 91 (10): 2833–49. doi:10.1890/10-0097.1.

Turner, Monica G, Robert V O'Neill, Robert H Gardner, and Bruce T Milne. 1989. "Effects of Changing Spatial Scale on the Analysis of Landscape Pattern." *Landscape Ecology* 3 (3–4). Springer: 153–62.

USDA Forest Service Northern Research Station and Forest Health Protection. 2016. "Alien Forest Pest Exploter - Species Map." http://foresthealth.fs.usda.gov/portal/Flex/APE.

Václavík, T, A Kanaskie, E M Hansen, J L Ohmann, and R K Meentemeyer. 2010. "Predicting Potential and Actual Distribution of Sudden Oak Death in Oregon: Prioritizing Landscape Contexts for Early Detection and Eradication of Disease Outbreaks." *Forest Ecology and Management* 260 (6): 1026–35. http://www.scopus.com/inward/record.url?eid=2-s2.0-77955509717&partnerID=40&md5=e5f33ee1d7b84ce42f6521232c88c049.

Valachovic, Y S, C A Lee, H Scanlon, J M Varner, R Glebocki, B D Graham, and D M Rizzo. 2011. "Sudden Oak Death-Caused Changes to Surface Fuel Loading and Potential Fire Behavior in Douglas-Fir-Tanoak Forests." *Forest Ecology and Management* 261 (11): 1973–86. http://www.scopus.com/inward/record.url?eid=2-s2.0-79954992343&partnerID=40&md5=2664521687dbdb6c6668e3baeca2d23f.

Vitousek, P M, Carla M D Antonio, Lloyd L Loope, and Randy Westbrooks. 1996. "Biological Invasions as Global Environmental Change." *American Scientist* 84 (5). Sigma XI-The Scientific Research Society: 468.

Vitousek, P M, Carla M D'Antonio, Lloyd L Loope, Marcel Rejmanek, and Randy Westbrooks. 1997. "Introduced Species: A Significant Component of Human-Caused Global Change." *New Zealand Journal of Ecology* 21 (1): 1–16.

Vogt, Kristiina. 1991. "Carbon Budgets of Temperate Forest Ecosystems." *Tree Physiology* 9 (1–2). Heron Publishing: 69–86.

Wagtendonk, Jan W Van, and Daniel R Cayan. 2008. "Temporal and Spatial Distribution of Lightning Strikes in California in Relation to Large-Scale Weather Patterns." *Fire Ecology*.

Waring, Richard H. 1983. "Estimating Forest Growth and Efficiency in Relation to Canopy Leaf Area." *Advances in Ecological Research* 13. Elsevier: 327–54.

Waring, Richard H, and Steven W Running. 2010. *Forest Ecosystems: Analysis at Multiple Scales*. Elsevier.

"Web Soil Survey." 2014. Soil Survey Staff, Natural Resources Conservation Sevice, United States Department of Agriculture. http://websoilsurvey.nrcs.usda.gov/.

Welsh, Cedar, Kathy Lewis, and Alex Woods. 2009. "The Outbreak History of Dothistroma Needle Blight: An Emerging Forest Disease in Northwestern British Columbia, Canada." *Canadian Journal of Forest Research* 39 (12): 2505–19. doi:10.1139/X09-159.

Yorks, Thad E, Donald J Leopold, and Dudley J Raynal. 2003. "Effects of Tsuga Canadensis Mortality on Soil Water Chemistry and Understory Vegetation: Possible Consequences of an Invasive Insect Herbivore." *Canadian Journal of Forest Research* 33 (8). NRC Research Press: 1525–37.

Zhang, Lin, Daniel J Jacob, Eladio M Knipping, Naresh Kumar, J William Munger, C C Carouge, A Van Donkelaar, Y X Wang, and D Chen. 2012. “Nitrogen Deposition to the United States: Distribution, Sources, and Processes.” *Atmospheric Chemistry and Physics* 12 (10). Copernicus GmbH: 4539.